Université de Montréal

Nanovecteurs pour cibler *Pseudomonas aeruginosa* dans la Fibrose Kystique

par

Juliana Campos Del' Orto

Sciences pharmaceutiques

Faculté de pharmacie

Mémoire présenté à la Faculté des études supérieures en vue de l'obtention du grade de Maitre en sciences (M.Sc.) en sciences pharmaceutiques option technologie pharmaceutique

Juin 2014

Université de Montréal

Faculté des Études Supérieures et Postdoctorales

Ce mémoire intilulé:

Nanovecteurs pour cibler *Pseudomonas aeruginosa* dans la Fibrose Kystique

Présenté par:

Juliana Campos Del' Orto

A été évalué par les membres du jury :

Patrice Hildgen, directeur de recherche

Jeanne Leblond- Chain, co-directrice de recherche

Valérie Gaëlle Roullin, présidente- rapporteur

Valéry Waters, examinatrice externe

Juin 2014

RÉSUMÉ

La production excessive de mucus visqueaux dans les poumons des patients atteints de la fibrose kystique (FK) gêne la diffusion des médicaments et entraîne des infections bactériennes. En effet, l'infection pulmonaire par *Pseudomonas aeruginosa* (PA) est la principale cause de mortalité. Les travaux effectués dans cette thèse avaient pour but de développer des nouvelles formulations de nanoparticules (NP) et de liposomes (LP) chargées avec des antibiotiques pour erradiquer le PA chez les patients atteints de KF. Tout d'abord, les polymères PEG-g-PLA et PLA-OH ont été synthétisés et caractérisés. Ensuite, l'efficacité d'encapsulation (EE) de la tobramycine, du sulfate de colistine et de la lévofloxacine (lévo) a été testée dans des NP de PEG-g-PLA et / ou PLA-OH. Les premiers essais d'optimisation ont montré que les NP chargées avec la lévo présentaient une augmentation de l'EE. La lévo reste alors le médicament de choix. Cependant, la meilleure charge de médicament obtenue était de 0,02% m/m. Pour cette raison, nous avons décidé d'évaluer l'encapsulation de la lévo dans les LP. En fait, des LP chargés de lévo ont présenté une EE d'environ 8% m/m. De plus, la taille et la charge de ces LP étaient appropriées pour la pénétration du vecteur dans le mucus. Le test de biofilm n'est pas reproductible, mais le test standard a montré que la souche mucoïde de PA était susceptible à la lévo. Ainsi, nous avons comparé les activités des LP fraîchement préparées (vides et chargés) et de la lévo libre sous la forme planctonique de PA. Les résultats ont montré que des LP vides ne gênent pas la croissance bactérienne. Pour la souche mucoïde (Susceptible à la lévo) les LP chargés et le médicament libre ont présenté la même concentration minimale inhibitrice (CMI). Toutefois, les souches non mucoïdes (résistant à la lévo) ont présenté une CMI deux fois plus faible que celle pour le médicament libre. Finalement, les LP se sont avérés plus appropriés pour encapsuler des médicaments hydrophiles que les NP de PEG-g-PLA. En outre, les LP semblent améliorer le traitement contre la souche résistante de PA. Toutefois, des études complémentaires doivent être effectuées afin d'assurer la capacité des liposomes èa traiter la fibrose kystique.

Mots-clés : antibiotique , nanoparticules polymèriques, PEG-g-PLA, liposomes, *Pseudomonas aeruginosa*, biofilm, Fibrose Kystique.

ABSTRACT

The increased production of viscoid mucus in the lungs of cystic fibrosis (CF) patients hinders the diffusion of therapeutics and favor bacterial infections. Indeed, lung infection by *Pseudomonas aeruginosa* (PA) relates with increased mortality in CF patients. This work is aimed at developing new antibiotic loaded nanoparticles and liposomes formulations to eradicate PA in CF. Firstly, PEG-g-PLA and PLA-OH polymers were synthesized and characterized. Afterwards, the loading efficiency (LE) of tobramycin, colistin sulfate and levofloxacin was evaluated in PEG-g-PLA and/or PLA-OH nanoparticles (NP). Early stage of optimization showed that levofloxacin NP exhibited increased LE thus this drug was selected for further optimization. However, the highest levofloxacin LE accomplished was 0.02% w/w. Thus, we decided to evaluate the levofloxacin LE into liposomes (LP). In fact, levofloxacin LP exhibited drug loading of 8% w/w with a size and charge suitable for mucus penetration. Preliminary evaluation of free tobramycin, colistin sulfate and levofloxacin against PA showed that the biofilm test was not reproducible. However, the traditional test in the planktonic form of PA showed that the mucoid strain was susceptible to levofloxacin. Thus, we evaluated fresh LP (blank and loaded) and free levofloxacin formulations against the planktonic form of PA (mucoid and non-mucoid strains). Results showed that blank LP did not interfere with the bacterial growth. Loaded LP presented similar minimal inhibitory concentration (MIC) for the susceptible mucoid strain and half MIC for the resistant non-mucoid strain when compared to the free drug. To conclude, LP seemed more appropriate to encapsulate hydrophilic drugs than polymeric PEG-g-PLA nanoparticles. Also, levofloxacin loaded LP seemed to improve the treatment against resistant strain of PA when compared to the free drug. However, further studies need to be performed to conclude whether levofloxacin LP are a promising option for the treatment of CF.

Keywords: antibiotics, polymeric nanoparticles, PEG-g-PLA, liposomes, *Pseudomonas aeruginosa*, biofilm, Cystic Fibrosis.

TABLE OF CONTENTS

LIST OF TABLES

LIST OF FIGURES

ABREVIATIONS

AML	Adherent Mucus Layer
ASL	Airway Surface Liquid
ATCC	American Type Culture Collection
ATP	Adenosine tri-phosphate
CAMBH	Cation Adjusted Mueller Hinton Broth
CF	Cystic Fibrosis
CFTR	Cystic Fibrosis Transmembrane Conductance Regulator
CFU	Colony Forming Units
CLSI	Clinical and Laboratory Standards Institute
DCM	Dichloromethane
DE	Double Emulsion
DLS	Dynamic Light Scattering
DMF	Dimethylformamide
DNA	Deoxyribonucleic acid
DNFB	2,4 - Dinitrofluorobenzene
DPI	Dry Powder for Inhalation
DSPC	1,2-Distearoyl-sn-glycero-3-phosphocholine
DSPE-PEG	1,2-distearoyl-sn-glycero-3-phosphoethanolamine-N-[biotinyl(polyethylene-glycol)-2000]
EE	Encapsulation Efficiency
ELSD	Evaporative Light Scattering Detection
EPS	Extracellular polysaccharide
ESE	Emulsification Solvent Evaporation
GC	Growth Control
GPC	Gel Permeation Chromatography
HILIC	Hydrophilic Interaction Column
HPLC	High Performance Liquid Chromatography

HPV	Human Papilloma Virus
I	Intermediate
IV	Intra venous
LE	Loading Efficiency
LML	Luminal Mucus Layer
LOD	Limit of Detection
LOQ	Limit of Quantification
LPS	Lipopolysaccharide
MBIC	Minimal Biofilm Inhibitory Concentration
MHA	Mueller Hinton Agar
MIC	Minimal Inhibitory Concentration
mM	Mili mol
Mn	Number average molecular weight;
MPP	Mucus Penetrating Particle
MPS	Mononuclear Phagocytic System
MRSA	Methicilin-Resistent *Staphylococcus aureous*
MS	Mass Spectrometry
mV	Milivolts
Mw	Weight average molecular weight
MWCO	Molecular Weight Cut off
nm	nanometers
NP	Nanoparticles
NPP	Nanoprecipitation
OD	Optical Density
PA	*Pseudomonas aeruginosa*
PCA	Poly(cyanoacrylate)
PDI	Polydispersity index
PEG	Poly(ethylene glycol)

PEG-g-PLA	Poly(ethylene glycol)-grafted-poly(lactic acid)
pH	Potential of Hydrogen
PLA	Poly(lactic acid)
PLA-OH	Poly(lactic acid) polymer altered during the synthesis of PEG-g-PLA (intermediate product).
PLC	Poly(ε-carprolactone)
PLGA	Poly(glycolic acid)
PMMA- MA	Poly(methyl methacrylate-co-methacrylic acid
PNP	Polymeric Nanoparticle
ppm	Parts per milion
PVA	Polyvinyl alcohol
R	Resistant
R^2	Correlation coefficient
S	Susceptible
RNA	Ribonucleic acid
SA	Sodium Alginate
SB	Stable bound
SC	Sterility Control
SD	Standard Deviation
SE	Single Emulsion
TB	Tobramycin
Tg	Transition temperature
TSB	Tryptic Soy Broth
USP- NF	United States Phamacopeia and National Formulary
UV	Ultraviolet
w/w	Percentage weigh by weight

ACKNOLEDGEMENTS

I thank God for always being by my side guiding my steps and making my dreams come true. You have provided me infinitely more then I would ever imagine.

I thank my beloved husband Marcelo Zanini for his support and cooperation. This accomplishment is also yours because I could never have made it without your incentive. I love you!

Also I thank my parents Pedro Del' Orto and Terezinha Del'Orto who have taught me the best values in life. Even being all the way in Brazil I can still feel your love here in Canada.

I am thankful for the opportunity that Professor Patrice Hildgen gave to me to study at Université de Montréal and for his friendship and guidance. Thanks for trusting in me!

I am also enormously thankful to Professor Jeanne Leblond-Chain's support and co-orientation. It was a great opportunity to work with you. Thanks for your dedication, expertise and friendship!

Similarly, I thank Professor Valérie Gaëlle Roullin that has recently jointed our university and already added so much to our team. Thanks for your precious cooperation and help. I am very lucky to have so many experts to count on.

I also thank the students and friends from Patrice's and Jeanne's lab : Jean-Michel Rabannel, Valérie Aoun, Igor Elkin, Mohamad Mokhtar, Mirza Hossain, Kevin Plourde, Warren Viricel, Amira Mbarek and Soudez Fakhari Tehrani (from Gaëlle's laboratory). I would have not finished this work without your help.

Friends such as professor Grégoire Leclair and professor Xavier Banquy, Marie-Éve Lèclair, Martin Jutras, Alexandre Melkoumov, Sarra Zaraa, Amandine Chefson and Mihaela Friciu also participated in my project providing kindness help whenever necessary. Thanks for your cooperation and friendship.

Finally, I thank Dr. Valérie Waters from the Hospital of Sick Kids in Toronto for kindly welcoming me and training me in the biofilm assay. I really enjoyed my time in Toronto. For sure you have a great team there.

CHAPTER 1:

Introduction

1.1. Cystic Fibrosis

1.1.1 Historical background

Cystic fibrosis (FC) was first pathologically distinguished from celiac disease in 1938. Autopsy studies from malnourished children characterized a newborn disease of mucus plugging of the glandular ducts named “Cystic Fibrosis of the pancreas”. This disease was characterized by pancreatic damage and lack of pancreatic enzymes secretion resulting in nutritional failure which was assumed to be related with increased vulnerability to lung infection. At this time, the life expectancy was 6 months and death normally occurred as a result of lung inflammation. The disease was also designed as “Mucoviscidosis” and later was referred as “generalized exocrinopathy” since many exocrine glands were affected. At this time, CF was already considered an autosomal recessive disease. Later, better elucidation of the disease was possible due to the advents of the sweat electrolyte defect discovered in 1953. They found that the sweat of CF patients possessed an increased concentration of salts. Afterwards, the development of the standardized sweat test in 1959 allowed the identification of mild cases. Thus, the disease was no longer considered only a disorder of mucus production (1). In 1983, the chloride transport was identified as the major defect in CF accompanied by increased sodium reabsorption. Although CF has been diagnosed since 1938, it is only in 1989 that the mechanism was discovered, thanks to the discovery of the CFTR gene (2). Located in the long arms of chromosome 7, the CFTR gene encodes a protein that functions as an anion channel: the phosphorylated-dependent epithelial chloride channel (3) **(Figure 1)**.

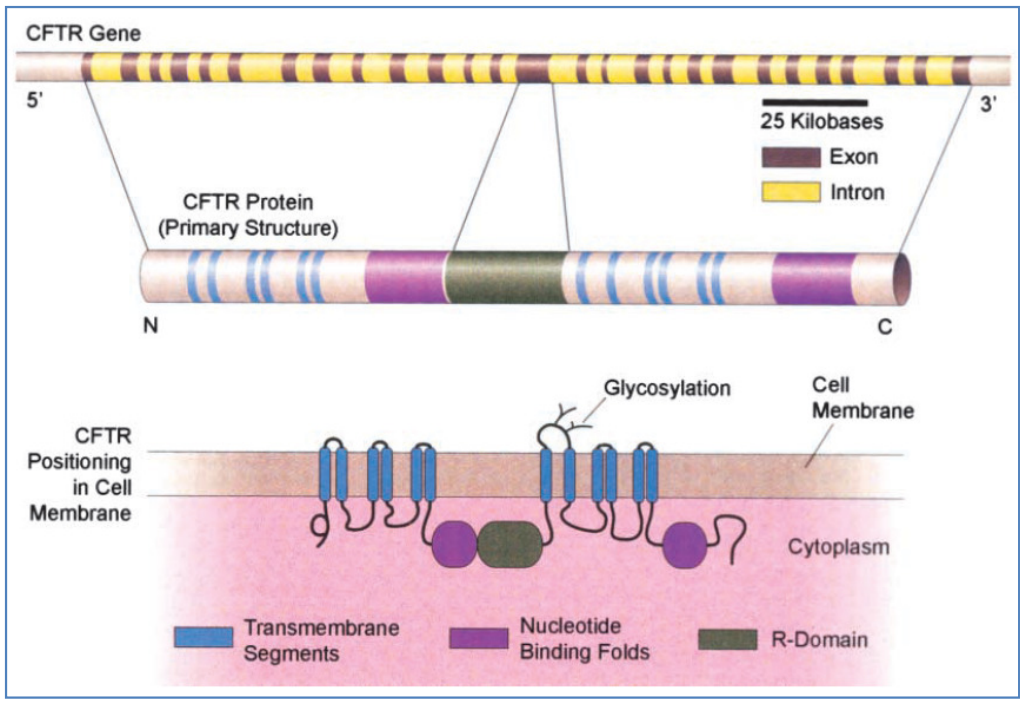

Figure 1. The cystic fibrosis (CF) transmembrane conductance regulator (CFTR) gene and its encoded polypeptide.*The human CFTR gene (top) is located on the long arm of chromosome 7 and consists of 27 exon regions that encode the 1,480 amino acid CFTR proteins (middle). The mature protein after proper folding, glycosylation, and insertion into the cell membrane is shown at the bottom. The CFTR protein is a member of the ATP-binding cassette (ABC) family of transporters. It contains two nucleotide-binding domains that bind and hydrolyze ATP, two dual sets of membrane-spanning segments that form the channel, and a central regulatory (R) domain. The R domain, unique to CFTR, is highly charged with numerous phosphorylation sites for protein kinases A or C.(Reprinted by permission from Reference 490).*
Taken from reference (3).

According to its primary structure, the CFTR channel is classified as a family member of the transport proteins class called ATP-biding cassette (ABC) transporter. These transporters utilize the energy of ATP hydrolysis to actively transport molecules across cell membranes. The CFTR channel is located in the apical membrane of epithelial tissues and is responsible for the regulation of chloride flow across epithelia cells. Thus, it has a crucial role in the control of transepithelial salt transport, fluid flow and ion concentration (4).

To date, more than 1900 mutations in the CFTR gene have been reported (5). In Canada, the most prevalent mutation (91.5%) is a deletion of a three-base pair which results in the loss of a phenylalanine residue at position 508 of the CFTR protein sequence (F508del) (6). Depending on the kind of mutation, the ion channel can work partially or completely fail

characterizing different symptoms and severity of the disease. However, the development of symptoms cannot be predicted based solely on DNA analysis, since some symptoms are also determined by phenotypic aspects, such as in the case of the pulmonary disease. However, the prediction of development of pancreatic disease is more genetically based.

1.1.2 Symptoms

As a variety of organs are lined by epithelial cells such as sweet ducts, airways, pancreatic ducts, biliary tree, intestines and vas deferens, cystic fibrosis leads to be a multi-systemic disease. The manifestations includes elevated sweat chloride concentration, lung disease, intestinal obstruction, pancreatic insufficiency with diabetes and impaired absorption, the latter due to inadequate secretion of digestive enzymes, biliary cirrhosis and congenital collateral absence of the vas deferens, often in combination (1, 7) .

Despite being a multi-systemic disease, approximately fifty percent of all patients are harmed with bacterial infection in the lungs (6). In addition, according to the Canadian Cystic Fibrosis Registry (2011), the main cause of death is pulmonary-related (6). Thus, given the impact of the pulmonary disease in the survival of CF patients, there is an unmet need for the development of new treatments for the chronic lung infections.

1.2. Lung Disease Phase in Cystic Fibrosis

1.2.1. Pulmonary dysfunctions due to CFTR mutations

The airways epithelium is formed by ciliated epithelial cells responsible to reabsorb electrolyte and goblet cells (glandular simple columnar epithelial cells). The latter are responsible for secreting mucins (the major component of mucus) and to generate the

airway surface liquid (ASL). As shown in **figure 2- scheme a**, the normal airways are covered by the periciliary liquid layer which is composed of the cilium and a mucus layer. The function of the periciliary layer to provide a low-viscosity solution for ciliary beat which allows the mucus transport, therefore its volume and ion concentration are tightly regulated. The mucus layer is formed by high molecular-weight mucins whose properties are altered by electrolyte concentration, water content and pH. Ultimately, the mucin structure consists of numerous diversified carbohydrate side chains which are suitable for binding a wide variety of particles, as a mechanism to clear the airway through the mucus transport. Most importantly, it is widely accepted that the sensible adjustment in the electrolyte transport by the airway epithelium and submucosal glands controls the volume and composition of the ASL. Thus, as shown in the **figure 2- schemes b and c,** loss or dysfunction of CFTR leads to failure or decrease in the chloride secretion. However, as the sodium absorption still takes place, it leads to chloride paracellular absorption and water influx generating dehydration of ASL and build up of high viscous mucus. As a consequence, the cilium beat is impeded and the mucus transport does not take place. All these impairments together favors infection by bacteria and limits the pulmonary host defense due to loss of mucociliary clearance of bacteria(8) (**Figure 2- schemes d and e**).

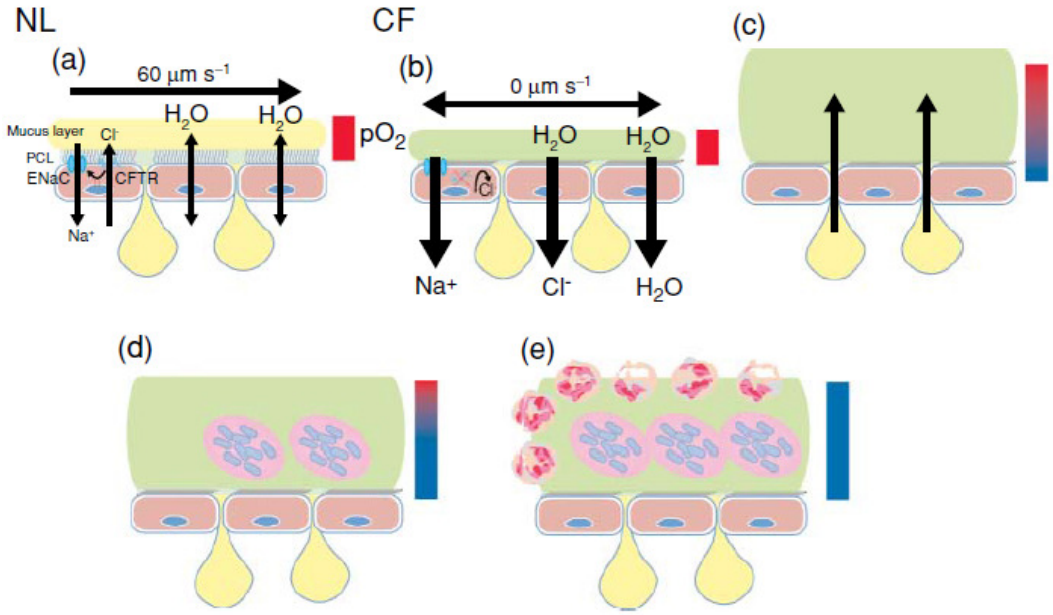

Figure 2: *Normal mucus clearance mechanisms and failure to adequately hydrate CF airway surfaces*. *(a) Normal airways coordinate rates of Na^+ absorption and Cl^- secretion to hydrate airway surfaces. (b) In CF, the absence of CFTR protein/function in the apical membrane leads to unregulated Na^+(Cl^- follows assively via paracellular path—not shown) and water absorption. The pathophysiologic sequence that follows CF dehydration is depicted in diagrams c–e. (c) Mucin secretion into adherent mucus plaque is depicted as emanating from goblet cells/glands. (d–e) Bacteria within mucus plaques/plugs are depicted as acrocolonies. Bars depict O_2 tension in ASL (red, oxygenated; blue, hypoxic). NL=normal lung; CF= Lung of patients with CF.*
Taken from reference (8).

1.2.2. Pulmonary Infection by *Pseudomonas aeruginosa*

Numerous microorganisms have been isolated from the lungs of CF patients such as *Aspergillus fumigatus* species, *Haemophilus influenzae*, *Stenotrophomonas maltophilia(9)*, *Burkholderia cepacia complex*, *Alcaligenes* species, atypical mycobacteria and methicilin-resistent *Staphylococcus aureous* (MRSA) (6) **(figure 3)**. In addition, viral infections also play an important role in the development of the CF disorder(10). However, the most prevalent bacteria are *Pseudomonas aeruginosa* and *Staphylococcus aureus depending on age* (6). *Pseudomonas aeruginosa* is a gram-negative bacillus, non-encapsulated and non-spore formers, which infects predominantly the lower respiratory tract.

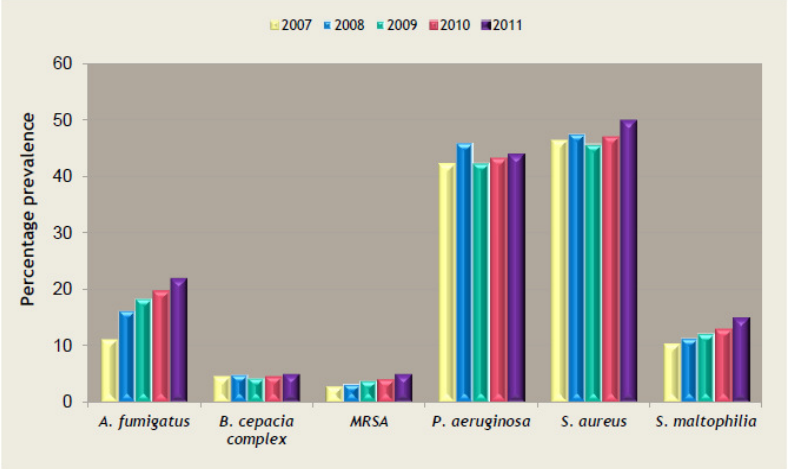

Figure 3: Prevalence of respiratory infections, 2007-2011. **Taken from reference (6)**.

Studies have shown that early infection in the airways of CF patients is most frequently caused by *S. aureus* and *H. influenzae*. In the other hand, the most prevalent pathogen isolated in adults is *Pseudomonas aeruginosa* **(Figure 4)**.

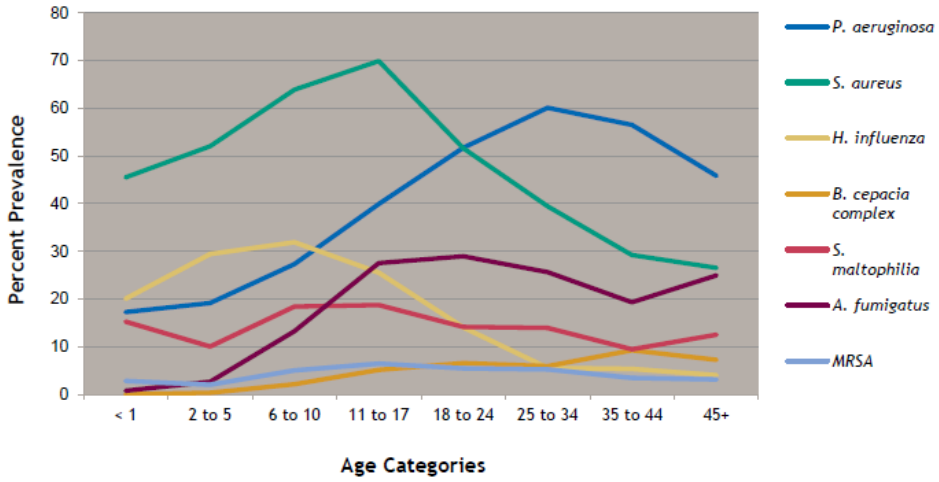

Figure 4: Age-specific prevalence of respiratory infection in CF patients, 2011. **Taken from reference (6).**

Indeed, pulmonary infection by *Pseudomonas aeruginosa* is closely related to an increase in mortality and morbidity of CF patients (6, 11) . However, it should be mentioned that other pathogens, such as *Burkholderia ssp. (12)*., *Achromobacter ssp. (13)* and *Stenotrophomonas maltophilia (9)* also contribute to morbidity and / or mortality .

Thus, these data support the importance of the development of new therapeutic strategies in order to prevent pulmonary exacerbations caused by these microorganisms. Pulmonary exacerbations are defined as the increased manifestation of respiratory symptoms such as cough and sputum production, often accompanied by systemic symptoms such as anorexia and malaise (14) . The occurrence of these symptoms defines the necessity of treatment adjustment in order to preserve pulmonary capacity and assure increased lifespan.

1.2.3. Biofilm formation

Numerous researchers have studied the underlying reasons why the immune system of CF patients is not effective to eliminate the early lung colonization by *P. aeruginosa.* However, how CFTR mutations enhance susceptibility to pulmonary infection and how this vulnerability could be prevented still remains unclear.

Cystic Fibrosis is correlated with increased proinfammatory signals; however this does not result in efficient clearance of bacteria. In fact, the failure to clear infection causes cyclic neutrophil influx which releases oxidants and proteases (15). This environment is characterized by low level of oxygen that triggers the change in the morphology of *Pseudomonas aeruginosa* from planktonic (mobile) to biofilm form (**figure 2 – diagrams d-e**). In addition, the bacteria which were strictly aerobic develop the ability to undergo anaerobic respiration (16). Mutations enable the bacteria to produce an extracellular polysaccharide (EPS) matrix composed mainly of alginate, the biofilm (**figure 5**).

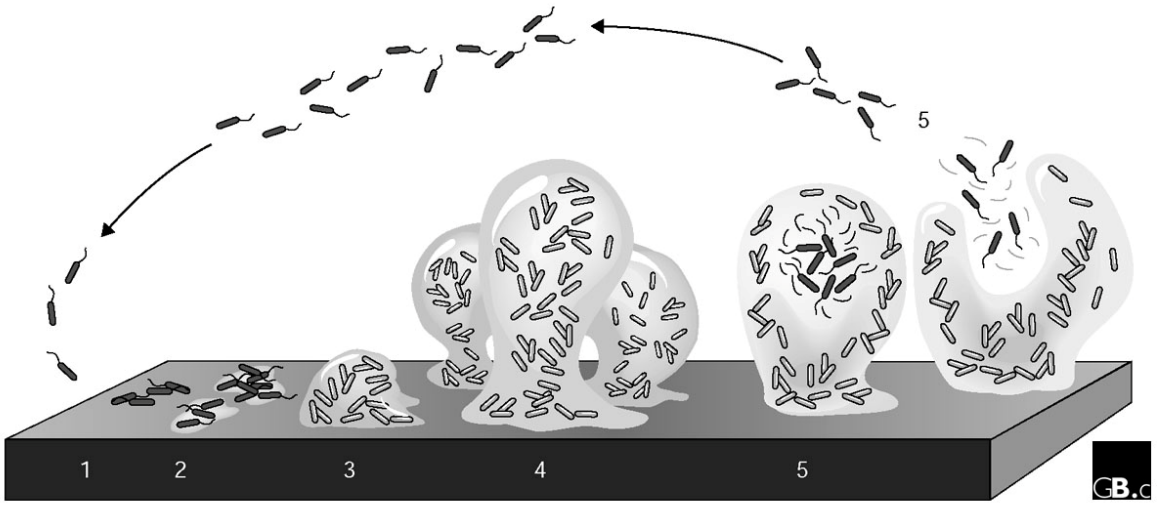

Figure 5: A model of the stages of bacterial biofilm development. At stage 1, the bacterial cells attach reversibly to the surface. Then, at stage 2, the cells attach irreversibly, a step mediated mainly by exopolymeric substances, and the cells lose their flagella-driven motility. At the next stage (3), the first maturation phase is reached, as indicated by early development of biofilm architecture. The second maturation phase is reached at stage 4 with fully mature biofilms, as indicated by the complex biofilm architecture. At the dispersion stage (5), single motile cells (dark cells on the figure) disperse from the microcolonies. Adapted from (17).Taken from reference (18).

In the biofilm form, the bacteria lose their flagellum which is recognized by the immunological system. In fact, *P. aeruginosa* isolated from chronically infected CF patients also have mutations enabling mucus production (mucoid strains) rendering them highly resistance to antibiotic and neutrophil-mediated killings. After maturation, these colonies of bacteria encased in the alginate matrix can return to the planktonic form (mobile) and disperse to colonize new niches (17). The genetic processes related to biofilm formation and dispersion has been extensively described in the literature (19).

1.2.4. Treatments

1.2.4.1. Treatment of the lung disease

The main goal of the treatment of the lung disease is to successfully eradicate microorganisms by antibiotic therapy. However, the establishment of chronic lung

inflammation is inevitable. Thus, other medications for chronic use are indicated to treat the symptoms due to pulmonary inflammation, as listed in table I (20).

Table I: Chronic medications for maintenance of lung health.

Class of drugs	Examples	Objective
Mucolytics	Dornase alpha (inhalation)	Increase mucus fluidity, hence aiding mucus clearance. Recombinant human DNase degrades the residual DNA caused by neutrophils infiltration.
Osmotic agents	Hypertonic saline (inhalation) Manitol (inhalation)	Reestablish the hydration condition of the ASL and improve the mucus transport rate. Osmotic agents draw water from the interstitium into the ASL which allows increased ciliary beat and cough clearance.
β2-adrenergic receptor agonists	Salbutamol, salmeterol (inhalation)	Treat reactive airway disease.

1.2.4.2. Treatment of lung infection caused by *Pseudomonas aeruginosa*

Antibiotic therapy against *P. aeruginosa* aims at increasing the life expectancy of patients by preventing pulmonary exacerbations which can result in irreversible loss of pulmonary capacity. Thus, aggressive and early antibiotic treatment of *P. aeruginosa* is associated with increased life expectancy (21, 22), since in most cases resistant bacterial cells selected over time in chronic infection cannot be eradicated. Although the pulmonary route is always favored due to decreased level of side effects and increased concentrations, the concomitant administration of systemic drugs (orally or intravenously) may also be indicated, depending on the severity of the infection. Indeed clinical practice is the main resource to guide physicians to the appropriate choice of the antibiotic therapy. However, the antibiotic arsenal is finite and limited to combat *P. aeruginosa* which exhibits a strong capacity to mutate into resistant forms and is hyper adapted to the lungs of CF patients. In addition, the slow development of new classes of antimicrobials suggests that it is worthwhile to invest in the development of new formulation for current drugs. In fact, pharmacotechnical research allows changes in the drug's pharmacokinetic properties which can be adapted to better target *P. aeruginosas* in the lungs. These innovative strategies

(presented in section 1.2.4.4), represent an important alternative to improve the bacterial eradication in cystic fibrosis, which is directly related to the longevity of CF patients.

1.2.4.3. Chronic *Pseudomonas aeruginosa* pulmonary infection

The use of aminoglycosides is recommended for the chronic suppressive therapy of *P. aeruginosa* in an alternating 28-day on/off regimen. Two different formulations are available including solution for inhalation and intravenous preparation also used for inhalation, as explained in table II.

Table II: Aerosolized aminoglycosides for the chronic suppressive therapy of *P. aeruginosas.*

Active (Trade Name)	Dose
TIS (tobramycin inhalation solution) – TOBI®	300 mg/ twice a day (23).
NIT (nebulized intravenous tobramycin) - Nebcin ®	Children: 70-120 mg twice or three times a day. Adults: 80-160 mg twice or three times a day (23).
NIT - (Sabex)	80-160 mg twice daily (23).
Amikacin® (Bristol) – intravenous formulation used by nebulization.	250 mg twice daily for children and 250-500 mg twice daily for adults (24).

Although there are no thorough studies to demonstrate the clinical efficacy of colistimethate sodium, this drug can also be prescribed to treat multi-resistant strains (24, 25). Thus, colistin (Coly-Mycin® M Parenteral - ERFA Canada Inc.) is indicated as another option and is supplied as an aerosol preparation (powder for reconstitution to 150 mg/2 mL). Colistin is also available as an intravenous formulation for nebulization (Colobreathe ®). The aerosol dosage recommended for Colobreathe ® is 25-150 mg (intravenous dry powder) twice or three times daily (24).

Beta-lactams are also available to fight pseudomonal infections in CF patients. Aztreonam, carbapenems, cephalosporins (ceftazidime and cefapime) and penicilins are indicated for intravenous administration (26-28).

1.2.4.4. Recently approved therapies

Given the advantages of the pulmonary administration over systemic routes for the treatment of cystic fibrosis, recent research efforts have focused in the development of new antibiotic formulations such as powder for nebulization or powder for inhalation, as listed in **table III.**

Table III: Recently approved aerosolized antibiotics for the treatment of cystic fibrosis.

Drug	Formulation	Comments
CMS[a] (Colomycin®-Forest and Promixin®-Profile Pharma)	Intravenous formulation used for nebulization.	Composed by colistimethate sodium (CMS). Administered by Jet nebulizer. Administration time is 15 minutes. Formulation must be refrigerated (29)
CMS[a] (Colobreathe®)	Dry powder for inhalation (DPI).	Composed by colistimethate sodium (CMS). Administrated with the Turbospin inhalation device. Administration time is approximately 1minute. Storage at room temperature (30).
Aztreonam lysine (AZLI, Cayston®, Gilead Sciences)	Powder for nebulization (aerosol).	Administrated with an electronic vibrating mesh nebulizer (Altera®). Administration time is 3 minutes. Formulation must be refrigerated. The CEDAC recommends the use of aztreonam inhalation solution for the treatment of chronic *P. aeruginosa* infection in patients with moderate to severe CF and deteriorating clinical condition despite treatment with inhaled tobramycin (31, 32).
Tobramycin (TOB Podhaler®- Novartis)[c]	DPI administrated with the Podhler (T-326) inhaler.	Tobramycin Inhalation Powder (TIP). Administration time is under 6 minutes. Storage at room temperature (33).

CEDAC: Canadian Expert Drug Advisory Committee: CF: Cystic Fibrosis.
[a]Approved in the European Union (EU).
[b]Approved for the treatment of CF patients infected with *P aeruginosa* in Australia and USA, and conditionally approved in Canada and EU. The Canadian Expert Drug Advisory Committee (CEDAC) recommends the use of aztreonam inhalation solution (28-day cycles) for the treatment of chronic P. aeruginosa infection in patients with moderate to severe cystic fibrosis and deteriorating clinical condition despite treatment with inhaled tobramycin.
[c]Approved in European Union, Canada, Switzerland and other countries.

It has to be mentioned that the solution for inhalation requires the use of a nebulizer and compressor combination that can be noisy and difficult to transport. Additionally, nebulizers require long time for administration which may include the cleaning step of the equipments. Thus, the development of powder for inhalation must be encouraged since the advantage to

have rapid drug delivery with a portable inhaler includes potentially improving patient adherence.

All formulations discussed in **table III** are composed of free drugs. Indeed, they are aerosolized formulations which bring therapeutic improvements the treatment of CF since they enable the pulmonary administration of antibiotics. However, additional benefits would be achieved with the application of an aerosolized sustained delivery formulation (drug encapsulated into nanocarriers), as will be discussed afterwards.

1.2.5. Causes for treatment failure

1.2.5.1. Patient compliance

The new advances in the treatment of cystic fibrosis and aggressive management of lung disease have resulted in great improvements of the patient's length and quality of life. However, as the number of treatments expands, the medical regimens become increasingly tiresome and time-consuming (34). Therefore, treatment burden for patients with cystic fibrosis is extremely high, and includes a range of inhaled and systemic medications, physiotherapy and exercises, often taking more than 2 hours a day (35).

Non adherence to treatment may cause accelerated disease and increased number of hospital admissions. The overall rate of treatment adherence in children with CF was found to be below 50% (36).

The most important reasons for patient non adherence to treatment include time management difficulties, oppositional behavior from children, poor taste when using breathing nebulizer for a long period, forgetting to administer the drug and embarrassment to take a lot of drugs or receive physiotherapy at school (37).

Therefore, decreasing the frequency of drug administration, providing safe drug association in the same formulation, offering easy and fast administration (important factors in the case

of drugs for lung administration) and developing formulations with tolerable taste may be promising goals to increase patient adherence and efficacy of antibiotic treatment. For instance, sustained drug release can be achieved by encapsulation of drug in a biodegradable carrier thus resulting in decreased frequency of drug administration. Such goal has been achieved by the liposomal formulation Amikacin® which is now in phase IV of clinical trials (38).

1.2.5.2. *Pseudomonas aeruginosa* resistance to antibiotics

In spite of aggressive antibiotic therapy, *Pseudomonas aeruginosa* has demonstrated the ability to evade the mechanism of action of antibiotics. Some adaptive mechanisms of defense against antibacterial drugs can be listed **(table IV)** such as changes in the bacterium expression of proteins which are target for drugs, lack of membrane porins which are important for antibiotic diffusion and expression of drug efflux mechanisms (39, 40). These mutations can partially explain their ability to survive and persist for years in the CF patient's lungs.

Thus, as different classes of antibiotics show diverse modes of action, the rate and mechanisms of resistance vary according to the antimicrobial class as can be seen in the **table IV**.

Table IV: Main mechanisms of resistance of *P. aeruginosa* to certain classes of antibiotics.

Antibiotic Class	Examples	Mechanism of action	Resistance mechanism
Fluoroquinolones	Levofloxacin, ciprofloxacin	Inhibition of DNA synthesis by inactivation of topoisomerases II and IV (enzymes essential for DNA replication).	Expression of drug efflux pumps. Mutations in the topoisomerases II and IV (39).
Aminoglycosides	Tobramycin, gentamicin, amikacin.	Inhibition of protein synthesis by antibiotic binding to bacterial ribosomes and inhibition of ribosomal enzymes.	Expression of drug efflux pumps. Reduction in the active transport through the membrane. Modifying enzymes.
Beta-lactams	Imipenem, Meropenem, aztreonam, ceftazidime, cefapime.	Interference with cell wall synthesis.	Production of β-lactamase enzymes that inactivate the drug. Multi-drug efflux (40) .
Polymyxins	Colistin	Disrupt the bacterial cell wall through osmotic rupture.	Mutation in the lipid A reducing binding of polymyxins to lipopolysaccharide (h) (41).

Polymyxins had already been considered an alternative for the treatment of multi-resistant strains *of P. aeruginosa* (42). Their bactericidal activity consists of cell membrane disruption leading to leakage of cell contents and bacterial death. This is achieved at least in part by binding to lipopolysaccharide (LPS), a major component of the Gram-negative cell surface, through interactions with phosphates and fatty acids of lipopolysaccharides core and lipid A moieties. However, spontaneous polymyxin-resistant mutants of *Pseudomonas aeruginosa* have already been isolated (41). Indeed, lipid A of these mutants contained aminoarabinose which reduces binding of polymyxins to LPS, whereby resistance arises (43).

The increase in bacterial resistance to antibiotics is also related to the route of administration. Thus, in the case of cystic fibrosis, the pulmonary route is preferred since it allows increased local concentration of antibiotics and longer contact time with the pathogen. Moreover, the local mechanism of action provided by pulmonary delivery decreases the occurrence of side-effects and the possible occurrence of sub-inhibitory drug levels, as can occur in other routes (oral, intravenous) which favors drug resistance (44). In

addition, the extended antibiotic release achieved with a nanocarrier would in theory also help to maintain the therapeutic concentration of drug in the lungs.

In addition, a previous study done by our group (45) showed an increased antifungal effect of itraconazole, voriconazole and amphotericin B loaded PEG-g-PLA nanoparticles compared with the free drug against resistant strains of *Candida ssp* and *Aspergillus fumigates* (these strains presented over expression of efflux pumps). These studies showed that PEG-g-PLA nanoparticles with small hydrodynamic diameter (<200 nm) can be internalized in these yeast strains and might block the efflux pumps thereby overcoming fungal resistance to these drugs.

1.2.5.3. Antibiotic diffusion in the mucus

The mucus structure can interact with drugs hindering its diffusion through the mucus and the targeting of embedded bacteria. Various studies showed that positively charged, low-molecular weight drugs such as amikacin, tobramycin, gentamicin and some β-lactams antibiotics bind to negatively charged components in the mucus (46)**.** Therefore, bacteria are exposed to sub-inhibitory level of antibiotics which may induce bacterial resistance and biofilm formation (44, 47).

1.2.5.4. Biofilm formation

The implications of biofilm formation in the resistance to cystic fibrosis treatments have been extensively reported. Firstly, the alginate envelope (biofilm matrix) serves as a direct barrier against phagocytic cells and effective opsonisation (22). Moreover, alginate has immunomodulatory properties stimulating the release of inflammatory cytokines which increases lung inflammation and subsequent destruction. Intensive inflammation favors the development of hypoxic areas in the lungs that can trigger biofilm formation. The polysaccharide matrix can also contribute to antibiotic resistance, since some antibiotics

cannot penetrate its structure and sub-inhibitory level of antibiotic can result and bacterial selection and resistance (48). Likewise, within the biofilm some cells are dormant escaping the mechanism of action of some antibiotics, e.g. penicillins (49). Moreover, the oxidative stress inside the biofilm structure results in numerous genetic mutations that are transferred horizontally between the cells and confers resistance to antibiotics (50) (51). The main mechanisms of antibiotic resistance in biofilms are described in **figure 6.**

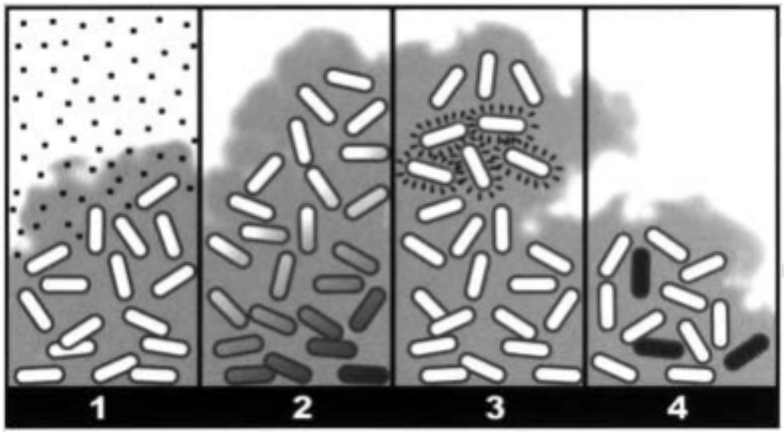

Figure 6: Four hypothesized biofilm resistance mechanisms. 1) The antibiotic (squares) penetrates slowly or incompletely; 2) A concentration gradient of a metabolic substrate or product leads to zones of slow or non-growing bacteria (shaded cells); 3) An adaptive stress response is expressed by some of the cells (marked cells); 4) A small fraction of the cells differentiate into a highly protected persister state (dark cells).Taken from reference (52)

1.3. Nanotechnology for pulmonary drug delivery

1.3.1. Nanocarriers for drug delivery in the lungs

As discussed before, controlled-release formulations are important tools for drug delivery in the lungs since they may increase and sustain local drug concentrations which contribute to decrease dose frequency and systemic toxicity and result in better patient compliance and augmented treatment efficiency.

A number of nanocarriers have been developed for drug release in the lungs; therefore we have selected the most well-known classes and described their main characteristics in **table V**.

Table V: Properties of the main nanocarriers produced for drug delivery to the lungs

Carrier properties	Liposomes	Polymeric Nanoparticles	Solid-Lipid nanoparticles	References
Incorporate both hydrophilic and hydrophobic drugs.	+	±	+	(53, 54)
Release drug over time.	±	+	±	(53, 55)
Reduce dose frequency.	+	+	+	(22, 55-58)
Maintain their integrity after nebulization.	±	+	+	(54, 55, 59-64)
Penetrate biofilms.	+	+	-	(38, 58, 64-66)
Penetrate the mucus.	-	+	-	(38, 63, 67, 68)
Stability during storage.	-	+	+	(53, 54, 63, 64)

The structural configuration of nanocarriers described in **table V** is displayed in **figure 7.**

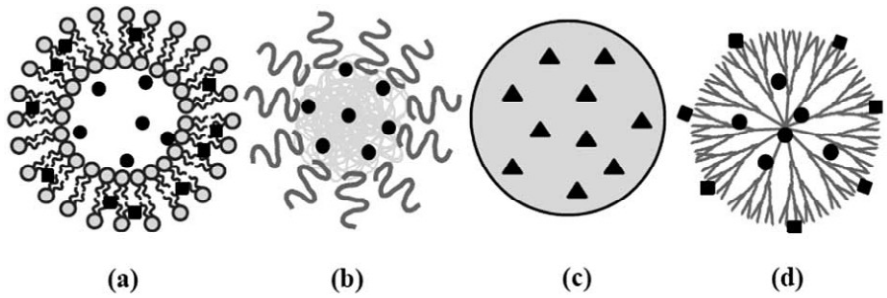

Figure 7: Schematic illustration of four nanoparticle platforms for antimicrobial drug delivery: (a) liposome, (b) polymeric nanoparticle, (c) solid lipid nanoparticle, and (d) dendrimer. Black circles represent hydrophobic drugs; black squares represent hydrophilic drugs; and black triangles represent either hydrophobic or hydrophilic drugs. **Taken from reference (53)**

Liposomes are formed by phospholipid dispersion in water solution that after saturation can form micelles able to entrap the drug added to this system. Liposomes are also the most investigated system for antibiotic controlled pulmonary delivery, since they may be prepared with phospholipids endogenous to the lungs. In addition, their lipid bilayer structure mimics the cell membrane and can fuse with infectious microbes to deliver high drug cargos into the cytoplasm, saturating their drug efflux pumps, therefore overcoming bacterial resistance (69, 70). Moreover, Meers *et al* have suggested that amikacin-loaded liposomes can also penetrate biofilms and infected mucus (38). Although studies have showed that liposomes positively charged can penetrate biofilms, positive charge appears to lead to more surface adsorption of liposomes at the expense of further penetration. In this respect, Meers *et al* hypothesized that the neutral or zwitterionic lipids used to prepare the amikacin-bearing liposomes in their study preclude strong ionic interactions and may help to enhance the penetration. Indeed, in this same study, inhaled liposomal amikacin formulation exhibited slow sustained released in normal rat lungs and was more efficacious than inhaled free amikacin in lungs infected by P. aeruginosas (38). However, liposomes are unstable during storage in the liquid and fragile carriers that can be physically destroyed in the nebulization process. Moreover, adjusting the drug release profile is a challenge if compared with other carriers such as nanoparticles. For instance, tobramycin liposome formulation showed increased both drug retention in the lung and antimicrobial activity compared with classical formulation. However, long-term efficacy could not be demonstrated by this formulation (22).

Dendrimers are defined as highly ordered and regularly branched globular macromolecules synthesized by stepwise iterative approaches. The structure of dendrimers consists of a core, layers of branched repeat units emerging from the core, and functional end groups on the outer layer of repeat units. Thus, hydrophobic drugs can be loaded inside the cavity core and the hydrophilic ones can be loaded in the outer layer through covalent conjugation or electrostatic interaction. Although some dendrimers exhibited sustained pulmonary drug release and antimicrobial activity itself (53, 56, 64), their activity was far from those of

commercialized drugs. In addition their synthesis and purification are time consuming, expensive and cumbersome, facts that justify the choice of other nanocarriers.

Solid lipid nanoparticles are carriers formed by solid lipids such as triglycerides, partial glycerides, fatty acids, steroids and waxes and they are able to encapsulate hydrophobic or hydrophilic drugs (66). However, they have not yet been fully exploited for pulmonary lung delivery. In addition, they can exhibit some drawbacks such as low drug loading and unpredictable drug release (58).

Conversely, polymeric nanoparticles (NP) are easier to formulate in order to reach pulmonary sustained release and its use for antimicrobial drug delivery has been extensively investigated, since this carriers offer several advantages. For instance, polymeric NP exhibit structural stability in biological fluids and under harsh and various conditions for formulation (such as spray drying, nebulization) and storage. In addition, by manipulating the formulation composition such as polymer chain lengths and concentration, surfactants and organic solvents, it is possible to tune polymeric NP properties such as size, charge, drug loading and drug release profiles. Furthermore, polymeric NP offer the possibility for insertion of chemical groups on its surface to improve mucus penetration and bacterial targeting, as will be discussed later.

1.3.2. Polymeric nanoparticles

A number of synthetic and natural polymers have been used for the synthesis of nanoparticles. However, synthetic polymers can be engineered to reach increased sustained release as compared with natural polymers such as albumin, gelatin, alginate, collagen, cyclodextrins and chitosan (71). Likewise, examples of synthetic polymers used for pulmonary applications include poly(lactic acid) (PLA), poly(glycolic acid)(PGA), poly(lactide-co-glycolide) (PLGA) and poly(ε-carprolactone) (PCL) (72). In addition, these polymers are considered non-toxic since they undergo hydrolysis upon implantation into the body, degrading into biologically compatible moieties (lactic acid and glycolic acid) which are

cleared from the body by the citric acid cycle. Therefore, degradation products are formed slowly assuring sustained release and do not affect normal cell function. Indeed, the polyesters PLA and PLGA are the most extensively investigated polymers for drug delivery (64). They have an hydrophobic core, therefore grafting of hydrophilic motifs such as poly(ethylene glycol) (PEG) on both polymer backbone have been studied (73, 74). The purposes for the PEG copolymerization are: 1) to facilitate the encapsulation of hydrophilic drugs, 2) to increase the resident time in the body, since hydrophobic particles are readily cleared by the mononuclear phagocytic system (MPS); 3) to modulate mucus adhesiveness in order to achieve mucus penetrating particles (64).

1.3.3. Engineered polymeric nanoparticles for drug delivery in the lungs

1.3.3.1. Mucus penetration particles

Although the proposal to develop an aerosolized sustained antibiotic release formulation for lung administration has the goal of achieving higher antibiotic levels in the lungs, the minimal inhibitory concentration (MIC) cannot be attained if the carrier does not diffuse in the mucus to target the bacteria. In fact, the build-up mucus acts as a physical, chemical and biological barrier to drug penetration, which also contributes to bacterial resistance to antibiotics. The mucus is composed mainly by mucins, but also contains DNA, lipids, ions, proteins, cells, cellular debris, and water (75). However, dysfunctions in the CFTR alter the mucus composition and generate increased viscosity which impairs the diffusion of drugs and carriers. Indeed, up to date no gene vector has been shown to penetrate the mucus in order to reach the epithelial cells, fact which explains the failure of clinical trials of gene therapy for cystic fibrosis (76). Therefore, our goal is to produce mucus inert polymeric nanoparticles as an antibiotic carrier able to penetrate the mucus.

Studies have elucidated the interaction between mucus structure and nanoparticle surface coating, in order to decrease NP retention in the mucus, therefore improving nanoparticle

diffusion (77). In addition to hydrophilic sites with negative charges imparted by the presence of carboxyl or sulfate groups on the mucin proteoglycans, the mucus also exhibit hydrophobic regions along mucin strands, stabilized by multiple internal disulfide bonds. These findings explain why the diffusion of both hydrophobic and cationic drugs such as tobramycin can be hindered in the mucus (78). However, the mucus is not impenetrable, as some viruses such as the human papilloma virus (HPV) can traverse it. In fact, a closer study of the HPV structure revealed that they are densely coated with both positively and negatively charged groups, leading to a densely charged yet net neutral surface. Based on these findings, Hanes and co-workers (67) rationalized that mucus penetrating particles must possess a high density on the hydrophilic surface able to minimize hydrophobic entrapment of mucus and be small enough to preclude significant steric inhibition by the dense fiber mesh, since the mucus structure contains multiple pores. Finally, the PEG properties such as being strongly hydrophilic and having a neutral charge make it an appropriate nanoparticle coating. However, as studies have also evidenced mucoadhesiveness properties of PEG, the rationale was to use a PEG molecule with controlled molecular weight. Thus, Hanes *et al* (67) hypothesized that the PEG molecular weight must be low enough to prevent adhesion via polymer interpenetration in the mucus (hydroplilic interactions). In addition, PEG density must be sufficient to effectively shield the hydrophobic core common to many biodegradable polymers resulting in decreased hydrophobic interactions between polymeric nanocarriers and mucus (67) (**figure 8**).

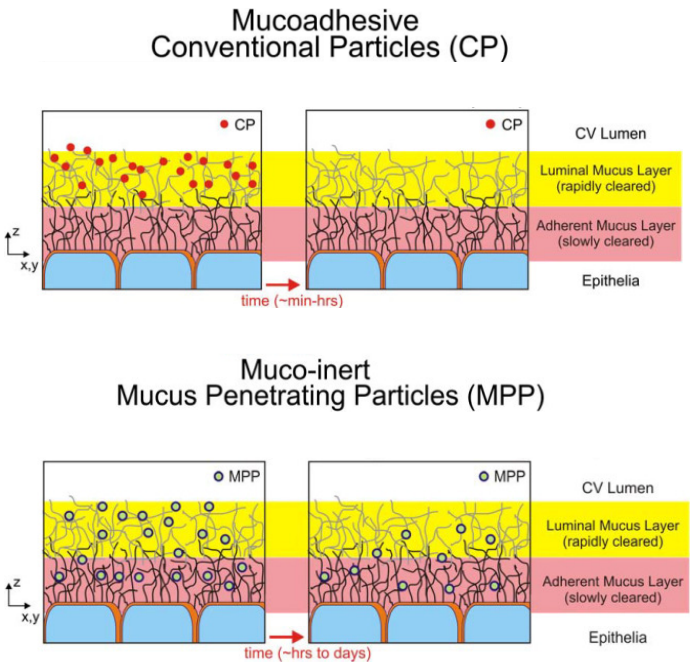

Figure 8: Summary schematic illustrating the fate of mucus-penetrating particles (MPP) and conventional mucoadhesive particles (CP) administered to a mucosal surface. MPP readily penetrate the luminal mucus layer (LML) and enter the underlying adherent mucus layer (AML). In contrast, CP are largely immobilized in the LML. Because MPP can enter the AML and thus are in closer proximity to the cells, cells will be exposed to a greater dose of drug released from MPP compared to drug released from CP. As the LML layer is cleared, CP are removed along with the LML whereas MPP in the AML are retained, leading to prolonged residence time for MPP at the mucosal surface. In the respiratory airways, CP are mostly immobilized in the luminal stirred mucus gel layer, whereas MPP penetrate the mucus gel and enter the underlying periciliary layer. Upon mucociliary clearance, a significant fraction of MPP remains in the periciliary layer, resulting in prolonged retention. Taken from reference (67).

1.3.3.2. Nanoparticles size and charge

Therefore, in order to prove the MPP theory, the nanoparticle diffusion in the mucus was evaluated by Hanes *et al* (77) as a function of PEG coating and nanoparticle size. Polystyrene particles as large as 200 nm in diameter that were densely coated with low molecular weight (2 KDa) polyethylene glycol (PEG) moved through undiluted CF sputum with average speeds up to 90-fold faster than similarly-sized uncoated polystyrene particles. Conversely, the transport of both coated and uncoated 500 nm particles was strongly hindered (77). These nanoparticles exhibited almost neutral surface (zeta potential higher than -10 mV) demonstrating that size (≤ 200 nm) and superficial charge (neutral) may also influence in the transport of nanoparticles in the mucus. Finally, this experiment proved that nanoparticles

with correct size, PEG coating and charge may overcome the mucus barrier for the transport of nanocarriers.

1.3.4. PEG-g-PLA nanoparticles as a model vector for pulmonary administration

The synthesis and characterization of PEG-g-PLA polymer have been previously proposed by our group of research (74). Briefly, PEG is grafted in the PLA backbone to form an amphiphilic polymer. When the outer phase in the emulsification process for nanoparticle production is water, this polymer can form nanospheres which are comprised by a hydrophobic core mainly composed of PLA and a hydrophilic surface composed of PEG coating (**figure 9**). In polymeric nanocapsules, a polymeric membrane forms a shell with an inner space loaded with the drug which are solubilized in aqueous or oily solvents. In contrast, nanospheres are solid nanoparticles with the drug homogeneously distributed in the polymeric matrices of variable porosity, as expected with PEG-g-PLA nanoparticles (79).

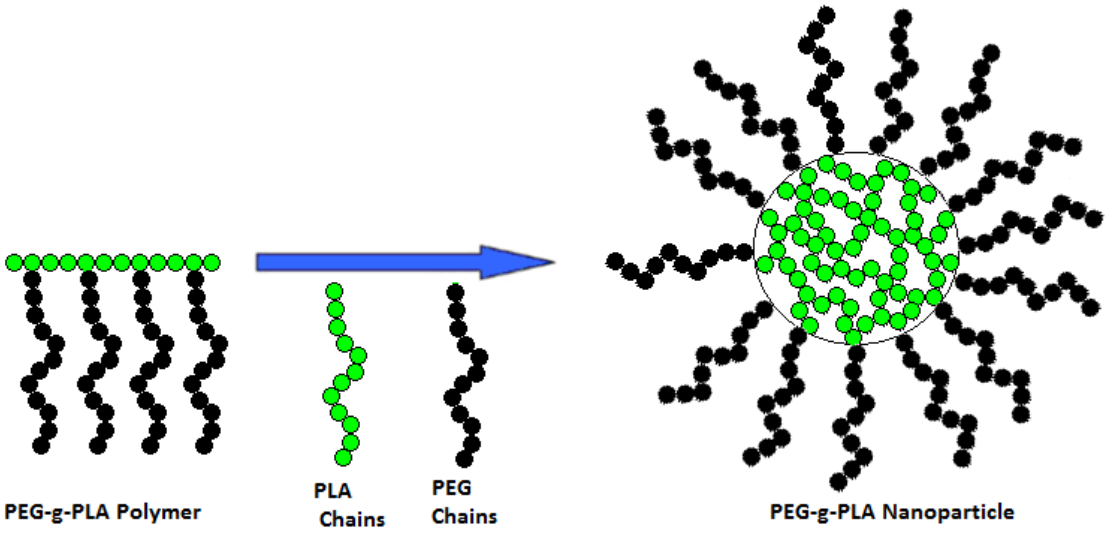

Figure 9: Scheme to represent the structure of PEG-g-PLA nanoparticles. Taken from reference (79).

The copolymer of PEG and PLA is amphiphilic (have an hydrophobic and an hydrophilic portion in the same polymer unit), fact which favors the encapsulation of hydrophilic and hydrophobic drugs (54). Hammady and co-workers have already reached the co-encapsulation of paclitaxel (a hydrophobic drug with a Log P value of 3.96 and water solubility of less than 0.01 mg/mL) (80) and endotelin (a hydrophilic drug with solubility of 1 mg/mL) for the anti-angiogenic treatment of diseases related with an angiogenic component (e.g. solid tumors, arthritis, psoriasis, diabetic retinopathy and atherosclerosis) (81). The majority of the antibiotics available for the CF treatment are hydrophilic; therefore, we believe that PEG-g-PLA might be an appropriate polymer to produce a pulmonary carrier for the CF treatment.

The antimicrobial activity of PEG-g-PLA nanoparticles formulations have also been investigated, as compared with the free drug. Two different copolymers of PLA and PEG were studied by Essa *et al*; branched PEGylated polymer in which PEG was grafted on PLA back bone (PEG-g-PLA) and multiblock copolymer of PLA and PEG, (PLA–PEG–PLA) (57). In addition, PLA nanoparticles were also analyzed. Itraconazole (ITZ) loaded nanoparticles were produced with the cited polymers and their *in vitro* antifungal activity was evaluated against both Candida and Aspergillus species. All ITZ-NPs were nearly spherical with smooth surface with a size range of 185–285 nm and zeta potential measured values were close to neutrality. In addition, ITZ release showed an initial burst followed by a gradual release profile: over 5 days for PEG-g-PLA and over 2 days for PLA-PEG-PLA nanoparticles. Most importantly, ITZ-loaded PEG-g-PLA nanoparticles inhibited fungal growth more efficiently in specific fungus strains (*Candida*) than either free ITZ or ITZ-loaded PLA nanoparticles suggesting that PEG-g-PLA–ITZ could be used efficiently as a nanocarrier to enhance antifungal efficacy (82).

Likewise, studies carried out by our group revealed that PEG-g-PLA loaded voriconazole nanoparticle formulation significantly improved the *in vitro* antifungal activity against *Candida ssp* (MIC of free voriconazole = 2.917 ± 0.137 $mg.L^{-1}$, n=3 and MIC of voriconazole-

loaded-PEG-g-PLA nanoparticles = 0.094 ± 0.01 mg.L^{-1}, n=3). However, just a slightly improvement was found in the same test against *Candida ssp* biofilms (45).

1.3.5. Recent drug carriers and other formulations under development

The new therapies under development for the treatment of cystic fibrosis are described in **table VI**.

Table VI: Recent formulations under development for CF treatment.

Drug	Nanocarrier	Administration	Development
Amikacin – Aricace ®, Insmed Incorporation	Liposomes	Powder for Inhalation	Phase III study (83)
Ciprofloxacin, Aradigm Corporation	Liposomes	Solution for nebulization	Phase II study (84)
Ciprofloxacin Pulmosphere, Bayer Schering Pharma	Free drug	Powder for inhalation.	Phase II study (85)
Fosfomycin/tobramycin (Gilead)	Free drug	Solution for nebulization	Phase II study (86)
Levofloxacin solution for inhalation (Mpex Pharmaceuticals)	Free drug	Solution for nebulization	Phase III (87) (88)

The most innovative formulas under development are the amikacin and ciprofloxacin liposomal formulations, since the use of a nanocarrier may enable sustained drug release (providing decreased side effects and reduced frequency of drug administration). In addition, nanocarries may enable mucus penetration thus preventing sub-inhibitory level of antibiotics and resulting in decreased bacterial resistance and biofilm formation. These benefits provided by nanocarriers may increase the efficacy of the antimicrobial formulation against the targeting bacteria; thereby improving the treatment of CF. However the other formulations improve the treatment by providing pulmonary administration as compared to oral or intravenous administration.

CHAPTER 2:

Hypothesis and objectives

2.1. Hypothesis

Based on the given facts, our hypothesis is that antibiotic-loaded PEG-g-PLA nanoparticles may improve the efficiency of the treatment against *Pseudomonas aeruginosa* in the lungs of CF patients, as compared with the free drug. The drugs chosen as models are colistin sulfate, tobramycin and levofloxacin, as an attempt to test three different classes of antibiotics extensively used for the treatment of CF.

We predict that PEG-g-PLA engineered nanoparticles may improve the treatment against *Pseudomonas aeruginosa* in Cystic Fibrosis patients based on the following concepts:

1) Engineered PEG-g-PLA nanoparticles with suitable size and charge are potentially mucus penetrating and might increase the targeting of mucus embedded *Pseudomonas aeruginosa*;

2) PEG-g-PLA nanoparticles might provide extended release of the encapsulated drug therefore increasing the exposure of *Pseudomonas aeruginosa* to therapeutic doses of drug and reducing bacterial resistance

3) PEG-g-PLA nanoparticles have the potential to circumvent bacterial resistance if the main mechanism of resistance presented by the strains under analysis is drug efflux (as in the case of *P. aeruginosa*), as have been showed in a precious research carried in our laboratory in *Candida ssp*. and *Aspergillus fumigatus* strains (45).

2.2. Objectives

Our main goal is to develop poly(ethylene glycol)-g-poly(lactic acid) (PEG-g-PLA) antibiotic-loaded nanoparticles with suitable physicochemical properties for antibiotic delivery in the lungs in order to increase the antimicrobial efficiency against *Pseudomonas aeruginosa*. In addition, PEG-g-PLA nanoparticles will be engineered to be mucus inert hence favoring

bacterial targeting through improved mucus penetration, as have been earlier discussed in the item 3.3.1.

The overall goal is to produce a solution for nebulization with the potential to be further incorporated to a solid vehicle to produce a powder for inhalation. The pulmonary administration of an antibiotic aerosolized sustained release formulation may result in higher efficiency of treatment and decreased induction of bacterial resistance, as compared with the free drug administration by systemic routes (as discussed in the item 1.2.5.2).

We will essay the encapsulation of tobramycin, colistin sulfate and levofloxacin into PEG-g-PLA nanoparticles, in order to develop new sustained release formulations. Studies showed that after pulmonary administration, levofloxacin reached high sputum and low serum concentrations (89). Additionally, higher reduction of *P. aeruginosa* in sputum and improvements in lung function was reached with inhalation if compared with oral intravenous administrations. Moreover, levofloxacin appears to be more potent against *P. aeruginosa* biofilms than aminoglycosides and aztreonam (89). Thus, a high and sustained level of levofloxacin achievable in the lungs following aerosol delivery of levofloxacin-loaded PEG-g-PLA nanoparticles suspension might be useful for the management of pulmonary infections caused by P. aeruginosa in CF patients. In addition, the development of PEG-g-PLA nanoparticles formulations to encapsulate other drugs such as colistin and tobramycin may also be encouraged, therefore targeting different mechanisms of antibiotic action. In fact, *Pseudomonas aeruginosa* has a diversified profile of resistance against many antibiotics resulting in an increasing demand of innovative formulations for the treatment of CF.

In addition, as liposomes have been thoroughly studied and some successful formulations for the treatment of cystic fibrosis are under phase III clinical studies (83, 84), we will also synthesize and characterize an antibiotic-loaded liposomes formulation (as a positive control) and compare their efficiency to kill *Pseudomonas aeruginosa in vitro*, as compared with antibiotic loaded nanoparticles. We hypothesize that nanoparticles will present the same or increased activity against *P. aeruginosa* when compared to liposomes.

Thus, the specific objectives at this work are: 1) Synthesize and characterize PEG-g-PLA and PLA-OH polymers; 2) Synthesize and characterize tobramycin, colistin sulfate and levofloxacin loaded nanoparticles and select the nanoparticle formulation with the highest loading efficiency to be further evaluated in microbiological testing; 3) Prepare and characterize antibiotic loaded liposomes (same drug as the optimized nanoparticle formulation); 4) Evaluate the antibacterial efficiency of antibiotic loaded nanoparticles and liposomes as compared to the free drug, through the microbiological susceptibility test in the biofilm and planktonic forms of *Pseudomonas aeruginosa.*

The description of each step of research for the completion of the specific objectives and the respective tests for the characterization of the final products are detailed in **table VII**.

Table VII: Plan of work.

Specific Objective	Steps	Characterization
I. Synthesis and characterization of PLA-OH and PEG-g-PLA polymer	Synthesis and characterization of polymers.	Polymer structure: ^{1}H NMR Polymer Mw, Mn, PDI: GPC
II. Synthesis and characterization of antibiotic loaded nanocarriers[a].	Development of quantitative method to dose the antibiotics.	Quantitative method: HPLC HPLC characterization: LOQ, LOD, R^2.
	Synthesis and characterization of polymeric nanoparticles.	Size and PDI: DLS Charge: Zeta Potential. Drug loading : HPLC Liposomes lipid concentration: Bartlett Assay
	Synthesis and characterization of liposomes.	
III. Assessment of free antibiotic versus antibiotic loaded nanocarriers[(a)] efficiency in eradicating planktonic and biofilm forms of PA in antimicrobial susceptibility testing.	Validation of microbiological susceptibility tests with free antibiotic against PA.	Broth Microdilution Test (plaktonic form of PA). Broth Microdilution Test with the Calgary Biofilm Device (biofilm form of PA).
	Test the free antibiotic, antibiotic loaded and blank nanocarriers[(a)] against the planktonic form of PA.	Determine the MIC of free antibiotic as compared to antibiotic loaded nanocarriers[(a)] to eradicate planktonic PA.
	Test the free antibiotic, antibiotic loaded and blank nanocarriers[(a)] against the biofilm form of PA.	Determine the MBIC of free antibiotic as compared to antibiotic loaded nanocarriers[(a)] to eradicate biofilm of PA.

[a]Nanocarriers: polymeric nanoparticles and liposomes; PEG: polyethylene glycol; PLA: polylactic acid. NP: nanoparticles; PA*: Pseudomonas aeruginosa*; ^{1}H NMR: Proton Nuclear Magnetic Resonance; PDI: Polydispersity index; GPC: Gel Permeation Chromatography; Mw: weight average molecular weight; Mn: number average molecular weight; LOQ: limit of quantification; LOD: limit of detection; R^2: correlation coefficient (statistics); DLS: Dynamic Light Scattering; HPLC: High Performance Liquid Chromatography; MIC: Minimal Inhibitory Concentration; MBIC: Minimal Biofilm Inhibitory Concentration.

CHAPTER 3

Experimental

3.1. Synthesis and characterization of PLA-OH and PEG-g-PLA polymers

i. Materials

3,6-Dimethyl-1,4-dioxane-2,5-dione (dilactide), Benzyl glycidyl ether 99%,Tin(II)-2-ethylhexanoate 99%, Palladium 5 wt. % activated charcoal, Thionyl Chloride ≥99.0%, 4-(Dimethylamino) pyridine ≥99% (DMAP), Pyridine anhydrous, 99.8% , Mineral oil, gas hydrogen, Celite® Standard Super-Cel®NF acid washed, chloroform, dichloromethane (DCM), ethyl acetate, hexane, tetrahydrofuran (THF), dimethyl sulfoxide-*d*6 99.9 atom % D (DMSO-*d6*), chloroform-*d* were purchased by Sigma-Aldrich (Oakville, ON, Canada). Spectra/Por® molecularporus membrane tubing MWCO 6-8000 was supplied by Spectrum Laboratories Inc. (Rancho Dominguez, CA, USA). Carboxylmethoxy PEG-2000 (PEG-COOH) was previously synthesized as reported in literature (74) and kindly provided by Pr. Hildgen (Université de Montréal, QC, Canada).

ii. Methodology

3.1.1. Synthesis of PLA-OH and PEG-g-PLA

3.1.1.1. Synthesis of PLA-BGE

The polymer poly(ethylene glycol)-g-poly(lactic acid) (PEG-g-PLA) was synthesized following the methodology described in Hildgen's previous publication, with some modifications (74). Firstly, PLA was synthesized by the co-polymerization of benzyl glycidyl ether and dilactide under argon atmosphere. Briefly, 15 g (0.104 mol) of dilactide previously dried under vacuum was mixed with benzyl glycidyl ether (BGE) (4.16×10^{-3} mol, 0.635 mL) and Tin (II)-2-ethylhexanoate as a catalyst (4.16×10^{-5}mol, 0.0135 mL). Then, bulk polymerization was carried at 165 ◦C for 15 h. The resulting polymer (PLA-BGE) was purified twice by

precipitation in 200 mL of hexane of the crude dissolved in 100 mL of DCM. The residue of DCM was removed by evaporation under reduced pressure (Buchi 461 water bath, BÜCHI Labortechnik AG, Flawil, Switzerland) and dried under vacuum for two days. The yield obtained was 89.5 % (14.03 g of PLA-BGE). Sample of 15 mg was removed for ^{1}H NMR analysis which data is found in results session, **figure 11**.

3.1.2. Synthesis of PLA-OH

Afterwards, purified PLA-BGE (13 g) was dissolved in 200 mL of ethyl acetate and the benzyl group was removed by hydrogenation using bubbling H_2 in the presence of palladium activated charcoal (2g) for 20 hours in mineral oil bath at 45◦C. According to ^{1}H NMR analysis **(figure 11)**, the BGE: PLA ratio obtained in the resulting PLA-BGE polymer was 1%. Thus, 13 g of PLA-BGE-(1%) is composed of lactide (12.71 g, 0.176 mol) and BGE (0.29 g, 1.76 X 10^{-3} mol). For the hydrogenation, the ratio of 1 g of Pt to reduce 1mM of benzyl group was applied (minimal Pt quantity equals to 1.76 g). Therefore, palladium was added in excess to assure complete removal of benzyl groups.

Palladium was removed by filtration on 8 g of Celite® washed with ethyl acetate. Ethyl acetate was removed by evaporation under reduced pressure. Purification and drying of the resulting polymer PLA-OH was done similarly as PLA-BGE. It was obtained 4.9 g of PLA-OH (yield= 38.2%) and sample of 15 mg was withdrawn for ^{1}H NMR analysis which data is found in **figure 12**.

For the pegylation, firstly PEG-COOH (1.5 g , 7.5 X 10^{-4} mol) was dissolved in 20 mL of chloroform and mixed with thionyl chloride ($SOCl_2$) (5 mL, 0.07 mol) in a round bottom flask under magnetic stirring for 2 hours, at room temperature. Chloroform was removed by evaporation under reduced pressure in a closed system which enabled the precipitation of $SOCl_2$ vapor in a trap with NaOH solution (2 N). The polymer was dried under vacuum overnight. Then, PEG-COCl (1.5 g, 7.5 X 10^{-4} mol) was dissolved in 40 mL of chloroform. To

this solution was added the previously synthesized PLA-OH (4.9 g, 0.382 mol and 6.60 X 10^{-4} mol of OH groups), anhydrous pyridine (3 mL), DMAP (20.1 mg, 1.65 X 10^{-4} mol) and the reaction was stirred under argon atmosphere and magnetic stirring overnight at room temperature. Subsequently, the reaction mixture was extracted three times with 400 mL of HCl solution 1N in order to remove non grafted PEG and excess of pyridine. The organic phase was collected and chloroform was removed by evaporation under reduced pressure. Purification was achieved by dissolving the PEG-*g*-PLA polymer in 20 mL of DCM and precipitating in 40 mL of hexane. After filtration, PEG-g-PLA was dissolved in 40 mL of THF and this polymer solution was dialyzed (MWCO 6-8000) against THF (400 mL) of THF for 24 hours (THF bath was replaced after 12 hours). This last purification step is aimed to remove non grafted PEG, given that it is also soluble in the organic solvents used before such as chloroform. After 24 hours, THF was removed by evaporation under reduced pressure and the purified PEG-g-PLA was dried under vacuum for two days. It was obtained 4.7 g of PEG-g-PLA polymer (yield of 75%). Samples were removed for ^{1}H NMR (15 mg) (**figure 13**) and Gel Permeation Chromatography (GPC) (2 mg) analysis.

3.1.3. Characterization of PLA-OH and PEG-*g*-PLA

The structural confirmation of both polymers was determined by ^{1}H NMR on the Brucker ARX 400MHz spectrometer (Bruker Biospin, Billerica, MA). Chemical shifts (δ) were measured in parts per million (ppm) using tetramethylsilane as an internal reference. 15 mg of PLA-BGE and PEG-g-PLA was dissolved in 0.8 mL of chloroform-*d* and 15 mg of PLA-OH was dissolved in 0.8 mL of DMSO-d*6*. In addition, to check the polymerization process, Mn, Mw and PDI of each polymer (2 mg/mL in THF) was assessed by Gel Permeation Chromatography (GPC) in a Waters Associate chromatography system (Waters, Milford, MA) equipped with a refractive index detector and a Phenomenex Phenogel of 5 µm column. Polystyrene standards were used for calibration with THF as the mobile phase at a flow rate of 1 mL/min.

iii. Results and discussion

The synthesis of PEG-g-PLA-2 was realized in three steps: 1) Co- polymerization of PLA and BGE to result in PLA-BGE; 2) Deprotection of PLA-BGE to result the PLA-OH; 3) PEG grafting to result in the polymer PEG-g-PLA.

The scheme for the synthesis of PEG-g-PLA-2 is showed in **figure 10** and the ^{1}H NMR data for the characterization of each sub-product is showed in **figures 11**, **12** and **13**.

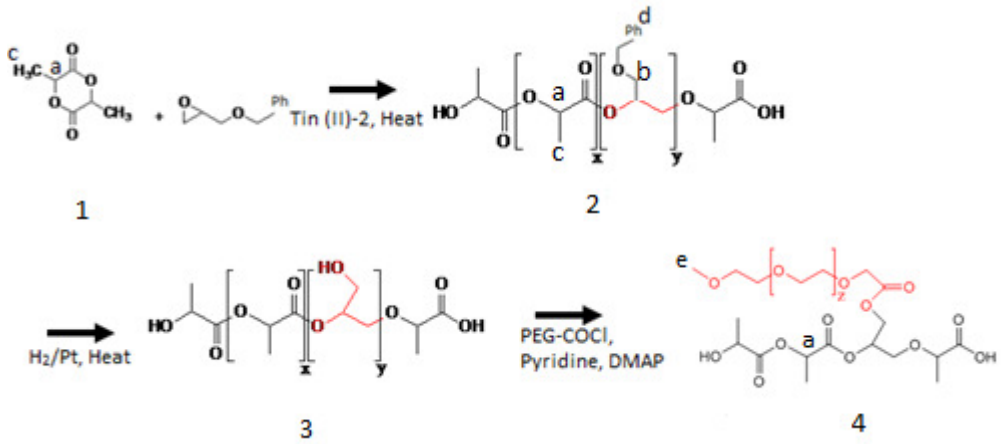

Figure 10: Synthesis and ^{1}H NMR characterization of PLA-BGE, PLA-OH and PEG-g-PLA.^{1} H

NMR analyses were performed to confirm the chemical structures of the polymers 2, 3 and 4.

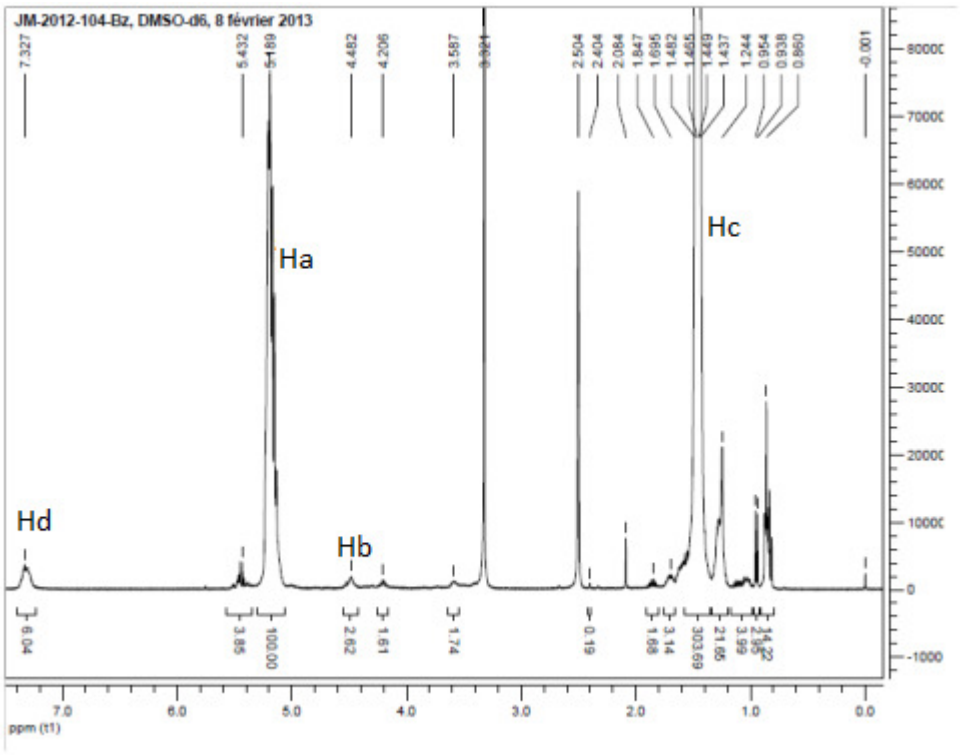

Figure 11: ^{1}H NMR spectra of PLA-BGE

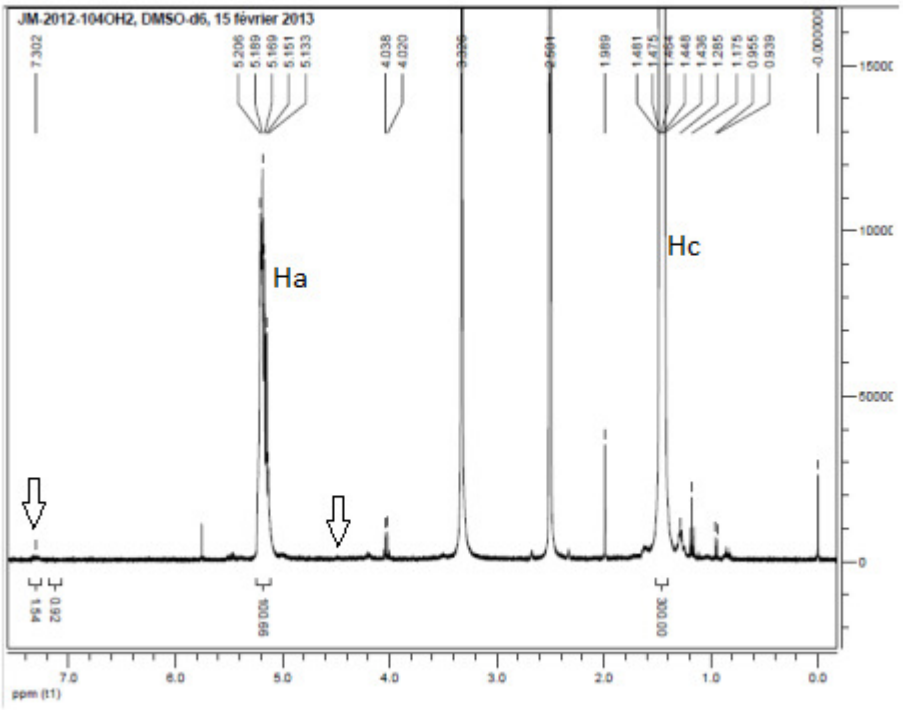

Figure 12: ^{1}H NMR spectra of PLA-OH

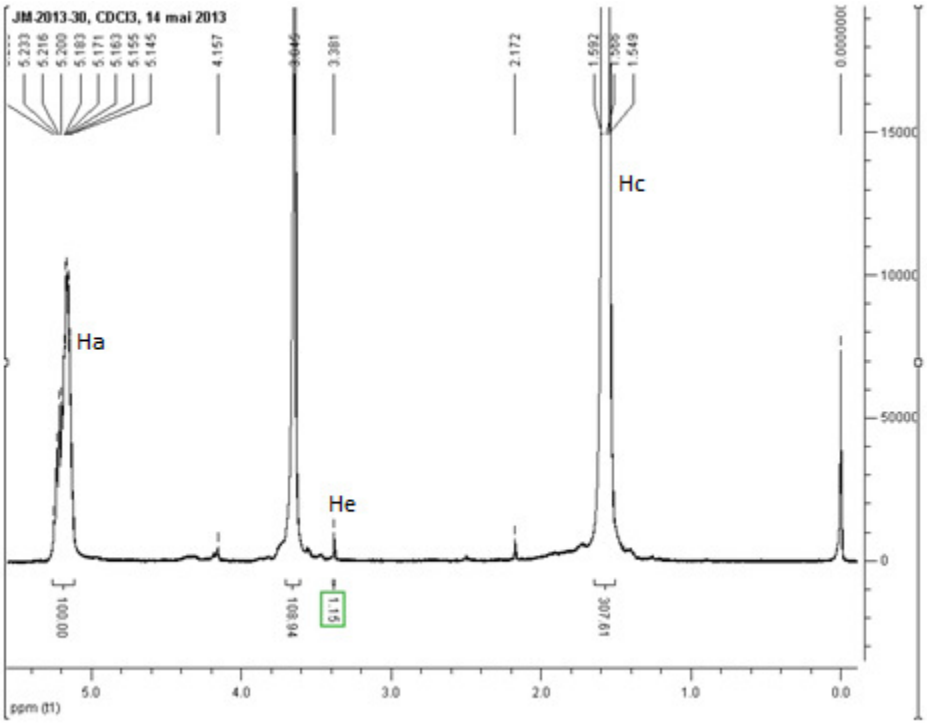

Figure 13: ^{1}H NMR spectra of PEG-g-PLA-2

The peak Hd at 7.3 ppm in **figure 11** refers to the 6 aromatic hydrogen groups from the PLA-BGE (marked with the letter d in the **figure 10**) and confirms that the benzyl glycidyl ether was co-polymerized with the PLA. Each peak of this spectrum was integrated and compared with the CH peak from the lactide at 5.1 ppm (Ha) in which was attributed the value of 100% to simplify the calculation. As each lactide presents just one group CH (marked with the letter a in the **figure 10**), the integration of the benzyl groups at 7.3 ppm divided by six (since it corresponds to 6 hydrogen groups) gives the percentage of grafting of BGE to PLA which equals to 1.0 %. The same spectrum also displays the peak at 4.48 ppm which refers to the CH_2-benzyl group (marked with the letter b in the **figure 10**), also proving that the co-polymerization occurred. After hydrogenation the latter peak and the benzyl peak at 7.3 ppm did not appear in the **figure 12,** confirming that the hydrogenation reaction successfully removed all protecting groups of OH.

Figure 13 shows the ^{1}H NMR data for the PEG-g-PLA-2, and the peak at 1.45 ppm (Hc) corresponds to the CH_3 group from the lactide (marked with the letter c in the **figure 10**). However, the ratio of PEG:PLA was calculated by comparing the CH peak of the lactide group at 5.2 ppm (100%) (marked with the letter a in the **figure 10**) with the CH_3 final group of the metoxy PEG-2000 at 3.38 ppm (marked with the letter e in the **figure 10**). As the CH_3 from PEG has three hydrogen groups, the value of its integration was divided by 3 to give the real grafting of PEG which equals to 0.4% (1.15%/3 = 0.4%).

Table VIII shows the ^{1}H NMR data and the results for the GPC analysis for both polymers which confirms that the intended syntheses were accomplished.

Table VIII: Polymers' batches characterization.

Polymer	Intended grafting (%)	Real grafting[a]	Mn[b]	Mw[b]	Mw/Mn[b]
PEG-g-PLA-1[c]	0.5	0.48	16223	31560	1.9
PLA-OH[d]	2.0	1.0	25250	37385	1.5
PEG-g-PLA-2[d]	1.0	0.4	29540	38400	1.3

[a]Calculated from peak intensity ratios of PEG at 3.38 ppm in PEG-g-PLA or benzyl at 7.3 ppm in PLA-BGE in relation to PLA at 5.2 ppm from ^{1}H NMR data.
[b]Determined by GPC analysis using narrow molecular weight polystyrene standards. Mw/Mn= polydispersity index of polymers (PDI).
[c]PEG-g-PLA-1 was provided by Patrice Hildgen's laboratory.[d]PLA-OH and PEG-g-PLA-2 were synthesized during this study.

The PEG-g-PLA-1 was previously synthesized by Hildgen's group and the batch PEG-g-PLA-2 was synthesized and characterized during this study, with PLA-OH as an intermediate product. According to the ^{1}H NMR analysis data displayed in **table XVIII**, the accomplished PEG grafting ratio for PEG-g-PLA-2 was 0.4%. The possible explanation for the low ratio PEG: PLA obtained was that the quantity of PEG-COOH added was not in default as compared to the PLA-OH quantity. However, as the molecular weight of PEG is high, even the apparent low value of 0.4% can make a difference in the polymer structure adding more hydrophilicity to the polymer as aimed, and it is close to batch 1, so good for comparison.

The GPC analysis provides two ways to express the molecular weight: the number molecular weight (Mn) and the weight molecular weight (Mw) and both shows that the polymerization successfully occurred and were similar from batch to batch (1 versus 2). The parameter (Mw/Mn) designed polydispersity index represents the variation of molecular weight within a given population of molecules, and when it is under 0.22 the polymer population can be considered as monodisperse. As showed in **table VIII**, we obtained a polydispersity index value of 1.9 for PEG-g-PLA and 1.5 for PLA-OH demonstrating a polydisperse population. Indeed, wider dispersion in the molecular weight was obtained for PEG-g-PLA, but it might not impair the nanoparticle formulation, since polymeric chains with different sizes can easily intercalate to form the nanoparticles.

In conclusion, 2 reproducible batches of PEG-g-PLA were obtained ready for the nanoparticle formulation. The batch of PLA-OH will be used in nanoparticle formulations to modify the PLA: PEG ratio and provide OH groups to the polymer, thereby potentially increasing hydrophilicity.

3.2. Synthesis and characterization of antibiotic loaded nanocarriers

3.2.1. Synthesis and characterization of tobramycin, colistin sulfate and levofloxacin nanoparticles

i. Materials

Tween 20, Span 80, Poly(ethylene glycol) monooleate (PEG-monooleate), Chloroform, Ethanol, Dichloromethane (DCM), Isopropanol, Acetonitrile HPLC grade, Trifluoroacetic acid (TFA), Phosphoric acid 85%, Triethylamine, Hydrochloric Acid, Sucrose 99%, Fluorescamine, Chitosan (Mw 60000-120000), Sodium Alginate, Pluronic F-126, Polyvinyl alcohol2000, 80% hydrolyzed (PVA) and Levofloxacin > 98% HPLC grade were purchased by Sigma-Aldrich (St. Louis, MO, USA). Tobramycin and Colistin Sulfate were purchased by AK Scientific (AK Scientific Inc., Union City, CA, USA), butyl Alcohol was purchased by Anachemia Science Canada Inc. (Lachine, QC, Canada) and Spectra/Por® molecularporus membrane tubing MWCO 6-8000 was purchased by Spectrum Laboratories Inc. (Rancho Dominguez, CA, USA).

ii. Methodology

3.2.2. Development of quantitative methods to dose antibiotics

3.2.2.1. Development of quantitative method to dose tobramycin

Tobramycin was analyzed by spectrometry of absorbance in the ultraviolet (UV) after prior derivation with fluorescamine (90). Briefly,0.1 mL of tobramycin standard solution and samples prepared in water were incubated with 0.1 mL of fluorescamine solution 0.5% (w/v) prepared in ethanol. The tobramycin standards for the calibration curve were prepared in the concentration of 32, 16, 8, 4, 2, 1 and 0.5 µg/mL. After one hour of incubation at room temperature, the absorbance was measured at 390 nm using the Microplate Reader Safire (Tecan Group Ltd., Männedorf, Switzerland), fitted out with a 96 well quartz plate.

3.2.2.2. Development of quantitative method to dose colistin sulfate

Colistin sulfate was quantified by High Performance Liquid Chromatography in the Shimadzu Prominence Ultra Fast Liquid Chromatogram equipped with Evaporative Light Scattering Detection (HPLC-ELSD) (91), since this drug does not present chromophores. All the parameters for the test are described in **table XI.**

Table IX: HPLC parameters used for the analysis of colistin sulfate

Column	C-18 Zorbax SB (5.0 X 150) mm
Flow rate	1 mL/min
Temperature	30ºC
Mobile Phase	A = Acetonitrile with Trifluoroacetic Acid (TFA) 37.5 mM B = Deonized water with TFA 37.5 mM
Gradient	From 10% A to 65% A in 6 min. Isocratic for 1 min. From 65% A to 10% A in 2 min.
Detection	ELSD. Temperature of vaporization: 60ºC. Pressure: 3.0 bar. Gain: 7.
Standards	Prepared in the mobile phase.
Retention time	6.6 and 6.9 minutes (corresponding to Colistin A and B, not necessarily in this order).

HPLC: High Performance Liquid Chromatography. ELSD: Evaporative Light Scattering Detector. min: minutes.

The plot log of mass (µg) versus log of area provided the calibration curve. The mass could be just for the most intense peak of for the sum of both peaks. The Limit of Quantification (LOQ) was calculated as LOD= 3.3 (SD/S) and the Limit of Detection (LOD) as LOD=10 (Sd/S) where SD is the standard deviation of Y and S is the slop of the curve.

3.2.2.3. Development of quantitative method to dose levofloxacin

Levofloxacin was quantified by High Performance Liquid Chromatography equipped with ultraviolet detection (HPLC-UV) in a Shimadzu Prominence Ultra Fast Liquid Chromatogram (92). All the parameters for the test are described in **table X.**

Table X: HPLC parameters used for the analysis of levofloxacin

Column	C- 18 Zorbax SB (5.0 X 150) mm
Flow rate	1 mL/min
Temperature	25ºC
Mobile Phase	A = Acetonitrile. B = Phosphoric acid 0.025 M adjusted to pH 3 with trietylamine
Isocratic	20% A and 80% B for 5 minutes.
Detection	UV = 294 nm
Standards	Prepared in the mobile phase.
Retention Time	1.7 minutes.

SB (stable bound). UV: ultra violet. nm:nanometers

The plot concentration (µg/mL) versus area provided the calibration curve. The Limit of Quantification (LOQ) was calculated as LOD= 3.3 (Sd/S) and the Limit of Detection (LOD) as LOD=10 (Sd/S) where Sd is the standard deviation of Y and S is the slop of the curve.

3.2.3. Organic solvent analysis for drug extraction from nanoparticles

A biphasic system with organic solvent/ water was used to extract the encapsulated hydrophilic drug from nanoparticles. Therefore, the aim of this study was to select the appropriate solvent for drug extraction from nanoparticles to ensure that the drug is not retained in the organic solvent. Thus, chloroform was analyzed for the extraction of colistin sulfate that is insoluble in chloroform. However, as levofloxacin is partially soluble in chloroform, its extraction was analyzed in chloroform, ethyl acetate and dichloromethane in order to select the best organic solvent. Briefly, drug standard (levofloxacin 10 µg/mL and colistin sulfate 200 µg/mL stock solutions were prepared in the aqueous mobile phase according to the HPLC method. Then, 1.2 mL of the drug stock solution was extracted by 2 mL of the selected organic solvent. The biphasic systems were vortexed for 1 minute and centrifuged at 2500 r.p.m for 5 min in the Centrifuge IEC Multi® / Multi RF TM (Thermo Fisher Scientific Inc.,Waltham, MA, USA). The aqueous supernatant was collected and analyzed by HPLC in triplicate. Blanks with mobile phase were also extracted in the organic

solvent and compared to the stock solutions and mobile phases without extraction. The recovery of drug in the water phase after extraction was calculated by comparing the drug peak intensity before and after extraction. Tobramycin is also insoluble in chloroform thus this solvent was selected for the extraction without previous solvent analysis.

3.2.4. Synthesis and characterization of nanoparticles

3.2.4.1. Synthesis of tobramycin, colistin sulfate and levofloxacin nanoparticles

Three methods were used for the synthesis of nanoparticles, as described in **table XI**.

Table XI: Applied methodologies for the production of tobramycin nanoparticles.

Method/ Drug	Phases	Reagents	Methodology
ESE- Double Emulsion (DE) w/o/w Tobramycin[a] Colistin Sulfate[b] Levofloxacin[b]	1- Internal water phase	Drug Distilled Water	Phases 1 and 2 were vortexed for 30 seconds. This first emulsion was mixed with phase 3 in the high pressure homogenizer Emulsiflex C30 (Avestin, Ontario, Canada) at 10000 psi for 4 min. NP suspension was collected and the organic solvent evaporated under reduced pressure for 3 hours. Then, NP suspension was centrifuged for one hour at 18500 r.p.m at 4˚C (Sorval® Evolution RC, Kendro, USA). The supernatant was discarded and the NP pellet collected and placed in the dialysis bag for 24 hours. After dialysis, the purified NP suspension was lyophilized (Freeze Dryer ModulyoD-115-230® (Thermo Fisher Scientific Inc., Waltham, MA, USA) to recuperate the powder of NP.
	2- Oil phase	Mixture of polymers[d] or only PEG-g-PLA Span 80 (0.4% w/v) N-butanol (16.6% w/v) Dichloromethane	
	3 External water phase	Water Tween 20 (2.5% w/v) PEG-oleate (0.5% w/v)	
Nano-precipitation (NPP) Tobramycin[a]	1- Internal water phase	Drug Water	First, the oil in water solution was prepared by mixing phases 1 and 2 under mixing. This emulsion was added to phase 3 under mixing, leading to immediate NP precipitation. Afterwards, residual organic solvents were extracted by evaporation under reduced pressure. NP were isolated by centrifugation at 6000 rcf for 1 hour at 4˚C (Sorval ® Evolution RC, Kendro, USA), dispersed in ultra pure water to a final volume of 5 mL, and dialyzed for 24 hours. Different helpers were added either in the internal e/or in the external water phases (see **table XI**).
	2- Oil phase	PEG-g-PLA 1% (w/v) Dichloromethane	
	3 - External water phase	Water/ethanol 50% (v/v)	
Nano-precipitation (NPP) Levofloxacin[b]	1 - Oil phase	Acetone Polymer Drug	Phase 1 was dropped into phase 2 under stirring to form the NP suspension. Acetone was removed under reduced pressure. Then, NP suspension was centrifuged for one hour at 18500 r.p.m at 4˚C (Sorval® Evollution RC, Kendro, USA). The supernatant was discarded and NP collected and dialyzed for 12 hours. Purified NP suspension was lyophilized in the Freeze Dryer ModulyoD-115-230® (Thermo Fisher Scientific Inc.,MA, USA) and collected as a powder.
	2- Water phase	Distilled water	
ESE- Single Emulsion (SE) (o/w) Levofloxacin[b]	1- Oil phase	Polymer, Organic solvent[c], Levo	Phase 1 was added to phase 2 in the high pressure homogenizer Emulsiflex C30 (Avestin, Ottawa, Ontario,Canada) at 10000 psi for 4 min. Then, it was processed as for the double emulsion.
	2- Water phase	Aqueous surfactant solution[e]	

ESE: Emulsification solvent evaporation.[a]Tobramycin NP was synthesized with PEG-g-PLA-1. [b]Colistin Sulfate and Levofloxacin NP were synthesized with PEG-g-PLA-2.[c] Organic solvents tested were DCM or the mixture DCM: DMF (1:1). [d]Mixture of polymers: PEG-g-PLA-2 and PLA-OH. [e]Surfactants used were PVA 0.5 % w/v or the mixture, Tween 20 (2.5 % w/v) and PEG-oleate (0.5% w/v). NP: nanoparticles. PVA: polyvinyl alcohol.

3.2.4.2. Characterization of nanoparticles

a. Nanoparticle size

After production, the nanoparticle size and the size distribution (the latter expressed by the PDI – polydispersity index) were measured at 25˚C and in triplicate (n=3) by Dynamic Light Scattering Dynamic Light Scattering (DLS) using the Zetasizer Nano ZS, Malvern (Malvern Instruments Ltd, Worcestershire,United Kingdom). Briefly, 0.1 mL of nanoparticles was diluted to 1 mL of ultra pure water.

b. Nanoparticle charge

Nanoparticle charge was measured at 25˚C and in triplicate (n=3) in the Zetasizer Nano ZS, Malvern (Malvern Instruments Ltd, Worcestershire,United Kingdom). Briefly, 0.1 mL of nanoparticle sample was diluted to 1 mL of sodium chloride solution 10 % w/v.

c. Drug content inside nanoparticles

Tobramycin, Colistin Sulfate and levofloxacin loaded nanoparticles were assessed to quantify the amount of encapsulated drug. Briefly, approximately 20 mg of nanoparticles were weighted and dissolved in 2 ml of chloroform under mixing for 1 minute. To extract the drug, 1.2 mL of ultra pure water or the respective mobile phase was added in the tobramycin and colistin sulfate/levofloxacin tubes respectively. Thus, after 1 minute under vortex a biphasic system was formed in each tube which contains the drug in the water phase. Afterwards, the biphasic system was centrifuged at 2500 r.p.m for 5 min in the Centrifuge IEC Multi® / Multi RF TM (Thermo Fisher Scientific Inc.,Waltham, MA, USA) and the aqueous supernatant was collected to be analyzed by absorbance (tobramycin nanoparticles) or by HPLC (colistin sulfate and levofloxacin nanoparticles). The encapsulation efficiency (EE) and the loading efficiency (LE), were applicable, were calculated as follows:

$$\mathrm{EE} = \frac{\text{total quantity of encapsulated drug (mg)}}{\text{initial quantity of drug (mg)}} \text{ x } 100$$

$$LE = \frac{\text{total quantity of encapsulated drug (mg)}}{[\text{initial quantity of drug (mg)} + \text{ initial quantity of polymer (mg)}]} \text{ X } 100$$

For the calculus of LE, the initial quantity of polymer was calculated as the total amount of polymer added in the formulation in mg, since we considered that the yield of the nanoparticle production was 100%. Thus, this calculus is accurate for the nanoparticles prepared by nanoprecipitation, since the nanoparticle suspension recovery after precipitation is 100%. However, for the single and double emulsion method a dead volume of nanoparticle suspension is lost inside the homogenizer Emulsiflex C30 (Avestin, Ontario, Canada). Therefore, the value of LE calculated for nanoparticles produced by single and double emulsion was estimated through this calculation.

iii. Results and discussion

3.3. Development of methodologies of analysis to quantify antibiotics

3.3.1. Development of quantitative method to dose tobramycin

Tobramycin belongs to the aminoglycoside antibiotic class, lacking chromophores for ultraviolet (UV) absorption or fluorescent groups. Thus, the derivation of tobramycin with fluorescamine enabled its spectrophotometric analysis by absorbance at 390 nm (92). The chemical structures of tobramycin and fluorescamine as well as the mechanism of the derivation reaction are represented in **figure 14**.

A- Scheme for the chemical reaction in which tobramycin is represented by R-NH_2. B: Tobramycin structure.

A

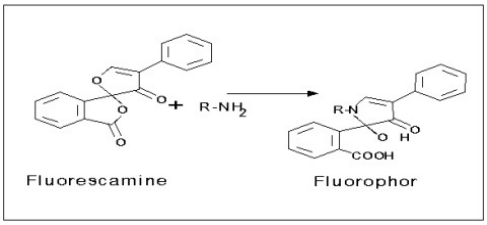

B

R-NH_2 =

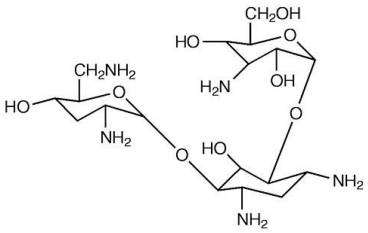

Figure 14: Derivation of tobramycin with fluorescamine for spectrophotometric analysis.

The limit of detection (LOD) and the limit of quantification (LOQ) found in this test were 0.5 and 10 µg/mL, respectively (n=3). The curve was linear between 0.5 to 64 µg/mL with the equation of y= 0.0245x - 0.0065 and R^2= 0.9999.

3.3.2. Development of quantitative method to dose colistin sulfate

Colistin is a cationic cyclic decapeptide linked to one of the two different fatty acid chain to form Colistin A or Colistin B (42) as showed in **figure 15**.

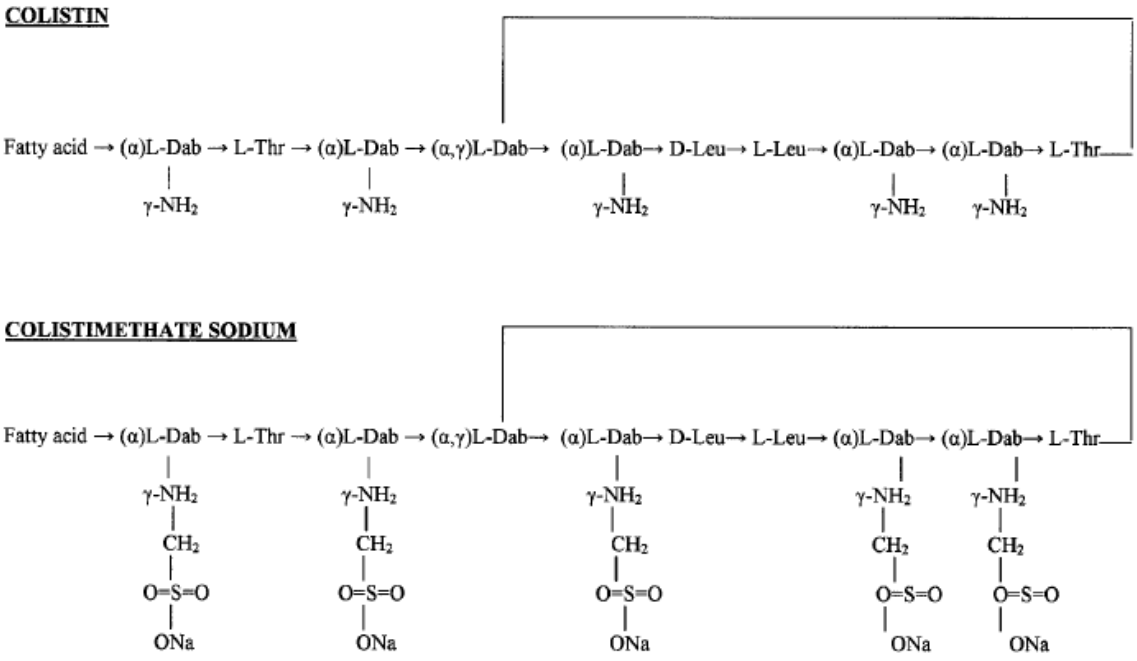

Figure 15: Chemical structure of colistin and colistimethate sodium. The fatty acid molecule is 6-methyloctanoic acid for colistin A and 6- methylheptanoic acid for colistin B. a and g indicate the respective -NH_2 involved in the peptide linkage. Dab, diaminobutyric acid; Leu, leucine; Thr, threonine. Taken from reference (42).

The mixture of Colistin A and B is commercially available in the salt form of colistin sulfate and colistimethate sodium. Colistimethate sodium is generally administrated by nebulization in the treatment of CF, since colistin sulfate causes throat irritation and severe cough (93). Thus, we first tried to develop an HPLC method for the quantification of colistimethate sodium (data not presented). However, the high hydrophilicity of colistimethate sodium prevents its retention on the reverse phase column (C18) so the drug is eluted too early. In normal phase (Hydrophilic Interaction Column - HILIC), the drug has such a high affinity for the stationary phase that it cannot be completely washed from the column. Another drawback is that colistimethate sodium is a pro-drug for colistin sulfate; therefore, it can undergo hydrolysis in aqueous medium. In this regard, we decided to select colistin sulfate as a model drug since this antibiotic is stable in water and less hydrophilic than

colistimethate sodium, thus favoring its HPLC analysis and encapsulation in the hydrophobic matrix of PEG-g-PLA polymer.

Colistin sulfate presented two peaks found between 6 and 7 minutes **(figure 16)** which corresponds to colistin A and colistin B (not identified/ assigned). The calibration curve can be calculated either based on the sum of the two peaks or just based on the most intense peak. The linearity was obtained in the range of 40 to 160 µg/mL. The limit of detection is 40 µg/mL. The limit of quantification for the analysis with both peaks is 60 µg/mL (with the equation of y= 1.7121x + 5.0278, R^2= 0.9985) and for the analysis considering just the most intense peak is 40 µg/mL (with the equation of y= 1.6484x + 4.9567, R^2= 0.9992). Thus, the calibration curve was set with the mass of the most intense peak (single peak instead of both peaks) which allowed the quantification of lower concentrations of colistin sulfate. Indeed, the values of LE and EE obtained for multiple batches of colistin sulfate were sometimes lower even than the lowest limit of quantification provided by the calibration curve considering the most intense peak.

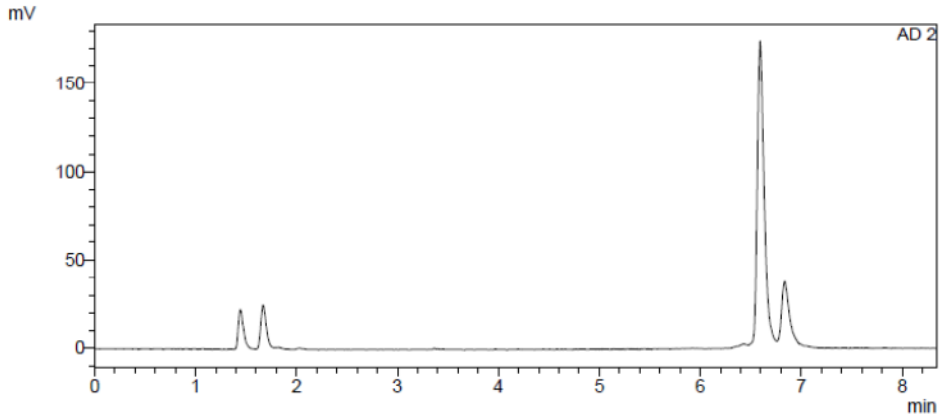

Figure 16: Colistin sulfate peaks at 6.6 and 6.9 minutes from the HPLC-ELSD analysis.

3.3.3. Development of quantitative method to dose levofloxacin

Levofloxacin (**figure 17**) has chromophores in its structure thus it is easily detected by UV at 294 nm. Levofloxacin displayed a single peak at 2.7 min (**figure 18**). The linearity was obtained in the range of 0.5 to 20 µg/mL (with equation of y= 95332x – 1555, $R^2 \geq 0.999$). The limit of detection (LOD) was 0.1 µg/mL and the limit of quantification (LOQ) was 3.0 µg/mL with n=9.

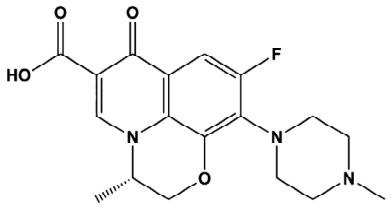

Figure 17: Chemical structure of levofloxacin. Taken from reference (94).

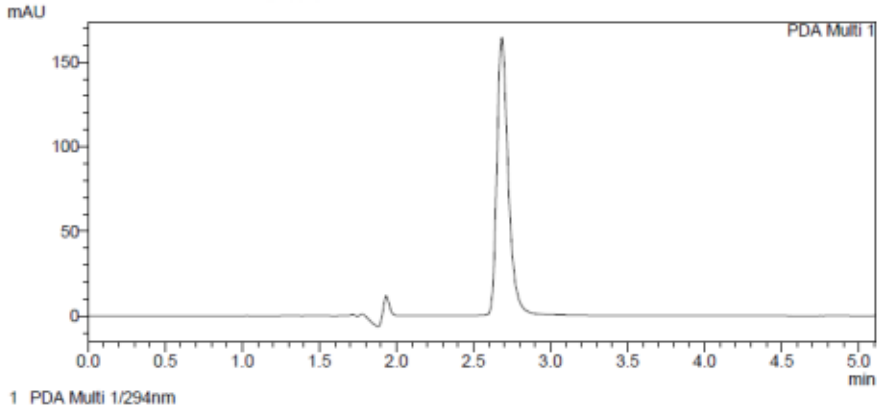

Figure 18: Levofloxacin peak at 2.7 minutes from the HPLC-UV analysis.

3.3.4. Organic solvent analysis for the drug extraction from nanoparticles

The results for the levofloxacin (10 µg/mL) recovery after drug extraction in dichloromethane, chloroform and ethyl acetate and the recovery of colistin sulfate (100 µg/mL) from chloroform are described in **the table XII**.

Table XII: Analysis of organic solvents for drug extraction of levofloxacin and colistin sulfate from nanoparticles.

Solvent	Levofloxacin Recovery (%)[a]	Colistin Sulfate Recovery (%)[b]
Dichloromethane	87.9 ± 5.7	-
Chloroform	96.9 ± 0.1	94.91 ± 1.7
Ethyl Acetate	96.5 ± 0.2	-

[a]Extraction made in triplicate and each test was injected in triplicate for HPLC analysis (n=9).
[b]Extraction made in duplicate and each test was injected in triplicate for HPLC analysis (n=6).

As displayed in table XII, levofloxacin exhibited the highest percentage of recovery in the water phase when extraction was made with chloroform and ethyl acetate. However, ethyl acetate was not selected for nanoparticle extraction due to problems with the separation of phases after centrifugation. In fact, an emulsion was formed in the interface water/ethyl acetate. Besides, ethyl acetate is less dense than water and these both drawbacks hindered the collection of pure water phase for HPLC analysis. Therefore, the presence of impurities was detected in the samples since the HPLC chromatogram showed two overlapping peaks with the same retention time as levofloxacin. So we selected chloroform for the extraction of levofloxacin. However, knowing that levofloxacin is partially soluble in chloroform, the standards and samples were treated with the same method of extraction. Indeed, even if part of levofloxacin was lost in the organic phase, the same drug ratio would be lost in the standards solutions and in the samples, thus minimizing errors in the drug quantification. DCM was not considered a better option since the percentage of recovery was lower than 90 %.

As colistin sulfate is not soluble in chloroform, we decided to use the same solvent for nanoparticle extraction after checking the efficiency of drug recovery, as showed in table XII. This checking was not done for tobramycin but it is also insoluble in chloroform which was used for drug extraction.

3.3.5. Synthesis and characterization of nanoparticles

3.3.5.1. Process of nanoparticle production

Several techniques have already been developed for nanoparticle production. However, the physicochemical properties of the drug and the polymer must be taken into consideration for the choice of the best method, in order to achieve an efficient drug entrapment. In this work we will discuss the nanoparticle preparation by the use of two techniques: emulsification solvent evaporation – ESE (single and double emulsion) and nanoprecipitation (NPP).

The single emulsification solvent evaporation technique is divided in two steps. First, the polymer and the drug are dissolved in an organic phase which is further emulsified in water by high pressure homogenization to prepare the emulsion oil in water (o/w). Afterwards, the organic solvent is evaporated inducing polymer precipitation as nanospheres or nanocapsules.

The nanoprecipitation technique (also known as solvent displacement) requires the dissolution of the drug and polymer in a water miscible organic solvent and its further precipitation in the water phase. In this case, the diffusion of the water-miscible solvent in water causes the precipitation of the polymer which is insoluble in water and the instantaneous entrapment of the drug. The organic solvent is further evaporated.

However, both mentioned methods are more efficient to encapsulate hydrophobic drugs and the drugs used in the treatment of the cystic fibrosis are generally hydrophilic.

As an alternative, a modification on the single emulsification- solvent evaporation technique has led to the protocol favored for encapsulating hydrophilic drugs: the double emulsion technique. First, the hydrophilic drug is dissolved in water with a stabilizer. The first emulsion is formed by dispersing this inner aqueous phase into an organic solvent containing the dissolved polymer. Then, the first emulsion is emulsified by high pressure

homogenization in an outer water phase with stabilizers to form the water/oil/water emulsion (w/o/w).

3.3.5.2. Synthesis and characterization of tobramycin loaded nanoparticles

The composition and characterization of tobramycin nanoparticle batches are described in **table XIII.**

Table XIII: Composition and characterization of tobramycin nanoparticles batches.

Batches[a]	Method	Drug (w/w) (%)[b]	Volume of the organic phase (mL)	Volume of the water phase (mL)[c]	Additive in the water phase	Size (nm)[d,e]	PDI[d,e]	EE (%)[f]	LE (%)[g]
TB_DE_1	DE	9	20	1 (I) 160 (O)	-	126.5 ± 0.8	0.249 ± 0.001	-	-
TB_DE_2	DE	11.25	16	1 (I) 160 (O)	Sucrose 5 % (w/v) (O)	251.1 ± 3.4	0.19± 0.03	-	-
TB_DE-3	DE	3.5	16	1 (I) 160 (O)	Sucrose 5 % (w/v) (O)	155.4 ± 3.1	0.260 ± 0.008	-	-
TB_NP_4	NPP	2	1	0.1 (I) 200 (O)	SA (I)[i] CH (O)[h] Ethanol 50% v/v	140.4 ± 2.2	0.12± 0.02	-	-
TB_NP_5	NPP	2	1	0.1 (I) 200 (O)	SA (I)[i] PVA[j] Ethanol 50% v/v	205.0 ± 6.8	0.23 ± 0.01	-	-

[a]PEG-g-PLA-1was used in each batch. [b]Ratio of drug weight and polymer weight by percentage. [c] Volume of water present in the inner phase (I) and in the outer phase (O). [d]All values indicate mean ± SD for n=3 independent measurements for the same batch. [e]Measured by Dynamic Light Scattering (DLS). [f]Encapsulation Efficiency (EE): (Total quantity of drug encapsulated/ Total amount of drug added) * 100.

[g]Loading Efficiency (LE): Total quantity of drug encapsulated / (Total amount of drug added + Total amount of polymer)*100

[h]CH: Chitosan (1:20) (helper polymer / PEG-g-PLA ratio (w/w).

[i]SA: Sodium alginate 0.04% (w/v).

[j]PVA: Polyvinyl alcohol (PVA/PEG-g-PLA-1 3:5 w/w)

TB: tobramycin; NP: nanoparticles; DE: double emulsion; NPP: nanoprecipitation; PDI: polydispersity index.

As can be showed in **table XIII**, even with the modification of parameters such as method of nanoparticle preparation, drug to polymer ratio, and inclusion of additives, nanoparticles were obtained in the appropriate size range for mucus penetration (67). However, the issue was the tobramycin encapsulation efficiency that remained lower than the HPLC limit of quantification despite further optimization.

The first nanoparticle method explored to produce tobramycin nanoparticles was the double emulsion technique. This method favors the encapsulation of the hydrophilic drug as compared with the single emulsion, since the drug is first entrapped within the polymer in the first emulsion w/o. Thus, the interaction of the drug with the polymer in the first emulsion decreases the chance of drug migration into the external water phase, as compared with the single emulsion process. In the batch 1, no tobramycin was detected in the spectrophotometric assay with fluorescamine. Thus, in the batch 2 the quantity of drug was increased and sucrose 5% (w/v) was added to the external water phase as an attempt to decrease drug leakage by equilibrating the osmotic pressure and viscosity. As no improvement in the encapsulated drug content was observed, the quantity of drug in the internal water phase was decreased as an attempt to decrease the difference of ionic strength between inner/outer water phase, and the concentration of sucrose was maintained at 5% w/v. However, no substantial difference was verified in the intensity of the OD (optical density) found in the quantification assay for the nanoparticle samples.

As an alternative to overcome this low drug entrapment, we also produced nanoparticles by nanoprecipitation. In the second methodology, polymers were added in the inner and/or outer phase as helpers to increase tobramycin encapsulation (90). In the batch 4, chitosan was added in the outer phase with the ratio of 1:20 (helper polymer / PEG-g-PLA ratio (w/w)). We predicted that chitosan have a better effect in reducing drug migration to the outer aqueous phase since it has higher molecular weight and concentration when compared with the sucrose previously used. In addition, chitosan has a positive charge in solution, such as tobramycin, thus resulting in an electrostatic repulsion of tobramycin and its migration to the inner aqueous phase. Conversely, in the batch 5 PVA was added in the

outer phase as a non-ionic stabilizer. In the batches 4 and 5 sodium alginate was added in the inner water phase as an attempt to attract tobramycin in the inner phase since sodium alginate is negatively charged in solution and tobramycin is positively charged. However, these changes showed to be inefficient to increase the drug loading.

The methodology to quantify tobramycin according to the United States Pharmacopeia and National Formulary (USP 29 – NF 24) (95) is by HPLC using pre-column derivatization with 2,4- Dinitrofluorobenzene (DNFB) which has limit of quantification of 3 µg/mL (96). However, we chose to apply a simpler method to quantify tobramycin such as spectrophotometry using fluorescamine as a derivatizing agent (97) which showed similar limit of quantification of 3 µg/mL. However, the LE and EE of tobramycin obtained inside nanoparticles was even lower than the 3 µg/mL indicating that the values of LE and EE calculated were not trustworthy and that the development of a new quantification method with higher sensitivity was required, prior to continuing with further optimization of nanoparticle production.

As a consequence, we tried to develop other method of quantification such as LC/MS/MS and bioluminescence. However, the drug interacted with the HPLC steel stainless material so that it was impossible to get a linear calibration curve. For the bioluminescence assay, the calibration curve did not showed linearity, pointing to some unknown interferences. Thus, we decided to screen another drug model for the nanoparticle formulation with a higher limit of detection in order to facilitate our analysis on the drug loading. In addition, this model drug should be less hydrophilic than tobramycin in order to increase its affinity for PEG-g-PLA polymer which is hydrophobic.

3.3.5.3. Synthesis and characterization of colistin sulfate and levofloxacin nanoparticles

Several batches of nanoparticles were synthesized and characterized regarding to size, charge and drug content with the objective to improve the encapsulation efficiency of colistin sulfate and levofloxacin, as describe in **tables XIV** and **XV**.

Table XIV: Composition of colistin sulfate and levofloxacin nanoparticle formulations.

Nº	NP formulation[a]	Method	Drug	Theoretical LE (w/w) %[b]	Rational
1	PEG-g-PLA (70%) + PLA-OH (30%)	DE	C	7.3	Add PLA-OH to enable hydrogen bonds with L thus favoring drug entrapment inside NP.
2	PEG-g-PLA (30%) + PLA-OH (70%)	DE	C	0.5	Increase the percentage of PLA-OH.
3	PEG-g-PLA (50%) + PLA-OH (50%)	DE	C	5.0	Surfactants in the oil phase were twice the regular concentration. The external water phase contains sucrose 10% w/v.
4	PEG-g-PLA (100%)	SE	C	10.0	DCM as organic solvent. PVA 0.5% (w/v) as surfactant. Lauric acid 6% (w/w)[c].
5	PEG-g-PLA (100%)	SE	C	10.0	DCM: DFM (1:1) as organic solvent. PVA 0.5% (w/v) as surfactant. Lauric acid 6% (w/w)[c].
6	PEG-g-PLA (100%)	SE	C	10.0	DCM: DFM (1:1) as organic solvent. Tween 20 (2.5 % w/v) and PEG-oleate (0.5% w/v) as surfactant. Lauric acid 6% (w/w)[c].
7	PEG-g-PLA (100%)	NPP	L	5.0	Water phase adjusted to pH 4.6 with HCl.
8	PEG-g-PLA (100%)	DE	L	0.5	Regular formulation
9	PEG-g-PLA (100%)	SE	L	2.0	Addition of PVA 0.5% w/v in the water phase.
10	PEG-g-PLA (100%)	NPP	L	5.0	Water phase composed of 50% ethanol.
11	PEG-g-PLA (100%)	NPP	L	5.0	Water phase composed of 50% isopropanol.
12	PEG-g-PLA (100%)	NPP	L	5	Water phase composed of ethanol 10% v/v.
13	PEG-g-PLA (100%)	NPP	L	5	Water phase composed of 10% ethanol and 1.1% w/v surfactant Pluronic F-127.
14	PEG-g-PLA (100%)	NPP	L	5	Water phase with pH adjusted to 4.6 with HCl and ethanol concentration of 20% v/v.
15	PEG-g-PLA (100%)	NPP	L	5	Water phase with pH adjusted to 4.6 with HCl and ethanol concentration of 30% v/v.
16	PEG-g-PLA (100%)	NPP	L	5	Water phase with pH adjusted to 4.6 with HCl and ethanol concentration of 40% v/v.
17	PEG-g-PLA (100%)	NPP	L	5	Distilled water.
18	PEG-g-PLA (100%)	NPP	L	5	Water phase with sucrose 10% w/v and ethanol concentration of 50% v/v.
19	PEG-g-PLA (100%)	NPP	L	5	Water phase with sucrose 10% w/v.
20	PEG-g-PLA (100%)	NPP	L	0.5	Water phase composed of 50% ethanol.
21	PEG-g-PLA (100%)	NPP	L	2.0	Water phase composed of 50% ethanol.
22	PEG-g-PLA (100%)	NPP	L	10.0	Water phase composed of 50% ethanol.

[a]PEG-g-PLA-2 was used in each batch.[b]mg of drug per 100 mg of polymer. [c]mg of lauric acid per 100 mg of polymer.
SE: single emulsion. DE: double emulsion; NPP: nanoprecipitation; LE: loading efficiency; NP: nanoparticles.
C: Colistin sulfate; L: levofloxacin. PVA: polyvinyl alcohol. DMF: Dimethylformamide.

Table XV: Characterization of colistin sulfate and levofloxacin nanoparticle formulations

Nº	NP formulation	Hydrodynamic diameter (nm)[a,b]	Drug	Polydispersity index[a.b]	Zeta potential (mV)[a,b]	LE (%)[c]	EE (%)[d]
1	PEG-g-PLA (70%) + PLA-OH (30%)	172.8*	C	0.622*	-11.8 ± 8.10	No peak	-
2	PEG-g-PLA (30%) + PLA-OH (70%)	131.6 ± 0.8	C	0.170 ± 0.010	-8.67 ± 6.1	Peak not quantifi a-ble	-
3	PEG-g-PLA (50%) + PLA-OH (50%)	121.3*	C	0.205*	-10.9 ± 7.37	No peak	-
4	PEG-g-PLA (100%)	131.1 ± 6.5	C	0.238	-	0.0127	0.1681
5	PEG-g-PLA (100%)	116.2 ± 1.9	C	0.222	-	0.0053	0.0724
6	PEG-g-PLA (100%)	166.6 ± 3.4	C	0.331		0.0028	0.0273
7	PEG-g-PLA (100%)	121.1 ± 1.3	L	0.140 ± 0.01	-28.2 ± 0.6	0.00195	0.04
8	PEG-g-PLA (100%)	131.6 ± 2.4	L	0.170 ± 0.021	-8.67 ±0.6	No peak	-
9	PEG-g-PLA (100%)	109.4 ± 2.5	L	0.086 ± 0.015	-	No peak	-
10	PEG-g-PLA (100%)	85.1 ± 3.0	L	0.101 ± 0.043	-	0.0245	0.4897
11	PEG-g-PLA (100%)	82.1 ± 1.5	L	0.144 ± 0.029	-	0.0120	0.2391
12	PEG-g-PLA (100%)	114.8 ± 2.9	L	0.26 ± 0.010	-5.33 ± 6.36	0.0160	0.3203
13	PEG-g-PLA (100%)	112.0 ± 5.5	L	0.088 ± 0.018	-2.64 ± 9.13	0.0025	0.0504
14	PEG-g-PLA (100%)	137.9 ± 1.7	L	0.125	-	0.0018	0.00009
15	PEG-g-PLA (100%)	134.5 ± 1.7	L	0.203 ± 0.006	-	0.0047	0.00023
16	PEG-g-PLA (100%)	110.6 ± 2.1	L	0.197 ± 0.027	-	0.0047	0.00023
17	PEG-g-PLA (100%)	118.9 ± 1.0	L	0.176 ± 0.021	-3.0 ± 16.0	No peak	No peak
18	PEG-g-PLA (100%)	157.2 ± 8.3	L	0.174 ± 0.045	-7.97 ± 7.76	0.001	0.0193
19	PEG-g-PLA (100%)	142.4 ± 3.3	L	0.223 ± 0.045	-1.44 ± 4.07	0.001	0.0206
20	PEG-g-PLA (100%)	153.1 ± 7.9	L	0.256 ± 0.024	-	No peak	-
21	PEG-g-PLA (100%)	127.4 ± 7.6	L	0.188 ± 0.051	-	No peak	-
22	PEG-g-PLA (100%)	95.9 ± 1.2	L	0.083 ± 0.005	-	0.001	0.01

[a]All values indicate mean ± SD for n=3 independent measurements for the same batch.
[b]Measured by Dynamic Light Scattering (DLS).
[c]Encapsulation Efficiency (EE): (Total quantity of drug encapsulated/ Total amount of drug added) * 100.
[d]Loading Efficiency (LE): Total quantity of drug encapsulated / (Total amount of drug added + Total amount of polymer)*100
*n=1.

The results in the **table XV** show that the nanoparticle size achieved by either NPP or ESE was < 200 nm in accordance with the literature to achieve efficient diffusion in the mucus (67). In addition, the PDI was lower than 0.2 which means a considerable low polydispersity of size, since particles with PDI< 0.1 are considered to have monodisperse distribution of size.

The zeta potential obtained for each batch is also displayed in **table XV**. All formulations exhibited zeta potential varying from (-1.44 which may be considered neutral) to -28.2 mV. According to the literature, particles with neutral charge present better penetration in the mucus (67, 77, 98, 99). Thus, the external charge found in our nanoparticles would not favor nanoparticle diffusion in the mucus. The reason for the negative surface is the carboxylic acid end groups of PLA. The external covering of PEG in the nanoparticles might shield this negative charge, but not completely. Although we have not produced blank nanoparticles, the literature shows that PEG-g-PLA blank nanoparticles exhibited charge of -1.30 mV but the formulation was different. Thus, for blank nanoparticles we expect neutral or slightly negative charge (79).

To increase the LE we modified:

a. Polymer composition

As described in **table XIV**, colistin sulfate nanoparticles were produced by double emulsion (emulsification- solvent evaporation technique - ESE). As the previous production of tobramycin loaded NP with PEG-g-PLA presented low loading efficiency (LE), based on the literature review we predicted that the addition of a polymer with higher hydrophilicity could improve the entrapment of such a drug. According to the literature, levofloxacin has already been encapsulated into PLGA nanoparticles (100) (101) with LE of 1,1 and 7.9 % w/w respectively. However, the polymer used in these works was PLGA 50/50 (DL-lactide/ glycolide) copolymer acid terminated, which is more hydrophilic than PLA based nanoparticles. Indeed, studies have showed that the component in the nanoparticle formulation which mainly impacts the LE of hydrophilic drugs is the hydrophilicity of the

polymer. Therefore, polymers with higher affinity for the drug will enhance drug loading. For instance, Barichello *et al*, tried to encapsulate lipophilic drugs (valproic acid, indometacin and cyclosporine A), hydrophilic drugs (vancomycin and phenobarbital) and ketoprofen (a drug sparingly soluble in water) in PLGA 75: 25 (DL-lactide/ glycolide) (102). The results of LE obtained confirmed the hypothesis that the most hydrophobic drugs would achieve the highest LE due to the hydrophobic nature of the polymer. Thus, favored interactions between drug and polymer would decrease drug leakage during nanoparticle formation. Following the same rationale, Cheow *et al* tried to encapsulate levofloxacin in PCL (polycaprolactone) and PLGA 50/50 (DL-lactide/ glycolide) .by NPP and ESE (single emulsion). In fact, PCL is a polymer less hydrophilic than PLA. Thus, the LE (% w/w) obtained with the nanoprecipitation method was 0.4 and 0.65 respectively. In addition, higher LE was obtained with PLGA by ESE (1.1 % w/w) (103).

Thus, PLA-OH was introduced in the batch 1 with concentration of 30% as an attempt to favor hydrogen bonds with levofloxacin and the drug entrapping inside the polymeric matrix. However, as showed in **table XV**, no peak was detected for the nanoparticles analysis by HPLC. Afterwards, we synthesized batch 2 with 70 % of PLA-OH and batch 3 with 50% of PLA-OH. However, the results of EE remained low suggesting that the addition of PLA-OH did not significantly altered the overall lipophilicity of the system and/ or did not increase the colistin affinity for the polymer mixture. In fact, Hammady *et al* (54), succeeded to encapsulate the hydrophilic calf thymus DNA in PEG-PLA block polymers. However, despite the difference of polymer morphology, calf thymus DNA is a bigger molecule with mean molecular weight of 8,418,000 (g/mol) if compared to colistin sulfate 1267.6 g/mol. In fact, the leakage of hydrophilic drugs to the external water phase is related with drug diffusion which is higher with small molecules, as seen with colistin. Thus, the encapsulation of calf thymus DNA in PEG-PLA block polymers might have been favored by its high molecular weight.

b. Surfactants composition

In the same work (54), Hammady emphasized the role of the surfactants to stabilize the first emulsion and avoid drug leakage. Thus, as our polymer presents different morphology, we tried to increase the quantity of surfactants in batch 3, without success. As the optimization of the NPP method is more complex if compared with ESE, and the first method does not offer advantages over the latter to encapsulate hydrophilic drugs; we decided to continue the optimization process with ESE by single emulsion.

c. Solvents and co-solvents in ESE by single emulsion

The aim in the batches 4, 5 and 6 was to verify if the mixture of DCM: DMF (1:1) could improve the LE. The rationale is to decrease the hydrophobicity of the organic phase by adding DMF which is more polar than DCM. Therefore the drug diffusion for the water phase should be decreased. In addition, the impact of two different surfactants was also verified. Most importantly, lauric acid was added as an attempt to form ion pairing with colistin sulfate thus hindering drug efflux to the water phase as demonstrated before by. Govender *et al* (104). In this work the approaches investigated for LE enhancement included the influence of aqueous phase pH, replacement of procaine hydrochloride with procaine dihydrate and the inclusion of helpers: (PLA) oligomers, poly(methyl methacrylate-co-methacrylic acid) (PMMA‑MA) or fatty acids into the formulation. Helpers were added to determine if an increased content of carboxyl groups in the matrix could increase the entrapment of the cationic drug. It was found that aqueous phase pH of 9.3, replacement of procaine hydrochloride with procaine dehydrate (less hydrophilic) and the incorporation of PMMA‑MA, lauric and caprylic acid into the formulation enhanced LE.

In fact, we probably varied too many parameters in a few batches. But the LE results exhibited in **table XV** showed that lauric acid might have improved the encapsulation of colistin sulfate if compared with the double emulsion method since we were able to detect a

peak and calculate the levofloxacin concentration. However, the mixture of solvent seemed less efficient to increase LE if compared with DCM. A possible hypothesis is that DCM improved lauric acid solvatation, lauric acid thus aiding the formation of the ion- pair if compared with the more hydrophilic organic phase formed by the mixture DCM/DMF. Most importantly, the application of the single emulsion method and other artifices (ion pairing, organic solvent polarity and use of different surfactants) was not efficient to significantly increase the LE of colistin sulfate in PEG-g-PLA nanoparticles.

d. Nanoparticle formation method

Afterwards, we followed with the production of levofloxacin nanoparticles by nanoprecipitation, double emulsion and single emulsion (batches 7, 8 and 9 respectively) as exhibited in **table XIV**. As the best result for EE so far was found with levofloxacin nanoparticles by nanoprecipitation showed in table XVI line 10, we decided to select this drug as a model drug for our polymer and to follow further optimizations with the NPP technique. Other reasons that guided our choice to work with levofloxacin are: 1) The HPLC test to quantify levofloxacin possess lower LOQ if compared with the HPLC method to quantify colistin sulfate which is important to evaluate improvements in the low EE in each batch; 2) Levofloxacin (log P = -2.1) (105) is less hydrophilic than colistin sulfate (log P = -3.15 for colistin A and log P= -3.60 for colistin B) (106), thus we hypothesized that levofloxacin might have higher affinity to PEG-g-PLA. 3) Colobreathe® study showed little improvement in FEV1 with colistin dry powder treatment compared to tobramycin(30). Therefore, levofloxacin is more appropriate than colistin to be further formulated as a powder to inhalation to treat cystic fibrosis. .

e. pH

Besides polymer composition, the variation of other parameters has also been studied as an attempt to increase the LE of hydrophilic drugs. For example, Mobarak *et al* tried to improve the LE of ciprofloxacin hydrochloride in PLGA (50: 50) by the double emulsion solvent evaporation technique (107). The variation of three different variables was evaluated: 1) application of probe sonication besides the high pressure homogenization and during the solidification step; 2) effect of polyvinyl alcohol addition in the formation of the o/w primary emulsion; 3) addition of sodium chloride in the external and extraction water phase; 4) pH adjustment of the external and extraction phases to 7.4. The best EE achieved was with the use of sodium chloride, buffer, and PVA. Sodium chloride adjusted the osmotic pressure in the external water phase in order to avoid drug leakage, pH adjustment to the least solubility of ciprofloxacin favored polymer/drug affinity and PVA was added to stabilize the first emulsion o/w thus, enhancing the drug entrapment. Besides, the sonication during solidification step did not increase the EE. However, the use of sonication in addition to homogenization to form the secondary emulsion helped to enhance the LE.

The pH impact on LE was also analyzed in our work. However, the results for the LE of batches 7 and 17 did not show a significant improvement in the LE. In fact, later it was checked that the lowest solubility of levofloxacin is at pH between 7 and 8 (105). Therefore, the best option should have been to adjust the water phase at pH=7.4 to have a better impact in the LE (decrease its solubility in the diffusion water phase thus decreasing leakage).

f. Co-solvents in NPP

In batches 10 and 11, water miscible co-solvents (ethanol and isopropanol respectively) were added in the diffusion phase water with the attempt to decrease the solubility of levofloxacin thus preventing drug diffusion. Actually, the best EE was reached with the batch 10.

g. Additives in NPP

Thus, in batches 12 and 13 we evaluated if the ethanol concentrations could be optimized to enhance LE. Besides, the impact of surfactant incorporation in the LE was also evaluated. In the formulations 14 to 17 we evaluated the impact of ethanol concentration and pH in the EE. However, the best conditions were in formulation 10. In batches 18 and 19, we evaluated the impact of adding a non ionic component in the diffusion phase in order to concentrate it, thus avoiding drug migration due to ionic strength.

h. Drug feeding ratio

Finally, as there was no improvement with any of these changes, we kept the parameters of batch 10 and varied the drug concentration in batches 17-19 with no success. However, the best LE achieved by levofloxacin encapsulation in PEG-g-PLA was 0.02% with the addition of ethanol 50% v/v in the external water phase of nanoprecipitation.

To conclude, the parameters used for the encapsulation of tobramycin, colistin sulfate and levofloxacin in PEG-g-PLA have already been used successfully to enhance the encapsulation of other hydrophilic drugs, mostly in PLGA matrices. Although we obtained nanoparticles with suitable size and polydisperity index for drug delivery in the mucus, the zeta potential obtained was negative, a fact that could hinder nanoparticles diffusion in the mucus. Most importantly, the LE obtained was low, probably due to low affinity of PEG-g-PLA and or PLA polymers to the hydrophilic drugs. New batches with pH optimization could be tested, since the pH range tested does not reflect the best difference in the drug solubility.

Indeed, as drug entrapment into liposomes does not depend on the interaction of drug and lipids, levofloxacin loaded liposomes will be synthesized and characterized as an attempt to develop a formulation with suitable drug loading to be tested in *Pseudomonas aeruginosa* to fulfill the objectives proposed for this work.

3.4. Synthesis and characterization of levofloxacin loaded liposomes

i. Materials

Methanol, acetonitrile, acetone, phosphorus standard solution 0.65 mM (phosphorus as KH_2PO_4 20 µg/mL in 0.05 N HCl), ammonium molybdate, ammonium sulfate, sodium metabisulfide, ascorbic acid, sulfuric acid, hydrogen peroxide, levofloxacin > 98% HPLC grade, sodium chloride (NaCl) and cholesterol were purchased by Sigma-Aldrich (Oakville, ON, Canada). 1,2-Distearoyl-sn-glycero-3-phosphocholine (DSPC) and 1,2-distearoyl-sn-glycero-3-phosphoethanolamine-N-[biotinyl(polyethylene-glycol)-2000] (DSPE-PEG(2000)-biotin) were obtained from Avanti Polar Lipids. Amicon Ultra-15 Centrifugal Filter Unit with Ultracel-10 membrane was obtained by EMD Millipore Corporation (Billerica, MA, USA). Spectra/Por® molecularporus membrane tubing MWCO 6-8000 was purchased by Spectrum Laboratories Inc. (Rancho Dominguez, CA, USA).

ii. Methodology

3.4.1. Preparation of liposomes

Blank and levofloxacin loaded liposomes composed of DSPC/Cholesterol/DSPE-PEG (60:45:5 mol%) was synthesized by the ammonium sulfate gradient method as described before, with some modifications (108). Briefly, blank liposomes were synthesized by adding to a 10 mL round-bottom flask the chloroform stock solutions of DSPC (116 µL, 38 mg/mL), cholesterol (37 µL, 42.1 mg/mL) and DSPE-PEG-2000 (32 µL, 44.3 mg/mL). Chloroform was evaporated under reduced pressure at 63 ˚C for 10 minutes in a Buchi 461 water bath (BÜCHI Labortechnik AG, Flawil, Switzerland). Eventual residue of chloroform was withdrew by a 30

minutes lyophilisation in a freeze dryer ModulyoD-115-230® (Thermo Fisher Scientific Inc.,Waltham, MA, USA). Afterwards, the resulting lipid film was hydrated with 1 mL of ammonium sulfate solution 120 mM (final lipid concentration of 10 mM/mL) with continuous stirring (60 r.p.m, 63˚C, 1 h.). 10 cycles of freezing and thawing process (in dried ice and water bath at 63˚C, respectively) were applied followed by 21 cycles of extrusion in a mini extruder set, Avanti Polar Lipids Inc. (Al, USA) extruder charged with a 100 nm polycarbonate membrane. Finally, after checking the liposomes size by DLS (see 2.2.a for details), the liposomes suspension was diluted 1:4 (5 times) in NaCl 180 mM and dialysed in 1 L of NaCl 180 mM for 18 hours to remove non encapsulated ammonium sulfate. For the synthesis of levofloxacin loaded liposomes, the dialyzed liposomes were further incubated with levofloxacin stock solution (40 mg/mL in acetic acid 1% v/v) with the volume ratio of 1:4 (levofloxacin: liposome suspension) for 40 minutes under stirring in a mineral oil bath at 63˚C. The liposomes were purified from non-encapsulated levofloxacin by ultracentrifugation (in a centrifuge equipped with a 10 kDa membrane) at 4000 r.f.c for 40 min in a IEC Multi® / Multi RF TM centrifuge (Thermo Fisher Scientific Inc.,Waltham, MA, USA). Then, the purified liposome suspension was recovered from the filter using NaCl 180 mM and this same solution was used to complete the final volume to 4 mL.

3.4.2. Characterization of liposomes

a. Liposomes size

After production, liposomes size and size distribution (the latter expressed by the PDI – polydispersity index) were measured in triplicate (n=3), at 25°C by Dynamic Light Scattering (DLS) in the Zetasizer Nano ZS, Malvern (Malvern Instruments Ltd, Worcestershire,United Kingdom). Briefly, 5 µL of liposome suspension was added to 995 µL of ultra pure water.

b. Liposomes charge

Liposomes charge was measured in triplicate (n=3), at 25°C in the Zetasizer Nano ZS, Malvern (Malvern Instruments Ltd, Worcestershire,United Kingdom). Briefly, 10 µL of liposomes sample was diluted to 1mL with a sodium chloride solution 4 % w/v.

c. Lipid quantification

The quantity of lipid present in the final liposomes formulations was quantified according to the Bartlett Assay (109). Briefly, 60 µL of sulfuric acid was added to reference glass tubes containing 0, 25, 50, 100 and 125 µL of phosphorus standard solution and to the sample tubes containing 35 µL of liposomes. The tubes were vortexed and 10 µL of hydrogen peroxide was added in each tube. After 10 min incubation at 200 ˚C, the tubes were cooled in an ice bath and 670 µL of ultra pure and 20 µL of sodium metabisulfite (0.1 g/mL) were added into each tube. Then, the tubes were incubated at 100 ˚C for 5 minutes and cooled in an ice bath. Finally, 200 µL of ammonium molybdate (0.02 g/mL) and 20 µL of ascorbic acid (0.1 g/mL) were added into each tube and the tubes were incubated at 100 ˚C for 10 min and cooled in an ice bath. Standards and samples (100 µL) were transferred to a quartz 96 well plate and in which the absorbance of each solution was measured at 820 nm in a microplate Reader Safire (Tecan Group Ltd., Männedorf, Switzerland).

d. Drug content inside liposomes

Levofloxacin loaded liposome suspension was diluted in methanol (100: 900 µL) to disrupt lipid micelles and release the encapsulated drug. Then, 125 µL of this solution was added to a HPLC vial containing 875 µL of aqueous mobile phase. The levofloxacin HPLC analysis was performed using the same method developed to quantify levofloxacin in nanoparticles (see section 3.3.3). The standards of levofloxacin were prepared in the concentrations of 0; 1.25; 2.5; 5.0; 10; 20 and 40 µg/mL. EE and LE were calculated as following:

$$\mathrm{EE} = \frac{\text{quantity of encapsulated drug}}{\text{total quantity of added drug}} \text{ x } 100$$

$$LE = \frac{\text{quantity of encapsulated drug}}{(\text{total quantity of added drug} + \text{total quantity of lipid})} \text{ x } 100$$

iii. Results

3.4.3. Preparation of liposomes

Studies have shown that the encapsulation of amphipathic drugs can be increased by the method of ammonium sulfate gradient (108, 110) . Levofloxacin possess alkaline piperdino groups that display amine functionality which confers to this drug the possibility to be transported inside liposomes via a pH gradient formed by the ammonium sulfate. Briefly, amphipathic drugs in their neutral form are able to cross bilayer membrane faster than their neutral form. Indeed, the unprotonated levofloxacin crosses the liposomal membrane and is then protonated inside liposomes which is an H^+ rich environment. Consequently, the charged drug precipitates with sulfate and forms a salt that is entrapped inside the liposome thus helping to increase the drug loading (111) (**figure 19**).

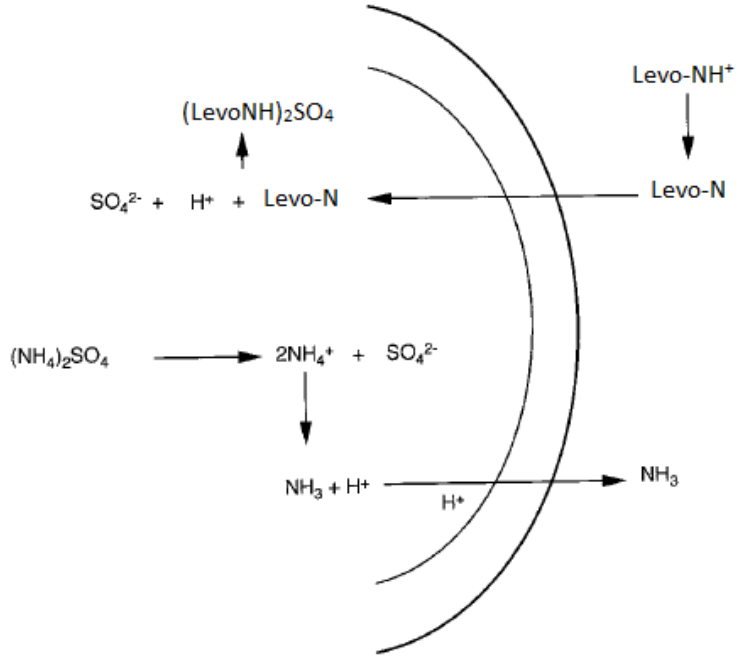

Figure 19: Ammonium sulfate gradient for weak bases. Liposomes are first prepared in the presence of ammonium sulfate (120mM). After removal of exterior ammonium sulfate by dialysis, levofloxacin (Levo) is added to the extraliposomal media. Ammonium sulfate can dissociate to form two ammonium cations and one sulfate annion. Ammonia (NH_3) is free to cross the liposomal membrane giving rase to a pH gradient across the membrane. Levo in its uncharged form can cross the membrane and form an insoluble gel under acidic conditions with the remaining sulfate effeivelly trapping it in the liposomal interior. Adapted from reference (112).

The lipid composition was guided by an attempt to reach a stable liposome formulation. DSPC was chosen since it possesses glass transition temperature (Tg) of 63˚C which results in higher formulation stability at room temperature and decreased drug leakage. Cholesterol chosen to add fluidity to the liposomes and DSPE-PEG was chosen since the hydrophilicity of PEG avoids aggregation of liposomes thus contributing to the stability of the lipophilic formulation.

3.4.4. Characterization of liposomes

The characterization of levofloxacin loaded and blank liposomes such as size, polydispersity index, charge, lipid concentration and drug loading are displayed in **table XVI.**

Table XVI: Characterization of blank and levofloxacin loaded liposomes.

Batches	Size (nm)[a,b]	PDI[a,b]	Zeta Potential (mV)[a,b]	Lipid concentration (mM)[c,d]	EE (%)[a,e]	LE (%)[a,f]
Levo Lip-1	155.7 ± 1.9	0.027 ± 0.006	-8.8± 0.3	2.065 ± 0.038	8.03 ± 0.08	7.04 ± 0.07
Levo Lip-2	152.6 ± 2.0	0.03 ± 0.01	-8.4 ± 0.3	2.342 ± 0.003	8.7 ± 0.1	7.53 ± 0.09
Levo Lip-3	150.6 ± 0.9	0.04 ± 0.02	-8.0 ± 0.6	2.040 ± 0.01	8.2 ± 0.2	7.1 ± 0.2
Blank Lip-1	158.2 ± 1.7	0.02 ± 0.02	-4.6 ± 0.5	2.103 ± 0.297	-	-
Blank Lip-2	160 ± 3.5	0.03 ± 0.03	-5.3 ± 0.6	2.259 ± 0.082	-	-
Blank Lip-3	157.5 ± 2.2	0.04 ± 0.04	-5.1 ± 0.9	2.239± 0.035		

[a]All values indicate mean ± SD for n=3 independent measurements for the same batch.
[b]Measured by Dynamic Light Scattering (DLS).
[c]Values calculated by the Bartlett Assay.
[d]All values indicate mean ± SD for n=2 independent measurements for the same batch.
[e]Encapsulation Efficiency (EE): (Quantity of drug encapsulated/ Total quantity of drug added) * 100.
[f]Loading Efficiency (LE): Quantity of drug encapsulated / (Total quantity of drug added + Total quantity of lipid)*100
PDI: polydispersity index. mV: milivolts.

As showed in table XVII, liposomes size was reproducible between different batches, lower than 200 nm and presented a monodisperse population (PDI< 0.2).

Liposomes charge was reproducible between the batches with values of approximately -8 mV for levofloxacin liposomes and -5 mV for blank liposomes. The slightly negative charge of blank liposomes can be explained by the presence DSPC with possesses negatively charged phosphate groups. However, the zeta potential is more negative in levofloxacin loaded liposomes due to the extra effect of negative ionized carboxylic groups present in levofloxacin.

Thus, liposomes size was suitable for particle diffusion in the mucus but the liposomes charge was slightly negative since neutral particles exhibit enhanced diffusion in the mucus (67, 77).

The lipid concentration determined by the Bartlett assay presented reproducible values of approximately 2 mM. After all dilutions during liposomes preparation the final lipid concentration expected is approximately 2 mM. Thus, as can be verified in **table XVI**, the Bartlett Assay results shows that no significant loss of lipid occurred during liposomes preparation.

The encapsulation efficiency obtained for the levofloxacin loaded liposomes was reproducible and around 8% w/w. Although the levofloxacin lost was considerable with the initial drug concentration of 40 mg/mL, the loading efficiency which expresses percentage w/w of drug/lipid obtained enabled to test the liposomes formulation in the microbiological test. According to the literature, and increased EE has been accomplished by Zhag *et a*l in a study of levofloxacin encapsulation into liposomes under similar conditions. However, the nanoparticle size found in this study was > 7 µm which may have helped to increase the LE (108).

The results of LE showed that liposomes are better nanocarriers to encapsulate hydrophilic drugs such as levofloxacin compared with polymeric nanoparticles. The main reason to explain this fact is that the entrapment of drug inside liposomes does not depend on the drug- lipid interaction as happens with the use of polymers. In addition, liposomes possess an aqueous core which is hydrophilic and compatible with levofloxacin while PEG-g-PLA nanoparticles possess a hydrophobic core which does not favor polymer interaction with levofloxacin. Thus, as seen in the nanoparticle chapter, nanoparticles were also obtained with suitable size (< 200 nm) and slightly negative charge. However, the best LE obtained was 0.02% in contrast with liposomes which exhibited LE= ~ 8%, a fact which proves that the

proposed liposomes formulation is a better alternative to encapsulate levofloxacin for the treatment of CF compared to PEG-g-PLA nanoparticles.

To conclude, liposomes were successfully developed and were of consistent size, charge, polydispersity, lipid concentration and drug loading in three different batches of loaded levofloxacin and blank liposomes. Indeed, this liposomes formulations present suitable size, charge and drug loading to be used to target *Pseudomonas aeruginosa* in Cystic Fibrosis, thus they will be further by antimicrobial susceptibility testing.

3.5. Assessment of free antibiotic versus antibiotic loaded nanocarriers efficiency in eradicating planktonic and biofilm forms of PA in antimicrobial susceptibility testing

i. Materials

Cation Adjusted Mueller Hinton Broth (CAMBH), Mueller Hinton Agar (MHA), Sheep blood defibrinated, resazurin sodium salt, Tryptic Soy Broth (TSB) and glycerol for molecular biology ≥ 99%, levofloxacin > 98% HPLC grade were purchased from Sigma-Aldrich (St. Louis, MO, USA). Tissue culture plate – 96 well flat bottom with lid and 10, 200 and µL 1000 µL pipet tips were purchased from Sarstedt (Montreal, QC, Canada). Nunclon Delta Surface 96 well plate was purchased from Thermo Fischer Scientific Nunc A/S (Roskilde, Denmark) and MBEC ^{TM} Biofilm Inoculator was purchased from Innovotech Inc. (Edmonton, AB, Canada). Tobramycin and Colistin Sulfate were purchased from AK Scientific (AK Scientific Inc., Union City, CA, USA).

ii. Methodology

3.5.1. Validation of antimicrobial susceptibility testing with free antibiotic against PA

3.5.1.1. Test conditions

3.5.1.1.1. Bacterial strains and culture conditions

Two different clinical strains of *Pseudomonas aeruginosa* (mucoid and non-mucoid) and the quality control strain ATCC 57853 (American Type Culture Collection, Manassas, VA), were kindly provided by Dr. Valerie Waters and Dr. Yvonne Yan from SickKids Hospital (Toronto, Canada). The clinical strains were isolated from the lungs of CF patients. After shipping, the strains were stored at -80°C in Tryptic Soy Broth with 15% glycerol. For antimicrobial susceptibility testing, the frozen strains were recovered on agar plates (Mueller Hinton agar with 5% v/v sheep blood) and incubated overnight at 37°C in the incubator Fisher Scientific™ Isotemp™ Standard Lab (Thermo Fisher Scientific Inc.,Waltham, MA, USA). After growth, isolates were subcultured under with similar incubation conditions. Cultures from the second passage were used for the testing.

3.5.1.1.2. Antibiotic formulations

The stock solution of free tobramycin, levofloxacin and colistin sulfate were prepared in ultra pure water at a concentration of 10 mg/mL. For the broth microdilution test in the planktonic form of PA, 256 µL of each stock solution was transferred to a 10 mL volumetric flask and the final volume completed with CAMBH to prepare the highest antibiotic concentration of 256 µg/mL. Serial twofold dilutions were performed to get standard solutions from 256 to 0.5 µg/mL. For the biofilm test, 32 µL of each stock solution (10 mg/mL) was transferred to a 10 mL volumetric flask and the final volume completed with

CAMBH to prepare the highest antibiotic concentration of 32 µg/mL and the serial twofold dilution was similarly performed in the range of 32- 0.0625 µg/mL.

3.5.2. Planktonic antimicrobial susceptibility testing against *Pseudomonas aeruginosa*

The minimal inhibitory concentration (MIC) was determined by using a modification of the Clinical and Laboratory Standards Institute (CLSI) approved microtiter serial dilution method (113) (114). The plates were set upas indicated in **figure 20**:

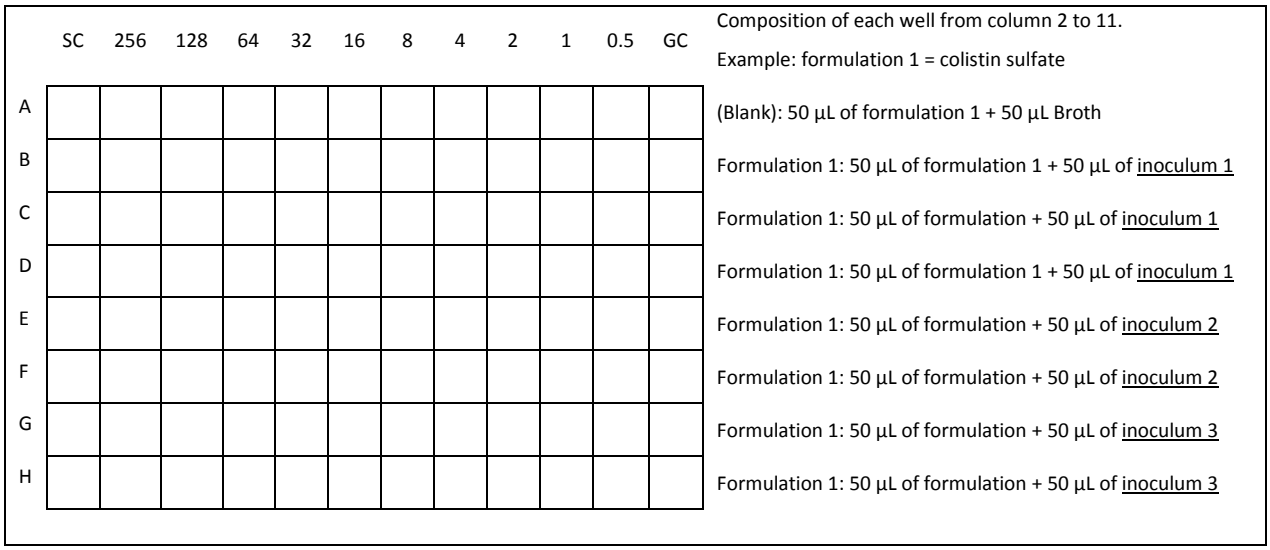

Figure 20: General scheme to illustrate the composition of plates for the regular microbiological test. SC (sterility control) = 100 µL of broth. GC (growth control) = 50 µL of broth + 50 µL of inoculum. Formulations (concentration range from 256 to 0.5 µg/mL): tobramycin, levofloxacin and colistin sulfate. Inoculums 1, 2 and 3: PA mucoid strain, non-mucoid strain and quality control strain, respectively. This is a general scheme; the inoculums were tested in duplicate or triplicate as showed in the table XVII.

As seen in the **figure 20,** appropriate controls (blanks), were included on each plate for the calculation of the bacterial counts after addition of resazurin as explained in the following item 1.2.3.

3.5.2.1. Preparation of the inoculums

Inoculums of mucoid, non-mucoid and quality control strains of *Pseudomonas aeruginosa* were prepared in the same way. Briefly, PA suspension from overnight growth on CAMBH was adjusted to 0.5 McFarland turbidity standard (1 X 10^8 CFU/mL). This initial concentration was obtained by adjusting the suspension absorbance between 0.08 - 0.13 at 625 nm. Then, each inoculum was further diluted 1:100 (1 X 10^6 CFU/mL) in CAMHB to form the final inoculum suspension to be added in the plate. After addition of the inoculums, each antibiotic concentration and the inoculums their selves were diluted 1:1. Thus, the antibiotic range in the test was from 0.25 to 128 µg/mL and the inoculum concentration per well was 5 X 10^5 CFU/ml.

3.5.2.2. Inoculum checks

After addition of the inoculum, microtiter plates were shaken briefly, and 10 µL was removed from 2 growth control wells (for each strain) and diluted 10:990 (10^{-2}) in CAMBH followed by a consecutive dilution 100:900 (10^{-1}) in CAMBH (total dilution of 10^{-3}). Then, 50 µL from last dilution was plated onto Mueller Hinton (MH) agar (it is expected 25 CFU/50 µL), and incubated for 24 to 48 h at 37°C to confirm 5 X 10^5 CFU/mL.

3.5.2.3. Incubation and addition of resazurin

Plates were then incubated for 24 hours at 37°C without shaking. Although the optimization of the microbiological test was done with the free antibiotics, this test was also designed to determine the MIC of nanocarriers which are opaque, thus hindering the determination of bacterial growth by the conventional method of turbidity or optical density (OD). Therefore, 50 µL of resazurin (0.02 % w/v) was added to each well after incubation, and the plates were incubated overnight at 37°C without shaking. Resazurin, a non fluorescing blue dye, is reduced to resorufin, a fluorescing pink dye, in the presence of actively metabolizing cells

(114). Therefore, MIC results were visually recorded the next day as the lowest concentrations of drug in which the wells remained blue. MIC results were further confirmed by measuring the fluorescence generated by the reduction product resorfurin on a Microplate Reader Safire (Tecan Group Ltd., Männedorf, Switzerland) at 560 nm excitation/590 nm emission. The change in metabolic activity for treated bacteria was calculated as follows:

$$x = \frac{(\mathrm{A} - \mathrm{B})}{(\mathrm{C} - \mathrm{D})} * 100$$

Where:

X= change in metabolic activity (%)

A= fluorescence of the visual MIC well

B= fluorescence of the well with the equivalent concentration of drug without bacteria (blank)

C= fluorescence of the well containing bacteria but no drug (GC)

D= fluorescence of the well containing medium only (SC)

The value for the MIC well should exhibit reduction ≥ 90%.

3.5.3. Antimicrobial susceptibility testing of the biofilm form of *Pseudomonas aeruginosa*

The minimal inhibitory concentration (MIC) -for the planktonic form of PA and the Minimal Biofilm Inhibitory Concentration (MBIC) - for the biofilm form of PA were determined in the Calgary Biofilm Device (115).

3.5.3.1. Preparation of the inoculums and biofilm formation

Bacterial suspension of mucoid and non-mucoid strains of PA from overnight growth on CAMBH was adjusted to 0.5 McFarland turbidity standard (1 X 10^8 CFU/mL, absorbance of 0.08 to 0.13 at 625 nm) and further diluted 300 :19700 µL in CAMHB (1 X 10^7 CFU/mL) and transferred to the Biofilm Inoculator 96 well plate as showed in **figure 21**. Since the biofilm generation time is different for each strain, the plates were set up with just one strain per plate.

	1	2	3	4	5	6	7	8	9	10	11	12	
	SC											GC	
A													Blank colistin sulfate (100 µL of sterile water) – no biofilm growth
B													100 µL inoculum 1
C													100 µL inoculum 1
D													100 µL inoculum 1
E													Blank levofloxacin(100 µL of sterile water) – no biofilm growth
F													100 µL inoculum 1
G													100 µL inoculum 1
H													100 µL inoculum 1

Figure 21: General scheme to illustrate the composition of the biofilm inoculators 96 well plates for biofilm formation.SC (sterility control) = 150 µL of sterile water. Inoculums 1 or 2: PA mucoid or non-mucoid strains (only one strain per plate). Antibiotics tested: colistin sulfate and levofloxacin.

Then, the plates were incubated at 37°C with shake at 110 r.p.m for 3.5 to 4.0 hours in a Thermo Scientific™ MaxQ™ 4000 Benchtop Orbital Shaker (Thermo Fisher Scientific Inc.,Waltham, MA, USA).

After 3.5 hours of incubation, the optical density of the wells was measured at 650 nm in the Microplate Reader Safire (Tecan Group Ltd., Männedorf, Switzerland) and the growth was stopped when the OD reached the range of 0.06 -0.07.

3.5.3.2. Inoculum checks

100 µL of each inoculum (mucoid and non-mucoid) was removed in duplicate from the final diluted inoculums and transferred to two tubes containing 400µL of sterile water. After vortex, three serial dilutions 100: 900 µL in ultrapure water were performed. Finally, 50µL from the 2 last dilutions were plated in duplicate onto agar plates and incubated for 24 to 48 h at 37°C to confirm 100 and 10 CFU/50 µL respectively.

3.5.3.3. Biofilm incubation with antibiotic solutions (Challenge Plate)

After growth, the peg lid containing the biofilm was removed and washed in a 96 well plate holding 200 µL of ultra pure water/ well to remove loosen planktonic cells and placed in the challenge plate containing the serial diluted antibiotic solutions, as illustrated in **figure 22**.

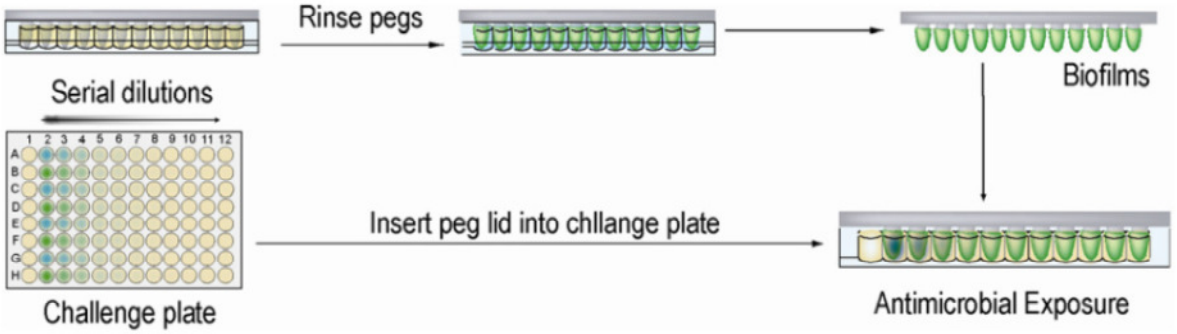

Figure 22: Scheme to illustrate the biofilm rinsing in water to remove loosen planktonic cells and exposure to the challenge plate. Taken from reference (116).

The general composition of the challenge plate is described in the **figure 23.**

	SC	32	16	8	4	2	1	0.5	0.25	0.125	0.0625	GC	
													Blank (100 µL of colistin sulfate solution)
B													100 µL colistin solution + biofilm of strain 1
C													100 µL colistin solution + biofilm of strain 1
D													100 µL colistin solution + biofilm of strain 1
E													Blank (100 µL of levofloxacin solution)
F													100 µL levo solution + biofilm of strain 1
G													100 µL levo solution + biofilm of strain 1
H													100 µL levo solution + biofilm of strain 1

Figure 23: General scheme to illustrate the composition of the challenge plate SC (Sterility Control) and Growth Control (GC) = 150 µL of broth. Remaining wells = 150 µL of serial diluted antibiotic solution (colistin sulfate or levofloxacin). Biofilm: PA mucoid and non-mucoid strains (only one kind of strain per plate). Levo= levofloxacin.

The challenge plates were incubated at 37°C for 24 hours without shaking.

3.5.3.4. Biofilm incubation in the recovery plate

After incubation, the peg lid was removed from the challenge antibiotic plate, washed in a 96 well plate holding 200 µL of ultra pure water/ well to remove loosen planktonic cells and placed in the recovery plate containing 150 µL of CAMBH/ well as illustrated in **figure 24**.

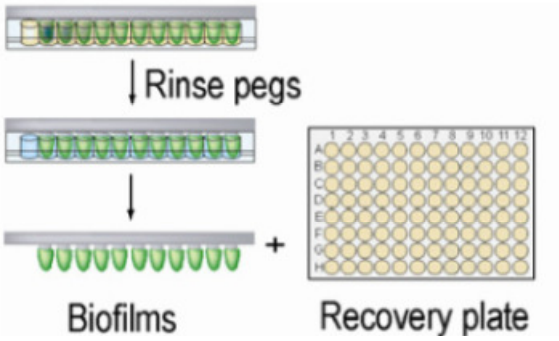

Figure 24: Scheme to illustrate the biofilm rinsing in water to remove loosen planktonic cells and exposure to the Recovery Plate. Taken from reference (116).

The recovery plate was incubated at 37°C for 24 hours without shaking.

3.5.3.5. Addition of resazurin

After incubation, 50 µL of resazurin (0.02 % w/v) was added to each well of the challenge and recovery plates which were incubated overnight at 37°C without shaking. The MIC was visually determined in the challenge plate as the first well which remains blue. To confirm the visual analysis, the spectrofluorimetric analysis was performed at 560 nm excitation/590 nm emission in the Microplate Reader Safire (Tecan Group Ltd., Männedorf, Switzerland). The value for the MIC well should exhibit reduction ≥ 90%. Similarly, the Minimal Biofilm Inhibitory Concentration (MBIC) was determined in the recovery plate.

3.5.4. Broth Microbiological Test of liposomes against *Pseudomonas aeruginosa*

The Broth Microdilution test was done as described in the section 3.5.2 with some modifications.

3.5.4.1. Antibiotics formulations

Free levofloxacin stock solution of 256 µg/mL and two times serial dilution in CAMBH in the range of 256 – 0.5 µg/mL were prepared as described before. Levofloxacin loaded liposomes stock solution of 256 µg/mL (4 mL) was prepared considering the concentration of levofloxacin determined by HPLC for each liposome formulation (see **table XVIII**). The resulting lipid concentration was calculated considering the lipid quantification by the Bartlett Assay (see **table XVIII**). Similarly, blank liposomes (4 mL) were prepared using the same lipid total quantity as loaded liposomes of 256 µg/mL. Levofloxacin loaded liposomes of 256 – 0.5 µg/mL were prepared by serial dilution in broth, and similar process was applied for blank liposomes.

3.5.5. Liposomes Broth Microdilution Test in the planktonic form of *Pseudomonas aeruginosa*

The test was performed as described before but with the addition of free levofloxacin, blank and levofloxacin loaded liposomes. In addition, blanks were added in order to calculate the resazurin reduction with 50 µL of broth and 50 µL of each formulation. After addition of inoculum, the formulations were diluted 1:1 therefore the concentration of each formulation tested was in the range of 128 – 0.25 µg/mL.

iii. Results and discussion

3.5.6. Validation of antimicrobial susceptibility testing with free antibiotic against PA.

In order to characterize the two strains obtained from SickKids Hospital, we checked the susceptibility of these strains to selected drugs (tobramycin, colistin sulfate and levofloxacin). Thus, we determined the Minimal Inhibitory Concentration (MIC) of the planktonic forms of mucoid, non-mucoid and quality control *Pseudomonas aeruginosa* strains according to the standardized Broth Microdilution Test proposed by the CLSI (Clinical and Laboratory Standards Institute (113).

Similarly, the Biofilm Minimal Inhibitory Concentration (MBIC) was assessed for the biofilm form of both clinical strains, according to Calgary Biofilm Device technology (115).

The experimental conditions of both tests were therefore optimized: tobramycin activity was evaluated just in the planktonic form of PA while colistin sulfate and levofloxacin activities were evaluated in the planktonic and biofilm forms of PA. In addition, colistin sulfate was evaluate the biofilm form of both strains and while levofloxacin was evaluated just in the biofilm form of the mucoid strain.

The results for the preliminary microbiological tests in the planktonic and biofilm forms of *Pseudomonas aeruginosa* are presented in **table XVII**.

Table XVII: *Pseudomonas aeruginosa* susceptibility to tobramycin, colistin sulfate and levofloxacin.

Test	Tobramycin	Colistin sulfate	Levofloxacin
Planktonic (MIC)	Mucoid = 1 µg/ml ($S^{b,c,g}$) Non-mucoid = 4 µg/ml ($I^{b,c,g}$) ATCC 57853 = 1 µg/ml^{b,f,h}	Mucoid = 4 µg/ml ($I^{a,d,g}$) Non-mucoid = 4 µg/ml ($I^{a,d,h}$) ATCC 57853 = 8 µg/ml^{b,f,h}	Mucoid = 1 µg/ml ($S^{a,e,g}$) ATCC 57853 = 1 µg/mL^{b,f,g}
Biofilm (MIC)	-	Mucoid = 1 µg/ml ($S^{a,d,h}$) Non-mucoid = 1 µg/ml ($S^{a,d,h}$)	Mucoid = 1.0 µg/ml ($S^{a,e,i}$)
Biofilm (MIBC)	-	Mucoid = 4 µg/ml ($I^{a,d,h}$) Non-mucoid = 1 µg/ml ($S^{a,d,i}$)	Mucoid = 8 µg/ml ($R^{a,e,i}$)

[a]All tests were made in triplicate for the each strain. [b]All tests were made in duplicate.
[c]Tobramycin - Susceptible (S): MIC is ≤ 2 µg/ml; Intermediate (I): MIC = 4 µg/ml; Resistant (R): MIC ≥ 8 µg/mL.
[d]Colistin sulfate - Susceptible (S): MIC is ≤ 2 µg/ml; Intermediate (I): MIC = 4 µg/ml; Resistant (R): MIC ≥ 8 µg/mL.
[e]Levofloxacin - Susceptible (S): MIC is ≤ 2 µg/ml; Intermediate (I): MIC = 4 µg/ml; Resistant (R): MIC ≥ 8 µg/mL.
[f]ATCC 57853: Tobramycin MIC range: 0.25-1 µg/mL; Colistin: 0.5-4 µg/mL; Levofloxacin: 0.5-4 µg/mL.
[g]The test was made in three different days. [h]The test was made in two different days. [i]The test was made just 1 time.
MIC: Mininal Inhibitory Concentration; MBIC: Minimal Biofilm Inhibitory Concentration.
ATCC: American Type Cell Collection.

The results showed that the planktonic form of the mucoid strain was susceptible to tobramycin (MIC= 1 µg/mL) while the non-mucoid strain presented intermediate susceptibility to tobramycin. The quality control strain presented MIC= 1 µg/mL, result within the expected range (0.25 – 1 µg/mL) (113) which validate the test.

In addition, the planktonic forms of both strains had intermediate resistance to colistin sulfate. However, the MIC= 8 µg/mL for the quality control strain was higher than expected (0.5 to 4 µg/mL) (113). However, the test had inter-day (n=3) and intra-day reproducibility (test done in two different days) suggesting that no mistake might have occurred. Moreover, the same quality control strain presented expected MICs for tobramycin and levofloxacin. Thus, the results of MIC for colistin sulfate can be considered valid despite no obvious explanation for the higher MIC found in the quality control strain.

The susceptibility test showed that the planktonic form of the mucoid strain is susceptible to levofloxacin and the MIC= 1 µg/mL and the MIC for the quality control strain was within the expected range of 0.5-4 µg/mL (113).

Thus, as showed in **table XVII**, the MIC found in the challenge plate of the Calgary biofilm device was in agreement with the MIC found in the regular microbiological test for levofloxacin. However, similar analysis for colistin sulfate presented divergent results. In fact, it was expected since studies carried out by Dr. Waters *et al* in Toronto (hospital of sickkids) showed that the MIC obtained from the peg panel is not comparable to the MIC obtained from separate MIC testing. Therefore, we will not consider the MIC provided by the biofilm test, just the MBIC.

Most importantly, although the biofilm test was done on four different days, the results were not reproducible, suggesting that this test must be further optimized.

It has to be noted that the Calgary biofilm characterizes MIC and MBIC in o high throughput way. The validation and reproducibility of this test is currently studied by Valerie Waters in Toronto. This is the reason why some optimization might be required to the application of this device.

To conclude, this preliminary test guided our choice to select levofloxacin as drug model for liposomes encapsulation (see section 3.5.1) since this drug was efficient to kill the mucoid strain of PA. In addition, the Broth Microdilution test was selected for further evaluation of levofloxacin loaded liposomes activity against PA since the Calgary Biofilm Test did not exhibit consistent MBIC.

3.5.7. Planktonic antimicrobial susceptibility testing of liposomes against *Pseudomonas aeruginosa*

As discussed in section 3.4.4, we prepared levofloxacin loaded liposomes with appropriate size and charge for drug diffusion in the mucus and with suitable loading efficiency to treat

PA in Cystic Fibrosis (LE ~ 8% w/w). Therefore we evaluated the antibacterial efficiency of levofloxacin loaded liposomes as compared with blank liposomes and the free drug since we expect that loaded liposomes will exhibit enhanced activity against PA.

The liposomes evaluation was performed by Broth Microdilution Testing and the results are displayed in **table XVIII**.

Table XVIII: MIC of free levofloxacin, loaded and blank liposomes against PA

Tests[a,b]	Formulation	Mucoid[c] MIC (μg/mL)	Non-Mucoid[c] MIC (μg/mL)	Quality Control[d] MIC (μg/mL)
1.1 and 1.2 (day 1)	Free Levo-1	-	64[e,f]	1[h]
	Levo Lip-1	-	32[e,f]	-
	Blank Lip- 1	-	> 128[g]	-
2.1 and 2.2 (day 2)	Free Levo-2	1[e,f]	64[e,f]	2[g]
	Levo Lip-2	1[e,f]	32[e,f]	-
	Blank Lip- 2	> 128[g]	> 128[g]	-
3.1 and 3.2 (day 3)	Free Levo-3	1[e,f]	64[g]	2[g]
	Levo Lip-3	1[e,f]	32[g]	-
	Blank Lip- 3	> 128[g]	> 128[g]	-

[a] Intra-day Reproducibility: two independent tests made in triplicate with the same formulation in the same day.
[b] Inter-day Reproducibility: 2 independent tests made in triplicate in 3 different days with new formulations in each day.
[c] Levofloxacin - Susceptible (S): MIC is ≤ 2 μg/ml; Intermediate (I): MIC = 4 μg/ml; Resistant (R): MIC ≥ 8 μg/ml.
[d] Quality Control strain ATCC 57853: levofloxacin MIC range of 0.5-4 μg/mL. [e] Result from test 1 found in duplicate (test 1 and 2 made in the same day with the same batch). [f] Result from test 2 found in triplicate (test 1 and 2 made in the same day with the same batch). [g] Result from test 1 and test 2 found in triplicates (test 1 and 2 made in the same day with the same batch). [h] Result from test 1 and test 2 found in duplicates (test 1 and 2 made in the same day with the same batch).MIC: Minimal Inhibitory Concentration. ATCC: American Type Cell Collection. Lip: liposomes. Levo: levofloxacin.

As showed in **table XVIII**, two independent tests were done in triplicate in the same day to test the intra-day reproducibility and these testes were repeated in three different days with new liposomes and free drug formulations to check the inter-day reproducibility.

The MIC found for the quality control strain was between 1 and 2 and this resulting range can be explained by small variations during the spectrophotometric analysis for the inoculum adjustment at 0.8 Mc Farland (OD= 0.08 – 0.13). Most importantly, the range

found was between the specification for the ATCC 57853 (MIC from 0.5 to 4 µg/mL) which validate the test and the MIC values obtained for the clinical strains. Furthermore, MIC range is in agreement with the results found in the preliminary tests. In addition, blank liposomes did not exhibit activity against PA, since the MIC found with this formulation was > 128 µg/mL.

Although the test was done in triplicate for each strain, the MIC values obtained were either in duplicate or triplicate depending on the test, as can be verified in **table XVIII**. Indeed, for the mucoid strain the MIC range obtained was between 1 and 2 µg/mL for both formulations (free drug and loaded liposomes). Therefore, levofloxacin loaded liposomes formulation did not exhibit increased efficacy to eradicate the mucoid strain of *Pseudomonas aeruginosa in vitro*. Indeed, these results were expected since the mucoid strain is already very susceptible to the free drug. A small concentration of the free drug is enough to eradicate this strain of *P. aeruginosa*. Thus, in this case the potential benefits of the liposomes formulation could hardly be evaluated by the MIC, but by other tests such as the comparative mucus penetration of free and loaded liposomes.

Conversely, for the non-mucoid strain the MIC range obtained for the free drug was from 64 to 128 µg/mL while the MIC range for levofloxacin loaded liposomes was from 32 to 64 µg/mL. Likewise, the blank liposomes formulation did not exhibit any activity against the non-mucoid strain. Therefore, the levofloxacin loaded liposomes formulation showed to be 2 fold times more efficient to kill *Pseudomonas aeruginosa in vitro* if compared with the free drug. In this case the liposomes seem to present a benefit over the free drug.

To conclude, despite the superior efficacy of the liposomes formulation to kill the non-mucoid strain of *Pseudomonas aeruginosa* showed in this study, a further investigation on the drug release from liposomes over 48 hours should be performed to elucidate if this better efficacy is either due to the extended delivery of levofloxacin or to the liposomes uptake by the bacteria.

These results tend to show that:

- Liposomes do not impair the delivery of drugs to *Pseudomonas aeruginosa*, since the antibiotic activity is similar or better than the free drug.

- When the strain is very susceptible to the free drug (such as the mucoid strain), it is difficult to verify any improvement in the antibacterial effect with the use of liposomes. Most probably, the small levofloxacin concentration released from liposomes is enough to kill the bacteria.

- When the strain is resistant to levofloxacin, liposomes might have a benefit over the free drug, since the MIC is reduced to a half. This superior activity might be either due to the extended delivery of levofloxacin or to the liposomes uptake by the bacteria. To confirm this result we need to study the drug release profile of the drug.

Chapter 4:

Conclusion and Perspectives

The main objective of this work was to develop an antibiotic formulation to treat pulmonary infections in Cystic Fibrosis (CF). This is the aspect of the disease with the highest impact in the patient's lifespan. Although a number of microorganisms have been isolated from the lungs of CF patients, the new formulation was evaluated in clinically isolated strains of *Pseudomonas aeruginosa* (mucoid and non-mucoid) kindly provided by Dr .Waters (SickKids, Toronto, Canada). Indeed, studies show that lung infection by *Pseudomonas aeruginosa* is related with increased morbidity and mortality of CF patients, hence the choice of this microorganism.

Based on the pathological aspects of Cystic Fibrosis, the new antibiotic formulation would:

- ✓ Circumvent the interaction of charged antibiotics with the mucus, a fact that hinders drug diffusion. As a consequence, sub-inhibitory antibiotic levels would favor bacterial resistance, biofilm formation and treatment failure.
- ✓ Have increased efficacy against *Pseudomonas aeruginosa* (planktonic and biofilm forms) in order to avoid cyclic bacterial infections and loss of lung capacity;
- ✓ Have the possibility to be formulated for pulmonary administration therefore decreasing side effects and improving the patient's compliance to the treatment.

In order to address these challenges we developed a polymeric PEG-g-PLA nanoparticle formulation since previous studies performed in our laboratory showed that: 1) PEG-g-PLA nanoparticles increased the efficacy of itraconazole against *Candida spp*.; 2) Experimental evidences showed that PEG-g-PLA nanoparticles might be related with decreased resistance in Candida strains (45); 3) PEG-g-PLA had been previously applied to encapsulate hydrophilic and hydrophobic drugs. Most importantly, nanoparticle with suitable size, charge, and PEG coating could improve particle diffusion in the mucus.

Tobramycin loaded nanoparticles were produced by emulsification solvent evaporation (ESE) – double emulsion (DE) and by nanoprecipitation (NPP). Tobramycin was chosen since this drug is a gold standard for the treatment of CF. Optimization of production was attempted

to increase the efficiency of tobramycin encapsulation. Experimental results demonstrated that size, polydispersity and charge of tobramycin nanoparticles were reasonable for mucus penetration. However, drug content inside nanoparticles was low for an antibiotic formulation. Indeed, tobramycin concentration inside NP was lower than the limit of quantification allowed by spectrophotometry analysis with prior fluorescamine derivatization. Thus, we attempted to develop other analytic methods for tobramycin quantification such as HPLC (ELSD and MS detection) with polar and reverse column phase. However, due to its high hydrophilicity, tobramycin could not be retained in the reverse column. Additionally, tobramycin strongly interacted with polar columns and both drawbacks hindered the development of a consistent method of quantification. In fact, PEG-g-PLA nanoparticles posses a hydrophobic core which is inappropriate for the encapsulation of highly hydrophilic drugs such as tobramycin. For these reasons, we decided to search for other drug with lower hydrophilicity aiming to reach higher loading efficiency.

The next step consisted in evaluating the encapsulation of colistin sulfate and levofloxacin in PEG-g-PLA nanoparticles. However, early steps of optimization showed that levofloxacin exhibited higher loading efficiency than colistin sulfate. In addition, the method of quantification for levofloxacin exhibited lower limit of quantification, a fact that helped to identify small increments in loading efficiency between the batches. Therefore, we decided to work in further optimization for the levofloxacin nanoparticles.

Results showed that irrespective of the method of nanoparticle preparation or drug composition, all nanoparticles exhibited size < 200 nm, PDI < 0.2 (monodisperse population) and charge range from -1.44 to -28.2 mV. These parameters favored mucus diffusion except the negative charge, since neutral particles exhibit better diffusion.

As an attempt to increase levofloxacin encapsulation, some parameters were altered such as 1) method of nanoparticle preparation; 2)polymer composition (addition of PLA-OH which is more hydrophilic than PEG-g-PLA); 3)surfactant composition; 4) solvent and co-solvent

composition; 5) pH; 6) drug feeding ratio and 7) additive composition. However, the best encapsulation efficiency reached was 0.02% w/w (formulation 10, **table XV**).

The drug loading results were in accordance with the literature. In fact, it has been shown that polymer composition mostly impacts the drug encapsulation. Thus, the main challenge to develop efficacious formulation for the treatment of CF is the polymer composition. As most of the drugs indicated for the treatment of CF are hydrophilic, in order to favor drug/polymer interaction to increase drug encapsulation the polymer must be hydrophilic. However, the polymer must possess a balanced hydrophilicity to avoid mucus interaction.

The second import observation is that the molecular weight may also have a significant impact in the drug loading. For instance, *Hammady et al* was able to encapsulate a high molecular weight hydrophilic component (calf thymus DNA) in a hydrophobic polymer (PEG-PLA).However, altering the molecular weight without losing drug activity is a complex task.

Therefore, we hypothesized that liposomes would be a better option to encapsulate hydrophilic drugs when compared to polymeric nanoparticles since the encapsulation process in liposomes does not depend on drug/lipid interaction.

Levofloxacin liposomes were prepared and exhibited size, charge and polydispersity appropriate for mucus penetration. Moreover, the loading efficiency was as optimized to 8% w/w which allowed to test of this formulation in *Pseudomonas aeruginosa*. Most importantly, results showed that liposomes were twice as efficient in killing the resistant non-mucoid strain of *Pseudomonas aeruginosa* (planktonic form) as compared to the free drug. However, further investigation in the drug release profile should be performed to elucidate if its higher activity was either due to extended drug release profile of liposomes or to nanoparticle uptake by the bacteria. In addition, the activity of liposomes formulation in biofilm should also be evaluated. However, the lack of a reproducible and representative biofilm microbiological test restricts the progress of studies in this specific field.

Although susceptibility tests evaluated the potential application of liposomes formulation to eradicate *Pseudomonas aeruginosa* in CF, studies to develop the final pulmonary

formulation must be performed since liquid liposome formulations are unstable. As an alternative approach, delivery by dry powder has been considered. Examples of techniques applied to prepare liposomes powders are lyophilisation (to dry the liposomes) and micronization by jet-milling (to adjust particle size to 1-6 μm for efficient drug delivery to the lungs). However, both freezing and drying can lead to structural and functional changes in liposomes. In addition, jet-milling is also expected to induce membrane deformation because of high-energy collision during milling, leading to perturbation of the liposome structure and leakage of encapsulated drug on hydration. Likewise, after micronization the final formulation must be evaluated to conclude if the drug loading of liposomes provides therapeutic doses of antibiotic per a reasonable quantity of powder.

The application of aptamers looks promising for the treatment of Cystic Fibrosis and is currently under investigation by our research group. Aptamers are an emerging class of nanocarriers composed of DNA or RNA strands whose composition can be optimised to favor the formation of a drug-aptamer conjugate. Therefore, aptamers could improve the encapsulation of hydrophilic drugs, such as tobramycin. As nucleotides are negatively charged, the conjugate drug-aptamer could be easily encapsulated into cationic liposomes. Thus, higher encapsulation efficiency might improve the treatment of CF and result in a final powder formulation with a higher concentration (suitable for pulmonary administration). In addition, liposomes may favor mucus penetration and aptamers may present a sustained release of drugs.

As have been showed and discussed, nanotechnology is a promising and challenging field of study to develop innovative formulations to treat the pulmonary phase of Cystic Fibrosis. However, the appropriate nanocarrier should be able to provide high drug loading in order to be further formulated as a powder for inhalation or nebulization. Moreover, nanocarriers must be mucus inert to aid the diffusion of hydrophilic drugs. Nanocarriers should also exhibit an extended drug release and/or be able to penetrate microorganisms. In this research we prepared and characterized PEG-g-PLA nanoparticles versus liposomes and the liposome formulation seemed to be able to address these challenges. However, further

studies must be performed to provide the final conclusion whether liposomes are in fact a suitable formulation for the treatment of Cystic Fibrosis.

Bibliography

1. Davis PB. Cystic Fibrosis Since 1938. American Journal of Respiratory and Critical Care Medicine. 2006;173(5):475-82.

2. Couzin-Frankel J. The Promise of a Cure: 20 Years and Counting. Science. 2009;324(5934):1504-7.

3. Gibson RL, Burns JL, Ramsey BW. Pathophysiology and Management of Pulmonary Infections in Cystic Fibrosis. American Journal of Respiratory and Critical Care Medicine. 2003;168(8):918-51.

4. SHEPPARD DN, WELSH MJ. Structure and Function of the CFTR Chloride Channel. Physiological Reviews. 1999;79(1):S23-S45.

5. Boyle MP, De Boeck K. A new era in the treatment of cystic fibrosis: correction of the underlying CFTR defect. The Lancet Respiratory Medicine. 2013;1(2):158-63.

6. Canada: CF. Canadian Cystic Fibrosis Registry 2011 Annual Report. Cystic Fibrosis Canada. 2011.

7. Sheppard MN, Nicholson AG. The pathology of cystic fibrosis. Current Diagnostic Pathology. 2002;8(1):50-9.

8. Boucher RC. Airway Surface Dehydration in Cystic Fibrosis: Pathogenesis and Therapy. Annual Review of Medicine. 2007;58(1):157-70.

9. Waters VJ, Gómez MI, Soong G, Amin S, Ernst RK, Prince A. Immunostimulatory Properties of the Emerging Pathogen Stenotrophomonas maltophilia. Infection and Immunity. 2007;75(4):1698-703.

10. Becq F, Mall MA, Sheppard DN, Conese M, Zegarra-Moran O. Pharmacological therapy for cystic fibrosis: From bench to bedside. Journal of Cystic Fibrosis. 2011;10, Supplement 2(0):S129-S45.

11. Emerson J, Rosenfeld M, McNamara S, Ramsey B, Gibson RL. *Pseudomonas aeruginosa* and other predictors of mortality and morbidity in young children with cystic fibrosis. Pediatric Pulmonology. 2002;34(2):91-100.

12. Fauroux B, Hart N, Belfar S, Boulé M, Tillous-Borde I, Bonnet D, et al. Burkholderia cepacia Is Associated with Pulmonary Hypertension and Increased Mortality among Cystic Fibrosis Patients. Journal of Clinical Microbiology. 2004;42(12):5537-41.

13. De Baets F, Schelstraete P, Van Daele S, Haerynck F, Vaneechoutte M. Achromobacter xylosoxidans in cystic fibrosis: Prevalence and clinical relevance. Journal of Cystic Fibrosis. 2007;6(1):75-8.

14. Rosenfeld M, Emerson J, Williams-Warren J, Pepe M, Smith A, Montgomery AB, et al. Defining a pulmonary exacerbation in cystic fibrosis. The Journal of pediatrics. 2001;139(3):359-65.

15. Tümmler B, Kiewitz C. Cystic fibrosis: an inherited susceptibility to bacterial respiratory infections. Molecular Medicine Today. 1999;5(8):351-8.

16. Hassett DJ, Cuppoletti J, Trapnell B, Lymar SV, Rowe JJ, Sun Yoon S, et al. Anaerobic metabolism and quorum sensing by *Pseudomonas aeruginosa* biofilms in chronically infected cystic fibrosis airways: rethinking antibiotic treatment strategies and drug targets. Advanced Drug Delivery Reviews. 2002;54(11):1425-43.

17. Stoodley P, Sauer K, Davies DG, Costerton JW. Biofilms as complex differentiated communities. Annual review of microbiology. 2002;56:187-209.

18. Sauer K. The genomics and proteomics of biofilm formation. Genome Biology. 2003;4(6):219.

19. Govan JR, Deretic V. Microbial pathogenesis in cystic fibrosis: mucoid *Pseudomonas aeruginosa* and Burkholderia cepacia. Microbiological Reviews. 1996;60(3):539-74.

20. Flume PA, O'Sullivan BP, Robinson KA, Goss CH, Mogayzel PJ, Willey-Courand DB, et al. Cystic Fibrosis Pulmonary Guidelines. American Journal of Respiratory and Critical Care Medicine. 2007;176(10):957-69.

21. Geller DE. Aerosol Antibiotics in Cystic Fibrosis. Respiratory Care. 2009;54(5):658-70.

22. Westreenen M, Tiddens HWM. New Antimicrobial Strategies in Cystic Fibrosis. Pediatr-Drugs. 2010;12(6):343-52.

23. Sawicki GS, Signorovitch JE, Zhang J, Latremouille-Viau D, von Wartburg M, Wu EQ, et al. Reduced mortality in cystic fibrosis patients treated with tobramycin inhalation solution. Pediatric Pulmonology. 2012;47(1):44-52.

24. Canadian consensus statement on aerosolized antibiotic use in Cystic Fibrosis. The canadian Cystic Fibrosis Foundation. 2006.

25. Flume PA, Mogayzel PJ, Robinson KA, Goss CH, Rosenblatt RL, Kuhn RJ, et al. Cystic Fibrosis Pulmonary Guidelines: Treatment of Pulmonary Exacerbations. American Journal of Respiratory and Critical Care Medicine. 2009;180(9):802-8.

26. Zobell JT, Young DC, Waters CD, Ampofo K, Cash J, Marshall BC, et al. A survey of the utilization of anti-pseudomonal beta-lactam therapy in cystic fibrosis patients. Pediatric Pulmonology. 2011;46(10):987-90.

27. Zobell JT, Young DC, Waters CD, Stockmann C, Ampofo K, Sherwin CMT, et al. Optimization of anti-pseudomonal antibiotics for cystic fibrosis pulmonary exacerbations: I. aztreonam and carbapenems. Pediatric Pulmonology. 2012;47(12):1147-58.

28. Zobell JT, Waters CD, Young DC, Stockmann C, Ampofo K, Sherwin CMT, et al. Optimization of anti-pseudomonal antibiotics for cystic fibrosis pulmonary exacerbations: II. cephalosporins and penicillins. Pediatric Pulmonology. 2013;48(2):107-22.

29. Ratjen F, Rietschel E, Kasel D, Schwiertz R, Starke K, Beier H, et al. Pharmacokinetics of inhaled colistin in patients with cystic fibrosis. The Journal of antimicrobial chemotherapy. 2006;57(2):306-11.

30. Schuster A, Haliburn C, Doring G, Goldman MH. Safety, efficacy and convenience of colistimethate sodium dry powder for inhalation (Colobreathe DPI) in patients with cystic fibrosis: a randomised study. Thorax. 2013;68(4):344-50.

31. Retsch-Bogart GZ, Quittner AL, Gibson RL, Oermann CM, McCoy KS, Montgomery AB, et al. Efficacy and safety of inhaled aztreonam lysine for airway pseudomonas in cystic fibrosis. Chest. 2009;135(5):1223-32.

32. Retsch-Bogart GZ, Burns JL, Otto KL, Liou TG, McCoy K, Oermann C, et al. A phase 2 study of aztreonam lysine for inhalation to treat patients with cystic fibrosis and *Pseudomonas aeruginosa* infection. Pediatr Pulmonol. 2008;43(1):47-58.

33. Konstan MW, Flume PA, Kappler M, Chiron R, Higgins M, Brockhaus F, et al. Safety, efficacy and convenience of tobramycin inhalation powder in cystic fibrosis patients: The EAGER trial. Journal of cystic fibrosis : official journal of the European Cystic Fibrosis Society. 2011;10(1):54-61.

34. Cohen-Cymberknoh M, Shoseyov D, Kerem E. Managing Cystic Fibrosis. American Journal of Respiratory and Critical Care Medicine. 2011;183(11):1463-71.

35. Sawicki GS, Sellers DE, Robinson WM. High treatment burden in adults with cystic fibrosis: Challenges to disease self-management. Journal of Cystic Fibrosis. 2009;8(2):91-6.

36. Conway SP, Pond MN, Hamnett T, Watson A. Compliance with treatment in adult patients with cystic fibrosis. Thorax. 1996;51(1):29-33.

37. Modi AC, Quittner AL. Barriers to treatment adherence for children with cystic fibrosis and asthma: what gets in the way? J Pediatr Psychol. 2006;31(8):846-58.

38. Meers P, Neville M, Malinin V, Scotto AW, Sardaryan G, Kurumunda R, et al. Biofilm penetration, triggered release and in vivo activity of inhaled liposomal amikacin in chronic *Pseudomonas aeruginosa* lung infections. Journal of Antimicrobial Chemotherapy. 2008;61(4):859-68.

39. Livermore DM. Multiple Mechanisms of Antimicrobial Resistance in *Pseudomonas aeruginosa*: Our Worst Nightmare? Clinical Infectious Diseases. 2002;34(5):634-40.

40. Abeylath SC, Turos E. Drug delivery approaches to overcome bacterial resistance to β-lactam antibiotics. Expert Opinion on Drug Delivery. 2008;5(9):931-49.

41. Moskowitz SM, Ernst RK, Miller SI. PmrAB, a Two-Component Regulatory System of *Pseudomonas aeruginosa* That Modulates Resistance to Cationic Antimicrobial Peptides and Addition of Aminoarabinose to Lipid A. Journal of Bacteriology. 2004;186(2):575-9.

42. Falagas ME, Kasiakou SK, Saravolatz LD. Colistin: The Revival of Polymyxins for the Management of Multidrug-Resistant Gram-Negative Bacterial Infections. Clinical Infectious Diseases. 2005;40(9):1333-41.

43. Johansen HK, Moskowitz SM, Ciofu O, Pressler T, Høiby N. Spread of colistin resistant non-mucoid *Pseudomonas aeruginosa* among chronically infected Danish cystic fibrosis patients. Journal of Cystic Fibrosis. 2008;7(5):391-7.

44. Hoffman LR, D'Argenio DA, MacCoss MJ, Zhang Z, Jones RA, Miller SI. Aminoglycoside antibiotics induce bacterial biofilm formation. Nature. 2005;436(7054):1171-5.

45. Aoun V. Développment de nouvelles formulations d'antifongiques et évaluation de l'activité sur *Candida spp* et *Aspergillus spp (Thèse de doctorat inédite).* Université de Montréal. 2014.

46. Aulton. Aulton's Pharmaceutics : The Design and Manufacture of Medicines2013.

47. McCaughey G, McKevitt M, Elborn JS, Tunney MM. Antimicrobial activity of fosfomycin and tobramycin in combination against cystic fibrosis pathogens under aerobic and anaerobic conditions. Journal of Cystic Fibrosis. 2012;11(3):163-72.

48. Major TA, Panmanee W, Mortensen JE, Gray LD, Hoglen N, Hassett DJ. Sodium Nitrite-Mediated Killing of the Major Cystic Fibrosis Pathogens *Pseudomonas aeruginosa*, Staphylococcus aureus, and Burkholderia cepacia

under Anaerobic Planktonic and Biofilm Conditions. Antimicrobial Agents and Chemotherapy. 2010;54(11):4671-7.

49. Keren I, Kaldalu N, Spoering A, Wang Y, Lewis K. Persister cells and tolerance to antimicrobials. FEMS Microbiology Letters. 2004;230(1):13-8.

50. Oliver A, Cantón R, Campo P, Baquero F, Blázquez J. High Frequency of Hypermutable *Pseudomonas aeruginosa* in Cystic Fibrosis Lung Infection. Science. 2000;288(5469):1251-3.

51. Høiby N, Bjarnsholt T, Givskov M, Molin S, Ciofu O. Antibiotic resistance of bacterial biofilms. International Journal of Antimicrobial Agents. 2010;35(4):322-32.

52. Stewart PS. Mechanisms of antibiotic resistance in bacterial biofilms. International Journal of Medical Microbiology. 2002;292(2):107-13.

53. Zhang L, Pornpattananangkul D, Hu CMJ, Huang CM. Development of Nanoparticles for Antimicrobial Drug Delivery. Current Medicinal Chemistry. 2010;17(6):585-94.

54. Hammady T, El-Gindy A, Lejmi E, Dhanikula RS, Moreau P, Hildgen P. Characteristics and properties of nanospheres co-loaded with lipophilic and hydrophilic drug models. International Journal of Pharmaceutics. 2009;369(1–2):185-95.

55. Nasr M, Najlah M, D'Emanuele A, Elhissi A. PAMAM dendrimers as aerosol drug nanocarriers for pulmonary delivery via nebulization. Int J Pharm. 2014;461(1-2):242-50.

56. Ryan GM, Kaminskas LM, Kelly BD, Owen DJ, McIntosh MP, Porter CJH. Pulmonary Administration of PEGylated Polylysine Dendrimers: Absorption from the Lung versus Retention within the Lung Is Highly Size-Dependent. Molecular Pharmaceutics. 2013;10(8):2986-95.

57. Essa S, Louhichi F, Raymond M, Hildgen P. Improved antifungal activity of itraconazole-loaded PEG/PLA nanoparticles. Journal of Microencapsulation. 2013;30(3):205-17.

58. zur Mühlen A, Schwarz C, Mehnert W. Solid lipid nanoparticles (SLN) for controlled drug delivery – Drug release and release mechanism. European Journal of Pharmaceutics and Biopharmaceutics. 1998;45(2):149-55.

59. Gaspar MM, Gobbo O, Ehrhardt C. Generation of liposome aerosols with the Aeroneb Pro and the AeroProbe nebulizers. Journal of Liposome Research. 2010;20(1):55-61.

60. Abu-Dahab R, Schäfer UF, Lehr C-M. Lectin-functionalized liposomes for pulmonary drug delivery: effect of nebulization on stability and bioadhesion. European Journal of Pharmaceutical Sciences. 2001;14(1):37-46.

61. Elhissi AMA, Faizi M, Naji WF, Gill HS, Taylor KMG. Physical stability and aerosol properties of liposomes delivered using an air-jet nebulizer and a novel

micropump device with large mesh apertures. International Journal of Pharmaceutics. 2007;334(1–2):62-70.

62. Chattopadhyay P, Shekunov BY, Yim D, Cipolla D, Boyd B, Farr S. Production of solid lipid nanoparticle suspensions using supercritical fluid extraction of emulsions (SFEE) for pulmonary delivery using the AERx system. Advanced Drug Delivery Reviews. 2007;59(6):444-53.

63. Nafee N, Husari A, Maurer CK, Lu C, de Rossi C, Steinbach A, et al. Antibiotic-free nanotherapeutics: Ultra-small, mucus-penetrating solid lipid nanoparticles enhance the pulmonary delivery and anti-virulence efficacy of novel quorum sensing inhibitors. Journal of controlled release : official journal of the Controlled Release Society. 2014;192:131-40.

64. Mansour HM, Rhee YS, Wu X. Nanomedicine in pulmonary delivery. International journal of nanomedicine. 2009;4:299-319.

65. Taylor D. Bacterial tellurite resistance. Trends in Microbiology. 1999;7(3):111 - 5.

66. Müller RH, Mäder K, Gohla S. Solid lipid nanoparticles (SLN) for controlled drug delivery – a review of the state of the art. European Journal of Pharmaceutics and Biopharmaceutics. 2000;50(1):161-77.

67. Lai SK, Wang Y-Y, Hanes J. Mucus-penetrating nanoparticles for drug and gene delivery to mucosal tissues. Advanced Drug Delivery Reviews. 2009;61(2):158-71.

68. Johansson EMV, Crusz SA, Kolomiets E, Buts L, Kadam RU, Cacciarini M, et al. Inhibition and Dispersion of *Pseudomonas aeruginosa* Biofilms by Glycopeptide Dendrimers Targeting the Fucose-Specific Lectin LecB. Chemistry & Biology. 2008;15(12):1249-57.

69. Andrade F, Rafael D, Videira M, Ferreira D, Sosnik A, Sarmento B. Nanotechnology and pulmonary delivery to overcome resistance in infectious diseases. Advanced drug delivery reviews. 2013;65(13):1816-27.

70. Mugabe C, Halwani M, Azghani AO, Lafrenie RM, Omri A. Mechanism of Enhanced Activity of Liposome-Entrapped Aminoglycosides against Resistant Strains of *Pseudomonas aeruginosa*. Antimicrobial Agents and Chemotherapy. 2006;50(6):2016-22.

71. Soppimath KS, Aminabhavi TM, Kulkarni AR, Rudzinski WE. Biodegradable polymeric nanoparticles as drug delivery devices. Journal of Controlled Release. 2001;70(1–2):1-20.

72. Huh AJ, Kwon YJ. "Nanoantibiotics": a new paradigm for treating infectious diseases using nanomaterials in the antibiotics resistant era. Journal of controlled release : official journal of the Controlled Release Society. 2011;156(2):128-45.

73. Garinot M, Fiévez V, Pourcelle V, Stoffelbach F, des Rieux A, Plapied L, et al. PEGylated PLGA-based nanoparticles targeting M cells for oral vaccination. Journal of Controlled Release. 2007;120(3):195-204.

74. Nadeau V, Leclair G, Sant S, Rabanel J-M, Quesnel R, Hildgen P. Synthesis of new versatile functionalized polyesters for biomedical applications. Polymer. 2005;46(25):11263-72.

75. Lai SK, Wang Y-Y, Wirtz D, Hanes J. Micro- and macrorheology of mucus. Advanced Drug Delivery Reviews. 2009;61(2):86-100.

76. Hida K, Lai SK, Suk JS, Won SY, Boyle MP, Hanes J. Common Gene Therapy Viral Vectors Do Not Efficiently Penetrate Sputum from Cystic Fibrosis Patients. PLoS ONE. 2011;6(5):e19919.

77. Suk JS, Lai SK, Wang Y-Y, Ensign LM, Zeitlin PL, Boyle MP, et al. The penetration of fresh undiluted sputum expectorated by cystic fibrosis patients by non-adhesive polymer nanoparticles. Biomaterials. 2009;30(13):2591-7.

78. Ramphal R, Lhermitte M, Filliat M, Roussel P. The binding of anti-pseudomonal antibiotics to macromolecules from cystic fibrosis sputum. Journal of Antimicrobial Chemotherapy. 1988;22(4):483-90.

79. Essa S, Rabanel JM, Hildgen P. Effect of aqueous solubility of grafted moiety on the physicochemical properties of poly(d,l-lactide) (PLA) based nanoparticles. International Journal of Pharmaceutics. 2010;388(1–2):263-73.

80. Surapaneni MS, Das SK, Das NG. Designing Paclitaxel Drug Delivery Systems Aimed at Improved Patient Outcomes: Current Status and Challenges. ISRN Pharmacology. 2012;2012:15.

81. Hammady T, Rabanel J-M, Dhanikula RS, Leclair G, Hildgen P. Functionalized nanospheres loaded with anti-angiogenic drugs: Cellular uptake and angiosuppressive efficacy. European Journal of Pharmaceutics and Biopharmaceutics. 2009;72(2):418-27.

82. Essa S, Louhichi F, Raymond M, Hildgen P. Improved antifungal activity of itraconazole-loaded PEG/PLA nanoparticles. J Microencapsul. 2013;30(3):205-17.

83. Okusanya ÓO, Bhavnani SM, Hammel J, Minic P, Dupont LJ, Forrest A, et al. Pharmacokinetic and Pharmacodynamic Evaluation of Liposomal Amikacin for Inhalation in Cystic Fibrosis Patients with Chronic Pseudomonal Infection. Antimicrobial Agents and Chemotherapy. 2009;53(9):3847-54.

84. Paul Bruinenberg JDB, David C Cipolla, Francis Dayton, Sujata Mudumba, Igor Gonda. Inhaled Liposomal Ciprofloxacin: Once a Day Management of Respiratory Infections. Respiratory Drug Delivery 2010; Vol 1:73-82.

85. Stass H, Nagelschmitz J, Willmann S, Delesen H, Gupta A, Baumann S. Inhalation of a Dry Powder Ciprofloxacin Formulation in Healthy Subjects: A Phase I Study. Clin Drug Investig. 2013;33(6):419-27.

86. Trapnell BC, McColley SA, Kissner DG, Rolfe MW, Rosen JM, McKevitt M, et al. Fosfomycin/Tobramycin for Inhalation in Patients with Cystic Fibrosis with Pseudomonas Airway Infection. American Journal of Respiratory and Critical Care Medicine. 2012;185(2):171-8.

87. Geller DE, Flume PA, Griffith DC, Morgan E, White D, Loutit JS, et al. Pharmacokinetics and Safety of MP-376 (Levofloxacin Inhalation Solution) in Cystic Fibrosis Subjects. Antimicrobial Agents and Chemotherapy. 2011;55(6):2636-40.

88. Geller DE, Flume PA, Staab D, Fischer R, Loutit JS, Conrad DJ. Levofloxacin Inhalation Solution (MP-376) in Patients with Cystic Fibrosis with *Pseudomonas aeruginosa*. American Journal of Respiratory and Critical Care Medicine. 2011;183(11):1510-6.

89. King P, Lomovskaya O, Griffith DC, Burns JL, Dudley MN. In Vitro Pharmacodynamics of Levofloxacin and Other Aerosolized Antibiotics under Multiple Conditions Relevant to Chronic Pulmonary Infection in Cystic Fibrosis. Antimicrobial Agents and Chemotherapy. 2010;54(1):143-8.

90. Ungaro F, d'Angelo I, Coletta C, d'Emmanuele di Villa Bianca R, Sorrentino R, Perfetto B, et al. Dry powders based on PLGA nanoparticles for pulmonary delivery of antibiotics: Modulation of encapsulation efficiency, release rate and lung deposition pattern by hydrophilic polymers. Journal of Controlled Release. 2012;157(1):149-59.

91. Clarot I, Storme-Paris I, Chaminade P, Estevenon O, Nicolas A, Rieutord A. Simultaneous quantitation of tobramycin and colistin sulphate by HPLC with evaporative light scattering detection. Journal of Pharmaceutical and Biomedical Analysis. 2009;50(1):64-7.

92. Hurtado FK, Nogueira DR, Bortolini F, da Silva LM, Zimmermann E, e Souza MJ, et al. Determination of Levofloxacin in a Pharmaceutical Injectable Formulation by Using HPLC and UV Spectrophotometric Methods. Journal of Liquid Chromatography & Related Technologies. 2007;30(13):1981-9.

93. Westerman EM, Le Brun PPH, Touw DJ, Frijlink HW, Heijerman HGM. Effect of nebulized colistin sulphate and colistin sulphomethate on lung function in patients with cystic fibrosis: a pilot study. Journal of Cystic Fibrosis. 2004;3(1):23-8.

94. Tarushi A, Polatoglou E, Kljun J, Turel I, Psomas G, Kessissoglou DP. Interaction of Zn(ii) with quinolone drugs: Structure and biological evaluation. Dalton Transactions. 2011;40(37):9461-73.

95. United States Pharmacopeia and National Formulary (USP 29-NF 24). Rockville, MD: United States Pharmacopeia Convention. 2007;2:2158.

96. Russ H, McCleary D, Katimy R, Montana JL, Miller RB, Krishnamoorthy R, et al. Development and Validation of a Stability-Indicating HPLC Method for the Determination of Tobramycin and Its Related Substances in an Ophthalmic Suspension. Journal of Liquid Chromatography & Related Technologies. 1998;21(14):2165-81.

97. Sampath SS, Robinson DH. Comparison of new and existing spectrophotometric methods for the analysis of tobramycin and other aminoglycosides. Journal of pharmaceutical sciences. 1990;79(5):428-31.

98. Suh J, Dawson M, Hanes J. Real-time multiple-particle tracking: applications to drug and gene delivery. Advanced Drug Delivery Reviews. 2005;57(1):63-78.

99. Wang Y-Y, Lai SK, Suk JS, Pace A, Cone R, Hanes J. Addressing the PEG Mucoadhesivity Paradox to Engineer Nanoparticles that “Slip” through the Human Mucus Barrier. Angewandte Chemie International Edition. 2008;47(50):9726-9.

100. Cheow WS, Chang MW, Hadinoto K. The roles of lipid in anti-biofilm efficacy of lipid–polymer hybrid nanoparticles encapsulating antibiotics. Colloids and Surfaces A: Physicochemical and Engineering Aspects. 2011;389(1–3):158-65.

101. Gupta H, Aqil M, Khar RK, Ali A, Bhatnagar A, Mittal G. Biodegradable levofloxacin nanoparticles for sustained ocular drug delivery. J Drug Target. 2011;19(6):409-17.

102. Barichello JM, Morishita M, Takayama K, Nagai T. Encapsulation of Hydrophilic and Lipophilic Drugs in PLGA Nanoparticles by the Nanoprecipitation Method. Drug Development and Industrial Pharmacy. 1999;25(4):471-6.

103. Cheow W, Chang M, Hadinoto K. Antibacterial Efficacy of Inhalable Levofloxacin-Loaded Polymeric Nanoparticles Against E. coli Biofilm Cells: The Effect of Antibiotic Release Profile. Pharm Res. 2010;27(8):1597-609.

104. Govender T, Stolnik S, Garnett MC, Illum L, Davis SS. PLGA nanoparticles prepared by nanoprecipitation: drug loading and release studies of a water soluble drug. Journal of Controlled Release. 1999;57(2):171-85.

105. Frick A, Möller H, Wirbitzki E. Biopharmaceutical characterization of oral immediate release drug products. In vitro/in vivo comparison of phenoxymethylpenicillin potassium, glimepiride and levofloxacin. European Journal of Pharmaceutics and Biopharmaceutics. 1998;46(3):305-11.

106. Jin L, Li J, Nation RL, Nicolazzo JA. Brain Penetration of Colistin in Mice Assessed by a Novel High-Performance Liquid Chromatographic Technique. Antimicrobial Agents and Chemotherapy. 2009;53(10):4247-51.

107. Mobarak DH, Salah S, Elkheshen SA. Formulation of ciprofloxacin hydrochloride loaded biodegradable nanoparticles: optimization of technique and process variables. Pharmaceutical Development and Technology. 2014;19(7):891-900.

108. Zhang X, Sun P, Bi R, Wang J, Zhang N, Huang G. Targeted delivery of levofloxacin-liposomes for the treatment of pulmonary inflammation. Journal of Drug Targeting. 2009;17(5):399-407.

109. Bartlett GR. Phosphorus Assay in Column Chromatography. Journal of Biological Chemistry. 1959;234(3):466-8.

110. Haran G, Cohen R, Bar LK, Barenholz Y. Transmembrane ammonium sulfate gradients in liposomes produce efficient and stable entrapment of

amphipathic weak bases. Biochimica et Biophysica Acta (BBA) - Biomembranes. 1993;1151(2):201-15.

111. Zucker D, Marcus D, Barenholz Y, Goldblum A. Liposome drugs' loading efficiency: A working model based on loading conditions and drug's physicochemical properties. Journal of Controlled Release. 2009;139(1):73-80.

112. Drummond DC, Meyer O, Hong K, Kirpotin DB, Papahadjopoulos D. Optimizing Liposomes for Delivery of Chemotherapeutic Agents to Solid Tumors. Pharmacological Reviews. 1999;51(4):691-744.

113. Institute. CaLS. Methods for dilution antimicrobial susceptibility tests for bacteria that grow aerobically. Approved standard M7-A7, 7th ed. Clinical and Laboratory Standards Institute, Wayne, PA

2006.

114. LiPuma JJ, Rathinavelu S, Foster BK, Keoleian JC, Makidon PE, Kalikin LM, et al. In Vitro Activities of a Novel Nanoemulsion against Burkholderia and Other Multidrug-Resistant Cystic Fibrosis-Associated Bacterial Species. Antimicrobial Agents and Chemotherapy. 2009;53(1):249-55.

115. Ceri H, Olson ME, Stremick C, Read RR, Morck D, Buret A. The Calgary Biofilm Device: New Technology for Rapid Determination of Antibiotic Susceptibilities of Bacterial Biofilms. Journal of Clinical Microbiology. 1999;37(6):1771-6.

116. Harrison J, Turner R, Ceri H. High-throughput metal susceptibility testing of microbial biofilms. BMC Microbiology. 2005;5(1):53.